Tampere University

PANU NORDBACK

Natural and Synthetic Biomaterials for Epithelial Repair

Skin and Urethral Regeneration

Tampere University Dissertations 121

Tampere University Dissertations 121

PANU NORDBACK

Natural and Synthetic Biomaterials for Epithelial Repair

Skin and Urethral Regeneration

ACADEMIC DISSERTATION
To be presented, with the permission of
the Faculty of Medicine and Life Sciences
of Tampere University,
for public discussion in the Yellow Hall F025
of the Arvo building, Arvo Ylpön katu 34, Tampere,
on 11th October 2019, at 12 o'clock.

ACADEMIC DISSERTATION
Tampere University, Faculty of Medicine and Life Sciences
Finland

Responsible supervisor and Custos	Assoc. Prof. Susanna Miettinen Tampere University Finland	
Supervisors	Assoc. Prof. Susanna Miettinen Tampere University Finland	Adj. Prof. Minna Kääriäinen Tampere University Finland
Pre-examiners	Adj. Prof. Ilkka Koskivuo University of Turku Finland	Adj. Prof. Esko Kankuri University of Helsinki Finland
Opponent	Prof. Martti Talja University of Eastern Finland Finland	

Cover design: Roihu Inc.

ISBN 978-952-03-1226-8 (print)
ISBN 978-952-03-1227-5 (pdf)
ISSN 2489-9860 (print)
ISSN 2490-0028 (pdf)
http://urn.fi/URN:ISBN:978-952-03-1227-5

PunaMusta Oy – Yliopistopaino
Tampere 2019

To Emma and Hugo

ABSTRACT

Epithelial defects in skin and urethra constitute a major problem, both to society and to individual patients. Acute and chronic wounds comprise a remarkable health issue for basic and special healthcare, with an estimated prevalence of 3.7/1,000. Urethral defects, caused by congenital issues, trauma, or infections, are another kind of clinical epithelial dilemma. Hypospadias is the most common penile congenital malformation, with 0.1–0.8% prevalence rate. Treatment of these epithelial skin and urethral defects is demanding.

In this thesis, the aim was to evaluate the suitability of biomaterial membranes for skin wounds and urethral repair using *in vitro* and *in vivo* models. Amniotic (AM) and chitosan (CM) membranes were studied on wound surface, whereas poly(L-lactide-co-ε-caprolactone) (PLCL) and poly(1,3 trimethylene carbonate) (PTMC) membranes were studied on urethral defects.

To study the effects of AM and CM, full-thickness wounds were excised and measured on the scalps of rats. The rats were randomized into AM or CM and control groups. The wounds were covered with AM or CM and Aquacel or Aquacel alone (control). The rats were followed up for 0, 3, 7, 14 or 21 days. Wounds and tattooed marks were measured, blood samples withdrawn for an interleukin 4 (IL-4) assay, and wound sites excised for histological analysis after follow-up.

Median wound areas were significantly ($p < 0.05$) smaller in the AM and CM groups, compared to their controls on day three. IL-4 levels were significantly ($p < 0.05$) lower in the CM group on days 7 and 14, compared to the control group. In wound histology, the CM group had a significantly ($p < 0.05$) lower leukocyte count on day 7, compared to the control. Chitosan degraded from the wound surface after day 7.

PLCL and PTMC membranes were studied for urethral defects. PLCL and PTMC membranes were imaged using X-ray microtomography (μCT) to identify their surface structure. Isolated human urothelial cells were cultivated on PLCL and PTMC membranes to verify cell attachment, viability, and maintenance of urothelial phenotype. A live/dead cell assay was performed in order to determine cell attachment and viability by 7 and 14 days of cultivation. In addition, the relative expression of cytokeratins (CK) 7, 8 and 19, and uroplakins (UP) Ia, Ib and III were

studied after 2-week human urothelial cell cultivation on PLCL, PTMC or polystyrene (control).

In the PLCL group, cellular attachment was significantly higher on the first day ($p < 0.05$). In turn, the qualitative analysis showed more urothelial cells on PTMC membrane after the first week. Live/dead staining confirmed that the majority of urothelial cells were viable on both membranes. qRT-PCR revealed the expression of CK7, CK8 and CK19 on PLCL, PTMC and the control, whereas the expression of CK7 and CK8 was significantly ($p < 0.05$) higher among PLCL-cultivated cells. CK19 expression was significantly ($p < 0.05$) lower in the PLCL group compared to the control. The expression of UPIII was significantly ($p < 0.05$) higher in the control than PLCL. The expression of UPIb and also UPIII was significantly ($p < 0.05$) lower among PLCL-cultivated cells compared to PTMC by two weeks' cultivation.

An oval urethral defect was excised from rabbits' penile urethra. PLCL or PTMC membrane was sutured to cover the defect. After 2, 4 or 16 weeks' follow-up, the rabbits were anesthetized, defect sites were imaged (X-ray), and then excised for histological and immunohistochemistry analyses.

In urethral defects, PLCL membrane was harder than PTMC. Urethrographic examination revealed no signs of urethral strictures at any time points. In the histological analysis, the urothelium was continuous at the 16-week time point in both groups. The progression of urothelium structure towards stratification was significant ($p < 0.05$) within the PTMC group between 2- and 16-week time points. Cytokeratin staining demonstrated progression of *de novo* urothelium in both groups. Furthermore, both membranes degraded after the 4-week time point from the defect site.

Based on the findings, all four biomaterials were found to be biocompatible and have potential for full-thickness epithelial repair. AM and CM enhanced early-stage wound healing. CM was found to reduce inflammation and affect the IL-4 pathway, but it degraded from the wound surface after day 7. For urethral regeneration, PTMC was discovered to have better handling properties, and it developed significant epithelial integrity, but PLCL was also found to be suitable.

TIIVISTELMÄ

Ihon ja virtsaputken epiteelivauriot muodostavat merkittävän kliinisen ongelman ja kuorman sekä perusterveydenhuollolle että erikoissairaanhoidolle. Akuuttien ja kroonisten haavojen esiintyvyydeksi on arvioitu 3.7/1000. Virstaputken epiteelipuutokset muodostavat toisenlaisen epiteeliin liittyvän ongelman. Ongelmat aiheutuvat yleensä synnynnäisten epämuodostumien, vammojen tai tulehdusten seurauksena. Virtsaputken alahalkio (hypospadia) on yleisin peniksen synnynnäinen epämuodostuma, jonka esiintyvyysasteeksi on arvioitu 0.1-0.8%. Näiden ihoon sekä virtsaputkeen liittyvien ongelmien hoito on haastavaa.

Väitöskirjatutkimuksen tavoitteena oli arvioida biomateriaalikalvojen soveltuvuutta ihon ja virtsaputken korjaamisessa. Amnion- ja kitosaanikalvoa tutkittiin ihohaavoilla, kun taas poly(L-laktidi-co-ε-kaprolaktoni) (PLCL) ja poly(1,3 trimetyleeni karbonaatti) (PTMC) -kalvoja tutkittiin virtsaputken epiteelivaurioissa.

Amnion- ja kitosaanikalvojen soveltuvuuden tutkimiseksi rottien päälaelle tehtiin ihokerrokset läpäisevä haava. Haava mitattiin ja eläimet satunnaistettiin amnion- tai kitosaanikalvoryhmiin sekä vastaaviin kontrolliryhmiin. Haavat peitettiin joko amnion- tai kitosaanikalvoilla ja Aquacelilla tai pelkällä Aquacelilla (kontrolliryhmä). Eläimiä seurattiin 0, 3, 7, 14 tai 21 päivää, jonka jälkeen haavat ja tatuoinnit mitattiin uudelleen, kerättiin verinäytteet interleukiini 4 -määritystä sekä haava-alueet histologista analysointia varten.

Haavakoon mediaanit olivat kolmen päivän kohdalla merkittävästi ($p < 0.05$) pienemmät sekä amnion- että kitosaanikalvoryhmässä kuin kontrolliryhmässä. Kitosaaniryhmän interleukiini 4 -tasot olivat merkittävästi ($p < 0.05$) matalammat 7 ja 14 päivän kohdalla kontrolliin nähden. Tulos valkosolumäärien osalta oli samansuuntainen 7 päivän kohdalla. Kitosaanikalvo hävisi haavapinnalta 7 päivän jälkeen.

Virtsaputken epiteelivaurioihin testattiin PLCL- ja PTMC-kalvoja. PLCL ja PTMC -kalvot kuvattiin mikrotietokonetomografialla pintarakenteiden selvittämiseksi. Ihmisen uroteelisoluja viljeltiin PLCL ja PTMC -kalvoilla solujen kiinnittymisen, elinvoimaisuuden sekä uroteelisolujen fenotyypin säilyttämisen osoittamiseksi. Live/dead-värjäyksellä varmistettiin solujen kiinnittyminen sekä

elinvoimaisuus. Lisäksi sytokeratiini (CK) 7, 8 ja 19 sekä uroplakiinien (UP) Ia, Ib ja III ilmeneminen määritettiin PLCL ja PTMC -kalvoilla sekä polystyreenillä (kontrolli) tehtyjen soluviljelyiden jälkeen.

PLCL-ryhmässä solujen kiinnittyminen kalvoille oli merkittävästi ($p < 0.05$) parempaa ensimmäisenä päivänä PTMC-ryhmään nähden. Tosin uroteelisoluja havaittiin viikon kohdalla enemmän PTMC-kalvolla. Live/dead-värjäys vahvisti, että suurin osa kalvoilla viljellyistä soluista oli elinvoimaisia. CK7, 8 ja 19 ilmenivät kaikilla viljelypinnoilla. CK7:n ja CK8:n ekspressio oli merkittävästi ($p < 0.05$) korkeampi PLCL-kalvolla. CK19 ekspressio oli merkittävästi ($p < 0.05$) matalampi PLCL-ryhmässä kontrolliin nähden. Kontrolliryhmän ekspressio UPIII:n osalta oli merkittävästi ($p < 0.05$) korkeampi kuin PLCL-ryhmän. UPIb:n sekä UPIII ekspressio oli merkittävästi ($p < 0.05$) matalampi PLCL-kalvoilla viljeltyjen solujen osalta PTMC-ryhmään nähden kahden viikon kohdalla.

Kalvojen soveltuvuutta virtsaputkessa tutkittiin poistamalla kanin virtsaputkesta soikea alue, joka peitettiin PLCL tai PTMC -kalvolla. Eläimiä seurattiin 2, 4 tai 16 viikkoa, jonka jälkeen eläimet jälleen nukutettiin ja virtsaputket varjoainekuvattiin. Biomateriaalilla peitetty virtsaputken osa kerättiin talteen histologisia sekä immunohistokemiallisia määrityksiä varten.

PLCL-kalvon todettiin olevan kovempaa kuin PTMC-kalvon. Virtsaputken varjoainekuvauksissa merkittäviä kaventumia ei havaittu. Histologisessa analyysissä uroteeli peitti tehdyn epiteelipuutoksen jatkumona 16 viikon kohdalla molemmissa ryhmissä. Uroteelin kehitys kerrostuneeseen suuntaan oli merkittävästi parempaa ($p < 0.05$) PTMC-ryhmässä 2 ja 16 viikon kohdalla. Molempien kalvojen osalta sytokeratiinivärjäys vahvisti epiteelikerroksen uudelleenmuodostumisen ja kalvojen havaittiin hajoavan 4 viikon seuranta-ajan jälkeen.

Löydösten perusteella kaikki neljä biomateriaalia osoittautuivat kelvollisiksi epiteelivaurioiden korjaamisessa valituissa käyttötarkoituksissa. Amnion- ja kitosaanikalvot edistivät haavan paranemista varhaisvaiheessa. Kitosaanikalvon havaittiin vähentävän tulehdusreaktiota ja vaikuttavan IL-4-välittäjäainereittiin. Virtsaputken korjaamistarkoituksessa PTMC oli PLCL:iin verrattuna helpompi käsitellä, minkä lisäksi epiteelikerros eheytyi sen päällä merkittävästi nopeammin.

TABLE OF CONTENTS

ABBREVIATIONS

AM	Amniotic membrane
cDNA	Complementary deoxyribonucleic acid
CK	Cytokeratin
CM	Chitosan membrane
CO_2	Carbon dioxide
DNA	Deoxyribonucleic acid
DPBS	Dulbecco's Phosphate-buffered Saline
EDTA	Ethylenediaminetetraacetic acid
ECM	Extracellular matrix
HE	Hematoxylin-eosin
IL-4	Interleukin 4
µCT	X-ray microtomography
NaCl	Sodium chloride
NaOH	Sodium hydroxide
NPWT	Negative pressure wound therapy
OECD	The Organization for Economic Co-operation and Development
PCL	Polycaprolactone
PFA	Paraformaldehyde
PGA	Polyglycolide
PLA	Polylactide
PLCL	Poly(L-lactide-co-ε-caprolactone)
PTMC	Poly(1,3 trimethylene carbonate)
qRT-PCR	Quantitative real-time reverse transcription polymerase chain reaction
RNA	Ribonucleic acid
UP	Uroplakin
VEGF	Vascular endothelial growth factor
w/v	Weight/volume (mass concentration)

LIST OF ORIGINAL COMMUNICATIONS

This thesis is based on the following original publications, which in the text are referred to using Roman numerals I-III. The original publications have been reprinted with the permission of the copyright holders.

I. **Nordback PH**, Miettinen S, Kääriäinen M, Pelto-Huikko M, Kuokkanen H, Suuronen R. Amniotic Membrane Reduces Wound Size in Early Stages of The Healing Process. J Wound Care. 2012 Apr;21(4):190, 192-4, 196-7.

II. **Nordback PH**, Miettinen S, Kääriäinen M, Haaparanta A-M, Kellomäki M, Kuokkanen H, Seppänen R. The Effect of Chitosan Membrane on Wound Healing and IL-4 Levels on Experimental Full-Thickness Cutaneous Wound. J Wound Care. 2015 Jun;24(6):245-6, 248-51.

III. Sartoneva R*, **Nordback PH***, Haimi S, Grijpma DW, Lehto K, Rooney N, Seppänen-Kaijansinkko R, Miettinen S, Lahdes-Vasama T. Comparison of poly(L-lactide-co-ε-caprolactone) and poly(trimethylene carbonate) membranes for urethral regeneration: an *in vitro* and *in vivo* study. Tissue Eng Part A. 2018 Jan;24(1-2):117-127.

* Contributed equally in the study

1 INTRODUCTION

Epithelium, one of the four basic tissue types, is our armor against various external threats. Epithelium covers the body's outermost layer, but also lines cavities, vascular and respiratory systems, urinary and gastrointestinal tracts, and glandular and reproductive systems, and covers our organs (Ross et al. 2010). Epithelia are not merely passive barriers against physical, chemical or biological threats, but also have multiple, specialized, and interacting functions. Epithelial cells act as gatekeepers allowing selective transfer for maintaining homeostasis, possess secretive actions, and provide sensation (Betts et al. 2018). Epithelial tissues can be classified according to their shape (squamous, cuboidal or columnar) and cellular layer structure (simple, stratified or pseudostratified) (Ross et al. 2010). Skin, our largest organ, is a good example of an epithelium, with a stratified squamous outmost layer, accompanied by two other distinctive layers possessing multiple crucial functions (Proksch et al. 2008). On the contrary, transitional epithelium (i.e. urothelium) is impermeable to salts and water, demonstrating how versatile epithelial tissues are (Holstein et al. 1991, Ross et al. 2010).

At times, the external burden exceeds our epithelial tolerance, causing an epithelial defect which triggers a complex healing cascade. Wound healing, for instance, is a multistage cascade including the collaboration of several different cell types and signal pathways (Martin 1997). Acute wounds can vary from precisely planned, small surgical incisions performed under optimal conditions, to excessively contaminated open wounds (Leaper and Harding 2006). Wound healing - even under optimal conditions - can become impaired, leading to a chronic wound (Werdin et al. 2009). Prolonged pressure, vascular problems and diabetes are the three most common factors contributing to the development of chronic wounds (Mustoe et al. 2006). The etiology has a major impact on treatment, and chronic wounds in particular often require special attention. Thus, preventive action cannot not be overlooked. Acute and chronic wounds altogether constitute a major dilemma to society and, of course, on an individual level, as well. The prevalence of patients with at least one acute or chronic wound has been estimated to be 3.7/1,000 (Posnett et al. 2009). Wounds comprise a burden to basic and special healthcare, causing estimated annual costs of €100–200 million in Finland alone (Jokinen et al. 2009).

On an individual level, wounds cause human suffering, decreased life quality and financial cost. These lend impact to the research of wound healing.

Beside skin wounds, the focus in this thesis was on urethral defects, an example of an epithelium-related clinical problem. Congenital defects, traumas and infections cause urethral defects. Hypospadias - a condition in which the urethra opens in an abnormal position - is among the most common congenital problems of the male reproductive system (Donaire & Mendez 2018). Its incidence in Finnish population (approx. 5.5 million) is approximately 100 new hypospadias annually (Jalanko 2017). The etiology of hypospadias is unclear, but genetical, endocrine and environmental factors are related to its incidence (Donaire & Mendez 2018). The treatment of hypospadias is surgical, but several complications, such as fistulas, strictures and diverticulas, remain major clinical problems (Keays & Dave 2017). Limited autologous grafts, donor site morbidity, and poor long-term outcome are also challenges in treating urethral defects (Orabi et al. 2013). Thus, there is a clinical need for new approaches, and tissue engineering has been suggested to have answers for novel urethral reconstruction.

The general development of biomaterials is a major theme of regenerative medicine. An optimal biomaterial should promote cell attachment, maintenance, proliferation, and differentiation, and provide structural and mechanical support. It should also possess qualities such as favorable host response, controllable biodegradability, suitable surface chemistry, low toxicity, and interconnecting pores (Patel et al. 2011, Keane & Badylak 2014). In addition, availability, ethical, and cost-effectiveness issues should also be considered.

AM is the innermost fetal membrane and has been under scientific investigation for over a century (Davis 1910). Anti-inflammatory, anti-angiogenic, antimicrobial and re-epithelializing characteristics, low immunogenicity, and affordability are all qualities which make AM a potential biomaterial in tissue engineering (Lo & Pope 2006). Recently, AM has been widely used in variable clinical practices in ophthalmologic surgery (Dua et al. 2004). As a dermatological application, AM has been studied in relation to its use for treating burns, chronic ulcers, epidermolysis bullosa and Stevens-Johnson syndrome (Lo & Pope 2009). Its known versatility has extended the field of AM research to specialties such as gynecology, gastrointestinal and thorax surgery (Trelford & Trelford-Saunder 1979, Mhaskar 2005, Gharib et al. 1996, Muralidharan et al. 1991). However, the precise mechanisms behind its effects have remained unclear, and most studies relate to ophthalmological applications.

Chitin is the world's second most common polysaccharide, extensively available from invertebrate skeletons and fungal cell walls (Younes & Rinaudo 2015). Chitosan

can be derived from chitin by chemical or enzymic deacetylation (Synowiecki & Al-Khateeb 2003). It is biocompatible, biodegradable, nontoxic, antimicrobial and hydrating (Jayakumar et al. 2011). These properties make chitosan an interesting material for use in regenerative medicine. Chitosan is known to have potential as a wound healing agent, but the mechanisms behind this are only partly known (Paul and Sharma 2004). The modifiability of chitosan from fibers to hydrogels, membranes, scaffolds and sponges, offers a wide range of possible applications (Pillai et al. 2009, Jayakumar et al. 2011). Beside dermatological applications, chitosan has been under investigation for treating nerve, cartilage and bone defects, and as a drug delivery system (Muzzarelli et al. 2009, Ahsan et al. 2017).

Polycaprolactone (PCL) is one the most widely used aliphatic polyesters in medical science (Fernandez et al. 2012). PCL can be copolymerized with various other polymers in order to alter its properties (Labet & Thielemans 2009). The copolymerization of PCL with lactide (PLCL) increases its ability to absorb water and degrade, affecting its mechanical, shape-memory, and drug-releasing properties, and making them more favorable for regenerative medicine applications (Fernandez et al. 2012). PLCL has been studied in a variety of applications, including for dermal, esophageal, vascular, bone, tendon, cartilage and nerve regeneration purposes (Im et al. 2018, Zhu et al. 2007 Shafig et al. 2015, Yassin et al. 2016, Vuornos et al. 2016, Jung et al. 2008, Wang et al. 2018). In urothelial tissue engineering, PLCL has been shown to be suitable for human urothelial cell attachment and proliferation (Sartoneva et al. 2011).

PTMC is an elastic aliphatic biocompatible polycarbonate ester (Shi et al. 2009). It can also be copolymerized with other polymers, such as PCL (Papenburg et al. 2009). The degradation of PTMC remarkably increases *in vivo*, compared to *in vitro*, due to enzymatic and macrophage-derived erosion (Bat et al. 2009). PTMC's stable construct and modifiable degradation rate offers ideal biomedical applicability. Thus, PTMC has been investigated for cardiovascular, nerve and bone regeneration, intra-abdominal adhesion reduction, and ophthalmological and dermal purposes (Song et al. 2011, Rocha et al. 2014, Vogels et al. 2015, Amsden & Marecak 2016, Han et al. 2009). PTMC has not been previously investigated for urethral regeneration.

2 REVIEW OF THE LITERATURE

2.1 Skin structure and function

Skin is composed of various layers (Figure 1). The main layers are epidermis and dermis, but the subcutaneous layer - also referred as hypodermis, underneath the dermis - can also be counted as a skin layer, due to its participation in skin functions.

Human skin has multiple appendages with different specific functions. Hair, nails, sweat glands, sebaceous glands, and neural structures can all be considered as skin appendages. Sweating has thermoregulatory and homeostatic roles in skin function. The sebaceous glands secrete sebum, an oily substance which lubricates the skin, making it water resistant, and lowering friction (Makrantonaki et al. 2011). Sebum also transports antioxidants, protects against natural light, and possesses antibacterial, pro- and anti-inflammatory functions (Makrantonaki et al 2011). Skin also contains two kinds of sensory nerves: free nerve endings and encapsulated nerve endings (Ross et al. 2010). There are four types of encapsulated nerve endings, each conducting different information: Merkel's cells (sensory), and Pacinian (pressure and vibration), Meissner's (touch) and Ruffini's (mechanical displacement) corpuscles (Ross et al. 2010).

Skin comprises 15–20% of total body mass, though the amount can vary considerably between individuals, due to different amounts of fat-rich hypodermis (Ross et al. 2010). Being the biggest organ and the outer covering of the body, it has several important functions. The most important function of the skin is to form a barrier between the organism and its surroundings (Proksch et al.2008). Skin also provides immunologic information, participates in homeostasis, produces sensory information, has endocrine functions, and takes part in excretion (Ross et al. 2010). If the skin gets injured, the dysfunction of these key missions can lead into life-threatening situations.

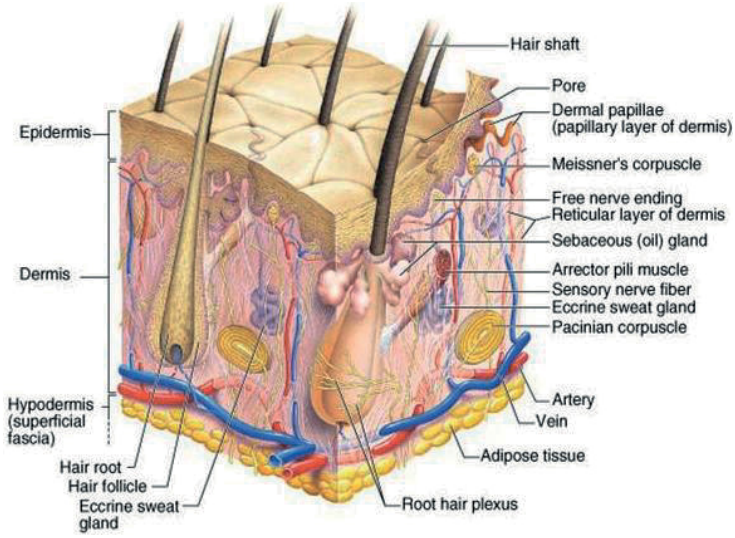

Figure 1. Normal skin structure (www.slideshare.net/bryndanair/skin-ap).

2.1.1 Epidermis

The epidermis - the outermost layer - is constituted of four distinctive sublayers (Figure 2). Listed from the bottom to the top: stratum basale or germinativum, stratum spinosum, stratum granulosum and stratum corneum. In palmoplantar skin, an additional zone between the corneum and granulosum also exists (Burns et al. 2008). The keratinocytes of the stratum lucidum are dead, flattened, and rich with eleidin protein, which gives the cells a transparent appearance and provides a water barrier (Betts et al. 2018). Within the epidermis there are keratinocytes, melanocytes, Langerhans' cells and Merkel's cells, but the dominant cell type is distinctly the keratinocyte.

The keratinocytes of the stratum basale are mitotically active and responsible for epidermal cell renewal and connectivity to the underlying basal lamina, keeping the epidermis at its place (Ross et al. 2010). The stratum basale, hair follicles and sweat glands possess epithelial progenitor cells, crucial for wound healing (Janis & Harrison 2016).

Melanocytes are also scattered within the stratum basale, where they produce and deliver melanin to adjacent keratinocytes. The functions of melanin are thermoregulation, camouflage, and protecting against ultraviolet radiation (Weiner et al. 2014). Melanin also dyes skin hair.

In addition to keratinocytes and melanocytes, Merkel's cells colonize the stratum basale. They are closely associated with the nerve fibers penetrating the epidermis, and together they produce sensory information (Ross et al. 2010).

In the stratum spinosum, the keratinocytes mature and move toward the surface. During maturation, their size increases and they start flattening in shape. The keratinocytes begin producing numerous keratohyalin granules when they reach the stratum granulosum. These contain cystine- and histidine-rich proteins, which induce the aggregation of keratin filaments, eventually leading to cell keratinization (Burns et al. 2008).

The highly differentiated keratinocytes of the stratum corneum are anucleate squamous cells full of keratin filaments. The terminally differentiating keratinocytes produce an insoluble protein surface inside their plasma membrane, and a lipid layer outside their plasma membrane, in order to compose a water-barrier responsible for body homeostasis (Ross et al. 2010).

The epidermis comprises the physical and chemical/biochemical barrier, but it is an adaptive immunological barrier (Proksch et al. 2008). Langerhans' cells located in the stratum spinosum act as antigen-presenting cells creating the immunological barrier (Ross et. al 2010).

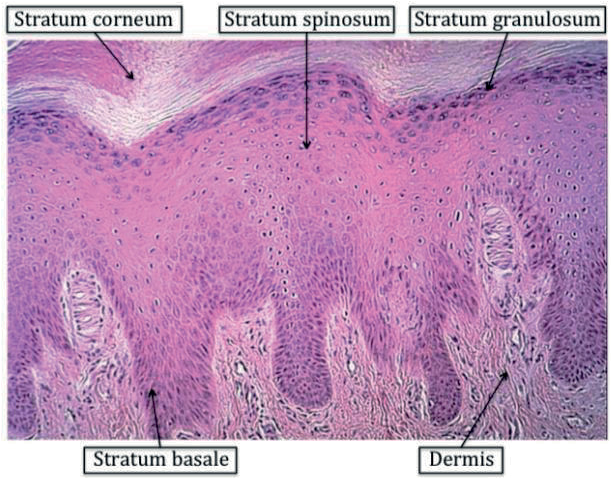

Figure 2. Microscopical image (HE staining) of the four distinctive epidermal layers and the dermis. The stratum lucidum is part of the stratum corneum, only found in skin on the palms of hands and soles of feet (not visible in the represented image). Image modified from an image from a free image database (www.studyblue.com).

2.1.2 Dermis

The papillary and reticular layers are the distinct sublayers of the dermis. The papillary layer, which is located just under the epidermis, consists of loose connective tissue, blood vessels, and nerve endings. The papillary layers' dermal papillae form a wavy border with the epidermis' epidermal ridges, protruding into the dermis. Collagen and elastic fibers compose a network giving the dermis tenacity. Blood vessels serve the avascular epidermis and the dermis itself. Sensory nerve endings produce sensory information from the surrounding environment (Ross et al. 2010).

The reticular layer of the dermis is thicker and less cellular than the papillary layer. It is comprised of thick, organized collagen, and elastic fibers, which form regular lines, called Langer's lines, visible to the naked eye, and giving our unique fingerprint and footprint patterns (Ross et al. 2010). The collagen and elastic fibers of the dermis give the skin its tensile strength. Considering wounds or surgery, Langer's lines are remarkable because incisions parallel to Langer's lines form smaller scars than incisions perpendicular to the lines. Dermal repair requires removal of the damaged collagen due to macrophage activity followed by fibroblast proliferation with production of new collagen and other extracellular matrix (ECM) components (Ross et al. 2010). Resulting scar tissue has a poorly organized collagen matrix and reduced mechanical durability compared to healthy skin structure (Martin 1997).

2.1.3 Subcutaneous layer (hypodermis)

Underneath the dermis, lies the subcutaneous layer, or hypodermis. Subcutaneous layer consists of adipose and connective tissue (Ross et al. 2010), and as an insulating tissue, has a role in body temperature regulation, and as an energy reservoir. Nutritional habits and other environmental factors have an impact on the amount of adipose tissue in the subcutaneous layer. Approximately 75% of all energy reservoirs of the body are stored in adipose tissue in the form of triglycerides, and although adipose tissue can be found internally - for instance in bone marrow, the greater omentum and retroperitoneal space - the subcutaneous layer stores a remarkable proportion of this (Aro et al. 2007, Ross et al. 2010).

2.2 Wound healing

Sometimes the burden from the external environment exceeds our tolerance, skin gets damaged and a wound results. If the wound is big or deep enough, there is a risk that - even under optimal conditions - the wound does not heal properly, and becomes chronic.

Wound healing can be divided into four different stages: hemostasis, inflammation, proliferation and maturation, or remodeling (Janis and Harrison 2016). Wound etiologies vary from acute to chronic. The etiology of the wound has a major impact on the correct selection of an appropriate treatment.

2.2.1 Wound etiologies

Acute wounds

Acute wounds can be classified as surgical incisions, lacerations, large open wounds and abrasions (Leaper and Harding 2006). Surgical incisions differ from traumatic wounds because they are planned to cause minimal tissue damage. Nevertheless, some forms of surgery - e.g. oncologic surgery - can result in excessive skin deficit, and need for special reconstructive management (Lee and Hansen 2009). Despite various techniques being used to reduce infection risk, bleeding, and deeper tissue damage, additional damage can still result, and wounds can become contaminated. A noteworthy example of a contaminated wound is a bite wound. An incision, whether surgical or traumatic, results in a penetrating wound, whereas laceration results in torn tissue, contusion to extensive tissue damage, and abrasion to a superficial epithelial wound (Leaper and Harding 2006). A wound can also consist of a combination of these wound types, and differ, depending on a vast variety of causes, such as punctures, gun shots and explosions, for instance.

Burn wounds are also a type of acute wound caused by heat, radiation, friction or electricity. The severity of burns is quantified according to the percentage of the total body's surface area burned, as well as burn depth, which are the primary prognostic indicators for mortality and morbidity. Burn depth can be classified as first- (superficial), second- (partial thickness), or third-degree (full-thickness) (Martin and Falder 2017). Various chemical substances can also cause wounds, typically considered to be burn wounds (Lee and Hansen 2009). Severe frostbite injuries of

the skin are also temperature caused wounds that can occur due to natural or iatrogenic origin (Lee and Hansen 2009).

Chronic wounds

Healing of an acute wound can become impaired, resulting in a delayed state of healing. Local and systemic factors such as hypoxia, wound infection, smoking, diabetes, nutritional deficiency, and certain drugs can all be associated with impairment of wound healing (Janis & Harrison 2016). Werdin et al. defined chronic wounds as wounds which have failed to proceed through an orderly and timely reparative process, to produce anatomic and functional integrity over a period of three months (Werdin et al. 2009). The definition of a chronic wound varies in the literature, and even 4–6-week old wounds can be classified as chronic (Lee and Hansen 2009). The main causative factors in chronic wounds are thought to be related to local tissue hypoxia, bacterial colonization, repetitive ischemia-reperfusion injury, or altered cellular and systemic stress responses in the elderly (Mustoe et al. 2006). Pressure ulcers, vascular ulcers, and diabetic ulcers are the three major types of chronic wounds, covering more than 90 percent of all chronic wounds (Mustoe et al. 2006).

Pressure ulcers are localized skin injuries primarily caused by prolonged or remarkable pressure. They manifest especially over bony prominences. High-risk patients for pressure ulcers are immobile, neurologically impaired (for instance paraplegia patients), and have poor nutritional status (Werdin et al. 2009). Pressure wounds may also appear in a more acute manner after sudden immobilization, such as intoxication or prolonged surgical operations.

Venous ulceration is caused by venous hypertension, which usually results from insufficient capability of venous valves in lower extremities to prevent blood reflux. Varicose veins, deep vein thrombosis, chronic venous insufficiency, poor calf muscle function, arterio-venous fistulae, obesity, and previous leg fracture are direct risks for venous ulceration (Grey et al. 2006). Arterial ulceration is caused by poor arterial blood flow, and often occurs after minor trauma or pressure. It is important to distinguish venous ulcers from arterial ulcers, due to different treatments. A stereotypic arterial ulcer is dry, necrotic and painful, and the surrounding skin is hairless, erythematous, atrophic, cold and pulseless (Chronic leg ulcers: Current Care Guidelines 2017). The risk factors for arterial ulceration are similar to atherosclerotic disease, such as smoking, hyperlipidemia, hypertension, obesity, diabetes, decreased activity, and genetics (Grey et al. 2006).

The primary risk factor predisposing to diabetic leg ulcer is peripheral neuropathy, but age, hyperglycemia, duration of diabetes, arterial disease, renal disease, visual impairment, and deformities also influence the course of ulceration (Neville et al. 2016). Risk factors relating to repetitive high vertical or shear stress lead eventually to ulceration (Armstrong et al. 2017). It has been estimated that globally, 6.3% of diabetics develop foot ulcers each year, and $60 billion is spent annually in the United States alone on curing them (Armstrong et al. 2017). Every 20 seconds, a lower limb is lost somewhere in the world due to diabetic leg ulcer, and diabetic foot infection is the most frequent disease-related complication leading to hospitalization (Grigoropoulou et al. 2017). Diabetic leg ulcers can thus be said to be common, complex and costly.

Diseases such as sickle cell disease, malignancies, pyoderma gangrenosum, Wegener's granulomatosis, monoclonal IgA gammapathies, and bacterial or fungal etiologies cause chronic ulceration (Wound Healing Society 2006). Also, lymphedema patients are at risk of developing chronic ulceration (Fife et al. 2017).

2.2.2 Stages of wound healing

Hemostasis

The hemostasis stage of wound healing begins seconds post-injury, and lasts in the order of several minutes (Janis et al. 2010). An injury damages vascular endothelium, exposing the basal lamina, and leading to platelet aggregation (Janis & Harrison 2016). The clotting cascade results in fibrin clot formation, and eventually ends extravasation (Buchanan et al. 2016). The injury also releases thromboxane and prostaglandins, which cause local vasoconstriction to enhance hemostasis (Janis et al. 2010). Simultaneous growth factor release starts ECM deposition, chemotaxis, epithelialization, and angiogenesis (Janis & Harrison 2016). Hemostasis has previously been described as being part of the inflammation stage, but recently has been referred to separately. The hemostasis stage is summarized in Figure 3.

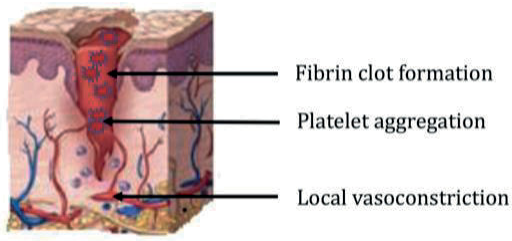

Figure 3. Illustration of the hemostasis stage of wound healing. Image modified from Jeschke & Rogers 2016.

Inflammation

The inflammation stage takes place 1–2 days after injury (Janis & Harrison 2016). It is characterized by leucocyte infiltration, in which neutrophils and monocytes use the blood clot formed by platelet activation as a scaffold from which to invade the wound (Buchanan et al. 2016). Fibroblasts and endothelial cells also target the area (Buchanan et al. 2016). The release of histamine, serotonin, kinins and bacterial products causes vasodilatation, and gains capillary permeability, which leads to local edema (Janis et al. 2010). At the injury site, monocytes transform into tissue macrophages, which debride injured tissue, and secrete cytokines and growth factors which promote fibroblast proliferation, angiogenesis, and keratinocyte migration (Janis & Harrison 2016). Macrophages also have a role in neutrophil apoptosis, which prevents the neutrophils from prolonging the inflammatory stage (Janis & Harrison 2016). Macrophages also produce wound healing-promoting growth factors (Janis et al. 2008). Inflammation is important in contamination control and proliferative stage induction, the role of which is to progress wound healing, instead of it entering unwanted chronic ulceration (Janis et al. 2010). The inflammation stage is summarized in Figure 4.

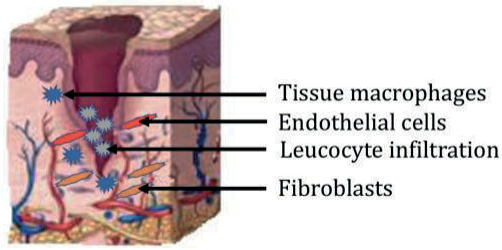

Figure 4. Illustration of the inflammation stage of wound healing. Image modified from Jeschke & Rogers 2016.

Proliferation

The proliferation stage follows the inflammation stage, and persists for up to 14 weeks (Buchanan et al. 2016). Epithelialization, angiogenesis and provisional matrix formation by fibroblasts are characteristic of this phase (Buchanan et al. 2016). The primary wound site - constituted of fibrin and fibronectin - is supplemented by fibroblast-produced glycosaminoglycans, proteoglycans, and other proteins (Janis et al. 2008). Fibroblasts secrete disorganized collagen (mainly type III) into the formed provisional matrix (Janis et al. 2010). Some wound site fibroblasts differentiate to myofibroblasts, which cause wound contraction (Janis et al. 2010).

The proliferative phase requires increased oxygen and nutrition supply to the wound (Janis & Harrison 2016). If the wound site is poorly perfused, it leads to low oxygen and high lactate levels, which also stimulate angiogenesis (Janis et al. 2010). Angiogenesis, a crucial part of the proliferation stage, is promoted by fibroblast, platelet-derived and vascular endothelial growth factors (VEGF) (Janis & Harrison 2016).

Epithelialization is conducted by the epithelial cells at the wound edge and/or by progenitor cells located in the adnexal structure, such as hair follicles, if they manage, from the primary injury (Buchanan et al. 2016). Epidermal, fibroblast and transforming growth factors, along with multiple cytokines, initiate epithelialization, in which keratinocytes detach and mitotically divide (Janis & Harrison 2016). In the proliferative stage, fibroblasts produce granulation tissue and initiate wound contraction (Buchanan et al. 2016). Epithelialization continues upon epithelial migration and proliferation until an intact epithelial barrier is formed (Janis et al. 2010). A moist environment promotes epithelialization (Janis et al. 2010). The proliferation stage is summarized in Figure 5.

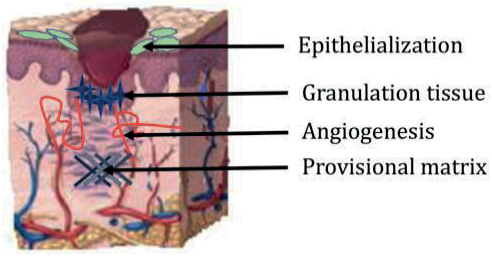

Figure 5. Illustration of the proliferation stage of wound healing. Image modified from Jeschke & Rogers 2016.

Maturation and remodeling

The maturation and remodeling phase should result in a quickly healed wound and minimally visible scarring (Janis & Harrison 2016). The remodeling stage takes up to one year from injury (Janis et al. 2008). Newly deposited collagen is reorganized and the number of cellular components is reduced from the wound surface (Buchanan et al. 2016). Type III collagen produced in the proliferative stage is replaced by stronger type I collagen, and collagen organization occurs (Janis et al. 2010). In the remodeling stage, the tensile strength of the wound site increases. It has been estimated that three months after injury, the tensile strength might recover to around 80% of that of the original uninjured skin site (Janis et al. 2008). The maturation and remodeling stage are summarized in Figure 6.

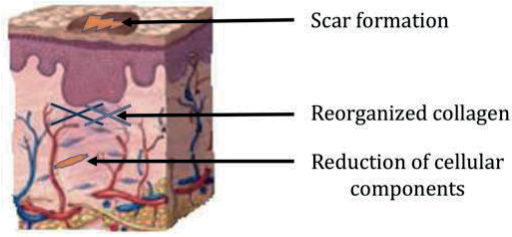

Figure 6. Illustration of the maturation and remodeling stage of wound healing. Image modified from Jeschke & Rogers 2016.

2.2.3 Cytokine IL-4

Wound healing is modulated by several cytokines, such as endothelial, fibroblast, and platelet derived growth factors, and interleukins 1, 8 and 10 (Janis & Harrison 2016). Cytokine IL-4 also has a role and is produced by activated $CD4^+$ T cells (Wills-Karp & Finkelman 2015). In the skin, $CD4^+$ T cells are located in close association with hair follicles, interfollicular dermis and epidermis. $CD4^+$ T cells are a subgroup of immune cells that mainly arise during thymic T-cell maturation that suppress pathogenic immune responses maintaining tissue homeostasis (Ali & Rosenblum 2017).

IL-4 enhances anti-inflammatory and reduces pro-inflammatory cytokines (Varin & Gordon 2009). It affects macrophage activity and increases ECM remodeling and angiogenesis (Wills-Karp & Finkelman 2015, Varin & Gordon 2009). IL-4 is related to keratinocyte differentiation and is thought to impair wound healing response by

decreasing fibronectin production in atopic dermatitis (Serezani et al. 2017). Fibronectin is a crucial glycoprotein that plays many roles in wound healing. Its main role is in ECM formation (Lenselink 2015). IL-4 is thus one of the cytokines related to inflammation and proliferation stages of wound healing.

2.2.4 Wound treatment

The management of wounds differs, depending on whether they are surgical incisions made under optimum conditions, or major traumatic wounds with serious damage of the underlying tissues. Chronic wounds often require special attention. Preventive management of risk factors that cause chronic wounds has individual and public importance. Pressure wounds, for instance, cause major costs, and prevention is more cost-effective than treatment (Tran et al. 2016). Wounds can also be classified by thickness, complexity, age and origin (Patrulea et al. 2015).

The Wound Healing Society has promoted the "TIME" acronym, where T stands for tissue, I for inflammation or infection, M for moisture balance, and E for wound edge quality (Werdin et al. 2009). These four issues should be assessed in order to optimize local wound healing conditions. Chronic wounds have especially multifactorial etiologies, and thus single-agent therapies are often considered ineffective (Mustoe et al. 2006). Wound infection is thought to impair all phases of the wound-healing cascade; decreases tissue oxygenation, prolongs the inflammatory phase, impairs angiogenesis and breaks down formed collagen, and thus has important clinical relevance (Lee and Hansen 2009). If the wound is suspected to be infected, a swab culture should be taken from wound or exudate to identify infective pathogens.

Treatment of acute wounds

Arterial, venous or capillary bleeding should be controlled, and the infection risk reduced with cleansing, debridement and use of prophylactic antibiotics, combined with tetanus prophylaxis in selected cases (Leaper and Harding 2006). Minor scratches usually heal without special attention, but it is always rational to attempt to prevent a wound, if possible. Methods to reduce the risk of trauma and choosing appropriate protective equipment prevent wounds. Factors associated with increased falling risk are also associated with wounds and can be prevented by focusing on reducing the risk of falling (Cheung 2016).

The incidence of acute burn wounds in developed countries has decreased with preventive acts such as fire-safe cigarettes and legislation, but worldwide burn injuries still remain a major source of death and disabilities (Bezuhly & Fish 2012). Minor burns can be treated with adequate debridement and dressing (Grunwald & Garner 2008). The clinical guide for sufficient debridement is based on the "three Ps": pale yellow fat, pearly white dermis, and patient vessels (Bezuhly & Fish 2012). Basic burn injury treatment also depends upon good nutritional status, sufficient pain control, and re-evaluation to examine healing progression and signs of infection (Grunwald & Garner 2008). For major burns, fluid resuscitation, antibiotic prophylaxis, surgical debridement and wound coverage using full- or split-thickness grafts, cultured epithelial cells or skin substitutes constitute the basis for treatment (Grunwald & Garner 2008). The treatment of major burns is challenging and is thus generally centralized at specialized centers.

Sutures, staples or adhesives, such as tissue glue or tapes can be used for wound closure (Hsiao and Council 2017). Sutures are the standard closure method. Several suture techniques and materials are available, from non-absorbable to absorbable sutures with different needles, length, construction, etc. The "golden period" for acute wound closure has been traditionally defined as 6 hours, based on laboratory and clinical studies (Lee and Hansen 2009). Due to practical realities, such as delayed patient presentation or operating room time, the "golden period" has to be discretionarily stretched. A simple wound can normally be closed primarily, but larger wounds require exploration, where vitality of skin, subcutaneous, muscle and bone tissue are assessed, and blood vessel and nerve damages examined (Lee and Hansen 2009). Devital, infected or necrotic tissue should be debrided.

Primary wound closure is not always purposeful and secondary intention should be considered. The advantage of secondary intention is that it does not have potential donor site morbidity compared to surgical inventions such as skin grafting (Buchanan et al. 2016). Adequate debridement is crucial, especially if the wound is left open. Wounds to be considered for open management are (Leaper and Harding 2006):

- Wounds caused by kinetic energy (such as explosions or gunshot)
- Devitalized tissue, due to poor perfusion
- Severely contaminated wounds
- Old (> 12–24 h) lacerations
- Shock of any etiology (usually hemorrhagic)
- Wounds containing foreign body (removal)

Treatment of chronic wounds

In chronic wounds, the most relevant part of the treatment is identifying and treating the etiology behind the wound, such as pressure, diabetes, venous insufficiency or arterial perfusion (Werdin et al. 2009). Systemic factors should also be noticed and taken care of if poor nutrition, infection or immunosuppression is noticed.

Patient positioning, special mattresses, pressure-relieving cushions and good nutritional condition are key components of pressure ulcer prevention. Poor glycemic control amongst diabetics should be taken care of. Rather than new, expensive therapies, prevention is preferable when treating diabetic leg ulcers, which can be managed following early recognition of peripheral neuropathy (Grigoropoulou et al. 2017).

In venous ulceration management, the keystone is compression, which increases the limbs hydrostatic pressure and decreases venous hypertension. Compression can be created using various compression bandage systems or even pneumatic devices, but compression stockings are the most used method. Ulcer revision, ulcer excision and skin grafting or correction of the superficial venous disease are surgical interventions that can be considered (Grey et al. 2006). Surgical interventions might decrease the recurrence rate of venous leg ulcers (Chronic leg ulcers: Current Care Guidelines 2017). Before surgical interventions, the patient's status should be stabilized and the wound environment optimized. Systemic factors, such as diabetes, smoking, nutrition and medications (especially exogenous steroids), and local factors, such as tissue oxygenation, infections, necrotic tissue, tissue perfusion, neoplasms, chemo- and radiation therapy should be taken under consideration in preceding surgical optimization (Myers et al. 2007).

Lower extremity ulcers should always be suspected for arterial disease, particularly among elderly patients with atherosclerotic risk factors, such as smoking, diabetes, hypertension, hypercholesterolemia or obesity (Wound Healing Society 2006). Wounds caused by arterial disease should be evaluated in special healthcare by a vascular surgeon for the possibility of limb revascularization (Chronic leg ulcers: Current Care Guidelines 2017). Wound etiology can also be a combination of venous ulceration and arterial disease.

Wound dressings

Wound dressings enhance local conditions, decrease healing time, provide cost-effective care and improve quality of life, if chosen correctly (Britto and Morrison

2017). An optimal wound dressing should decrease pain, apply hemostasis, protect the wound, prevent fluid loss, immobilize the injured area and promote wound healing. Wound dressing selection criteria are summarized in Table 1. Currently there are several hundred wound dressing options (Britto and Morrison 2017). The dressings can broadly be classified as interactive, active and passive dressings, based on their function (Chronic Leg Ulcers: Current Care Guidelines 2017). Interactive dressings aim for optimal wound site moisture, and are activated by exudates or added fluids. Active dressings contain bioactive material, such as growth factors or glycosaminoglycans, to promote wound healing. Passive dressings do not contain such additional material. Their function is to protect, absorb and prevent other dressings from attaching to the wound site.

Table 1. Wound dressing selection criterion (table based on Chronic leg ulcers: Current Care Guidelines 2017).

Wound type and coloration	Principle	Dressing
Epidermal wounds Pink	Protect wound surface	Lightly adhesive dressing protecting epithelial layer
Granulation tissue Red	Protect wound regeneration Keep wound surface moist	Moist wounds: absorb exudates Dry wounds: retain moist environment
Hypergranulation Light red Bottom protruding over wound surface	Remove hypergranulation and/or handle with silver nitrate	Light airy dressing
Fibrin coating Yellow	Soften and/or remove coating	Moist wounds: absorb exudates Dry wounds: retain moist environment
Necrotic tissue Black	Debride necrotic tissue	Moist wounds: absorb exudates Dry wounds: retain moist environment
Tendon and bone Light Hard or tendinous	Keep moist - do not allow bone or tendon to dry	Retain moist environment
Infected Redness, swelling, increased temperature, pain, exudates	Reduce bacterial contamination	Antibacterial, non-occlusive and absorbing dressings

Negative pressure wound therapy

Negative pressure wound therapy (NPWT) has achieved acceptance especially in secondary intention and clean chronic wounds, but it can also be considered for acute surgical wounds, diabetic foot ulcers, and prior to skin grafting or dermal substitutes, although it lacks consistent evidence (Buchanan et al. 2016). Mustoe et al. discussed a hypothesis that the positive effect of NPWT is based on: 1) reduced bacterial counts by exudate removal; 2) reduced edema, which enhances oxygenation

and nutrition; 3) preventing patient from adding pressure to the wound; and 4) drawing mesenchymal progenitor cells to the wounds surface, due to increased circulation (Mustoe et al. 2006). NPWT also seems to remove local inflammatory mediators, suppress maceration, and decrease wound closure time, complication rates, hospitalization time and costs (Buchanan et al. 2016). NPWT is nowadays well-established in clinical practice.

Reconstructive approaches

Wounds from different etiologies, such as trauma or oncological surgery, can primarily present major tissue deficiency, and thus reconstructive techniques should be considered. It has been estimated that a full-thickness wound of more than 4 cm does not heal without grafting (Vig et al. 2017). The anatomical location also influences the treatment decision. Reconstructive wound closure techniques can be systematically approached according to the "reconstructive ladder", on which reconstruction options proceed from simpler to more complex techniques (Figure 7). Sometimes it is appropriate to bypass techniques to obtain a more functional reconstruction, which is referred as the reconstructive elevator, rather than ladder (Buchanan et al. 2016).

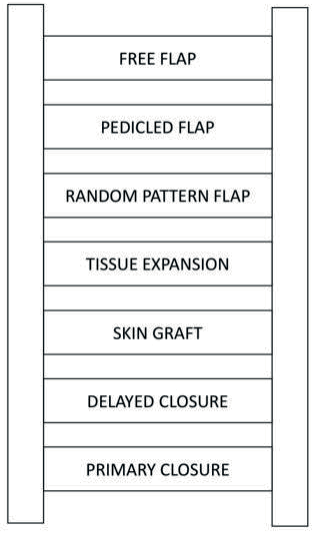

Figure 7. The reconstructive ladder.

Skin grafts can be used for wound construction in multiple situations, such as traumatic wounds, burns, scar contracture release, hair restoration, vitiligo, and for congenital or oncological skin deficiencies, but in more complex wounds they are normally avoided (Shimizu and Kishi 2012). Skin grafts can be classified as full-thickness, including the entire dermis, or split-thickness grafts. Split-thickness grafts contain only a portion of the dermis and can be further classified into mesh, stamp and chip skin grafts (Shimizu and Kishi 2012). Full-thickness grafts are usually used for small defects, whereas split-thickness skin grafts are used to cover moderate or large defects. Full-thickness grafts can be taken from auricular, nasolabial, supraclavicular, groin and lower abdominal regions, or from the eyelids or neck, whereas split-thickness grafts can be harvested from any area of the body, though anterior thigh remains as most commonly used donor site (Shimizu and Kishi 2012). From an aesthetical viewpoint, the donor site should be similar to the recipient site in skin consistency, thickness, color and texture.

Tissue expansion with an expander is also an option to reconstruct soft tissue defects, where it can provide matching color, texture and contour to the defect (Buchanan et al. 2016). In tissue expansion, nearby skin is first mechanically overstretched to provide sufficient coverage of the defect.

Random pattern, pedicle or free flaps, defined by their vascular supply, can also be used reconstructing skin defects. Local flaps consist skin and underlying subcutaneous tissue and provide suitable coloration, sensation and thickness to cover the defect (Buchanan et al. 2016). Z-plasty, bilobed and rhomboid flaps and V-Y-advancement are traditional examples of local (random) flaps. Regional or distant (pedicle) flaps can be considered if additional tissue coverage is needed. Muscle and musculocutaneous flaps are commonly considered for extremity, head, neck and trunk reconstruction, whereas fascial and fasciocutaneous flaps suit for more superficial reconstruction (Buchanan et al. 2016). Perforator flaps consist of skin and subcutaneous tissue, but not necessarily the underlining fascia and muscle, but they are technically more demanding (Buchanan et al. 2016). Free tissue transfer is preferred if local reconstructive options are negatively affected by the injury zone (Buchanan et al. 2016).

Dermal substitutes

If the patient has extensive wounds with insufficient donor site availability, dermal substitutes can be considered. There are three kinds of dermal substitutes: 1)

natural biological with intact ECM (allo- or xenografts); 2) processed biological with biological components; and 3) synthetic materials (Buchanan et al. 2016).

Tissue engineered skin substitutes have been developed aiming at ideal universal autologous graft, which would possess identical structure, composition and vitality, but the pathophysiologies of different wound types, such as burns and chronic wounds, have varying demands. Tissue engineered skin substitute options are summarized in Table 2. Dermal substitutes containing viable cultured cells are not yet commercially available in Finland (Chronic leg ulcers: Current Care Guidelines 2017).

Table 2. Summary of tissue engineered skin substitutes (based on Tenenhaus and Rennekampff 2016).

Substitute	Function	Note
Non-cultured products	Wound bed protection Promotes re-epithelialization Wound bed optimization for further grafting	Xenogenic (porcine) and allogenic skin E-Z Derm (silver-impregnated aldehyde porcine dermis formulation) Biobrane (nylon-silicon mesh with porcine collagen) Integra (bilayered silicone bovine collagen glycosaminoglycan template) Amniotic membrane Suprathel (trimethylene carbonate and ε-caprolactone copolymer)
Cultured products	Permanent or temporary wound coverage	Cultured keratinocytes (Epibase, Epicel SM, Tissue Repair, Keratinozyten Sheets) Cultured fibroblasts (Dermagraft, Hyalograft) Cultured composite skin constructs (NovaDerm, GraftSkin, OrCel)
Stem cells	Regenerative wound healing Fully developed skin construct	Basic and experimental studies
3D printing	Wound specific matrix	PrintAlive (bilayered hydrogel with fibroblasts and keratinocytes) SkinPrint (skin graft from hair follicle stem cells)
Whole-organ decellurization	Cellular microenvironment with organlike geometry and structure	Experimental studies (major revascularization and cell distribution challenges)

2.2.5 *In vivo* models of wound healing

Various mammalian species are used in skin research, but rodents - especially rats and mice - are most widely used. Both human and rodent skin has an epidermis with an underlying basement membrane and dermis, but anatomical differences between human and rodent skin are clear (Dorsett-Martin 2004). Layered skin structure differs underneath the dermis between loose-skinned and fixed-skinned animals. Loose-skinned animals, such as rats and rabbits, have a subcutaneous panniculus carnosus muscle located under the reticular layer of the dermis, which is thought to provide or promote skin twitching, thermoregulation capacity, contraction and revascularization (Naldaiz-Gastesi et al. 2016). Fixed-skin species, such as humans and pigs, generally do not have this muscle layer, but in human it can be identified in the skin of the neck, face and scalp, where it constitutes the platysma muscle (Ross et al. 2010). Humans use the platysma muscle to do facial expressions (Gottrup et al. 2004). Another major difference is that rat skin lacks both apocrine and eccrine glands, both of which can be found in human skin (Dorsett-Martin 2004). Human hair growth differs remarkably among individuals, and can be described as mosaic, whereas rat hair grows in patches (Dorsett-Martin 2004). Anatomically, pig and human skin are fairly comparable, and thus pigs are recognized as a model for human skin in many contexts, such as wounds, burns, toxicology, infections, radiation and stem cell research (Summerfield et al. 2015). Thicker subcutaneous (fat) layer, pigment divergence and absence of eccrine glands are the major differences in pig compared to human skin. Pigs are, on the contrary, more expensive and demanding in relation to laboratory facilities, compared to smaller species, such as rodents.

The wound healing process proceeds faster in animals, and therefore gives an advantage, considering that study designs require less time than in human designs (Dorsett-Martin 2004). Another major advantage is the possibility to harvest tissue samples from animal wounds at different stages, which can be considered unethical from human wounds, as the sample harvesting itself could complicate the healing process. Considering excisional wound healing models, wounds can be accurately reproduced and even allow multiple simultaneous investigations, which are prerequisites for a good animal model (Gottrup et al. 2000). Rats are widely available, reasonable sized, and their nature is tractable (Dorsett-Martin 2004). Short gestation, short lifespan, and well-known health and genetic backgrounds advocate the use of rat wound healing models (Dorsett-Martin 2004). Due to these qualities, rats have been widely used in wound healing studies.

In an excisional wound healing model, the wounds heal from the edges, but also by contraction, where the panniculus carnosus has a role in rats but not in humans (Gottrup et al. 2004). Acute wounds can be simulated using an animal model, but it is far more difficult to simulate human chronic wounds with an animal model (Gottrup et al. 2004). During the last decade some pathologic cutaneous pig wound-healing models have been validated including ischemic, diabetic, infectious, burn and scar hypertrophy models (Seaton et al 2015). These pathologic models still possess limitations concerning surgical technique, lack of long-term effects, and fundamental differences in healing compared to humans.

2.2.6 *In vitro* models in wound healing

In vitro models for wound research have been under development due to the mentioned limitations of *in vivo* experiments. Three-dimensional cell cultures are complex to construct but offer more information, as different cells function together more similarly to wound healing (Vidmar et al. 2017). HaCaT adult keratinocyte cell line, primary keratinocytes or epidermal stem cells are mostly used in monoculture models of skin wound healing, in which cytokine pathways, cell proliferation and migration are investigated (Vidmar et al. 2017). In co-culture models, it has been shown that, for instance, cell-cell interactions between keratinocytes and fibroblasts, ultrasound, and 1,25-dihydroxyvitamin D_3 treatment enhance wound healing (Sato et al. 1997, Ito et al. 2000).

Two main techniques are used to simulate a wound *in vitro*:

1) Scratch assay, in which a gap in the cell culture is created by scratching,
2) Microfluid technology, in which cell migration can be studied in micrometer dimension channels (Li and Lin 2011).

The future goal of *in vitro* wound healing models is to create a three-dimensional organoid microenvironment, with number of cell types and cell products replicating a wound (Vidmar et al 2017). The Organization for Economic Co-operation and Development (OECD) has published guidelines for *in vitro* skin absorption and irritation testing (OECD 2004, OECD 2015). The OECD guidelines serve as standard tools to assess the effects of chemicals on human health and the environment.

2.3 Urinary system and urothelium

The urinary tract begins from the renal pelvises, where the ureters begin. The urine flows from the ureters to the bladder, where it is stored and later voided through the urethra (Figure 8). The ureters, bladder and urethra serve as a reservoir and passage for the end products of the kidneys.

The transitional epithelium, i.e. urothelium, is characteristic of the urinary tract, where it can be found everywhere other than the distal urethra, which is covered by non-keratinized stratified squamous epithelium (Holstein et al. 1991). The distal male urethra is lined by pseudostratified columnar and stratified squamous epithelium, whereas the female distal urethra traditionally lacks pseudostratified columnar epithelium (Ross et al. 2010).

Urothelium is a stratified epithelium impermeable to salts and water. The cellular thickness varies from two cell layers in the minor calyces, to six layers in an empty bladder (Ross et al. 2010). Distension of the epithelium affects the number of layers seen. In the bladder, epithelial cells are cuboidal, protruding dome-shaped into the lumen. The urothelium is composed of umbrella, intermediate and basal cell layers (Khandelwal et al. 2009). The superficial cells are called umbrella cells that are characteristic with tight intercellular junctions, special intracellular plaques and morphology dependent on distension (Khandelwal et al. 2009). The intermediate cells are thought to be progenitors of the superficial cells with attachment to the basement membrane (Yamany et al. 2014). The basal cells lie on top of connective tissue and serve as precursor for the other cells (Apodaca 2004). Underneath the urothelium lies a dense collagenous lamina propria. Beneath the lamina propria in the ureter and urethra, two smooth muscular layers can be found: the inner longitudinal layer and the outer circular layer (Ross et al. 2010).

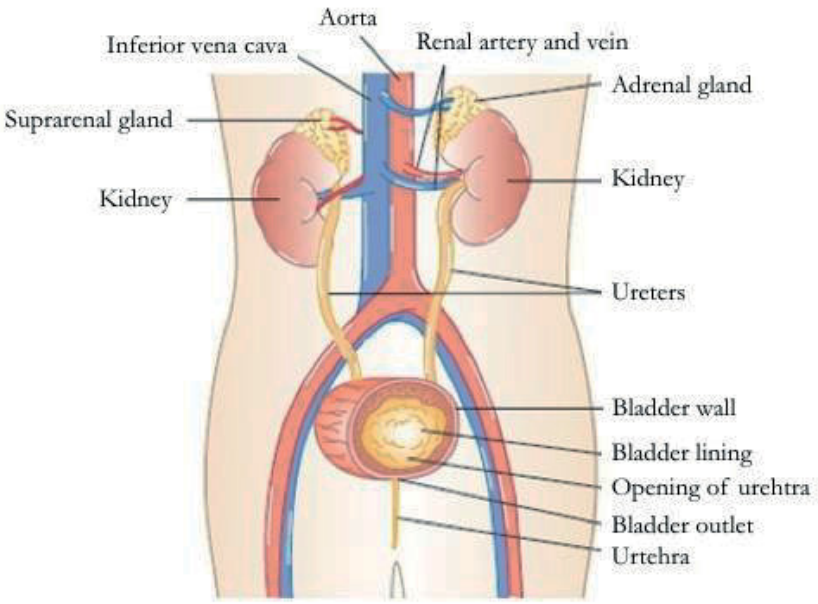

Figure 8. Schematic macro anatomy illustration of normal urinary system. Image modified from a free image database (www.jouefct.com).

2.3.1 Ureters and urinary bladder

Ureters and urinary bladder are similar in structure, being lined by urothelium, submucosa, muscular and adventitia layers (Ross et al. 2010). Only at the distal end of the ureters there is an additional outer longitudinal smooth muscle layer on top of the circular layer. The outermost layer of the ureters is the adventitia (Ross et al. 2010).

The urinary bladder works as a temporary reservoir for urine and has two ureteric orifices and one internal urethral orifice. The smooth muscle of the bladder forms the detrusor muscle, which voids urine to the urethra when contracting (Figure 9). Around the urethral orifice, the muscle fibers are organized as an involuntary internal urethral sphincter (Ross et al. 2010).

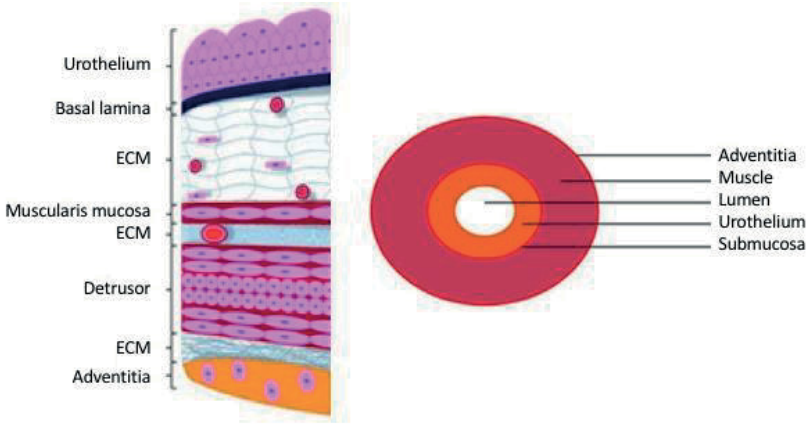

Figure 9. Schematic illustration of bladder cell layers (left) and urethral architecture (right). Image modified from Orabi et al. 2013.

2.3.2 Urethra

The size, structure and functions of the urethra differ between males and females. Male urethra can be divided in to three segments: prostatic, membranous and penile urethra (Ross et al. 2010). The prostatic urethra is the proximal part of male urethra running through the prostate gland, from which small prostatic ducts and ejaculatory ducts enter the urethra. The membranous segment is located between the prostate apex and penile bulb, where the urethra passes through the urogenital diaphragm and enters the perineum. The part where the urethra passes the urogenital diaphragm is a voluntary external sphincter of the urethra in males and females. The membranous segment is where urothelium ends, and is lined with stratified or pseudostratified columnar epithelium (Ross et al. 2010). The penile urethra is surrounded by the corpus spongiosum and ends at the external urethral orifice. The penile segment of the urethra is lined with pseudostratified columnar epithelium, but at its distal end the epithelium changes to stratified squamous epithelium. The ducts of urethral (Littré) and bulbourethral (Cowper's) glands open and empty into the penile segment.

The female urethra is short (3–5 cm) compared to male urethra (approx. 20 cm). The mucosa of the female urethra has longitudinal folds of urothelium, which changes to stratified squamous epithelium before its termination (Ross et al. 2010). Numerous small urethral glands open to the proximal urethra in females. The paraurethral glands open their ducts on each side of the external urethral orifice.

2.4 Urethral defects

2.4.1 Urethral regeneration

The turnover rate of urothelium is slow compared to the epidermis. The homeostatic urothelium turnover rate is estimated to be 3–6 months, whereas epidermal rate takes only days (Khandelwal et al. 2009). Urothelium, however, demonstrates rapid response to acute injuries, highlighting its crucial barrier function (Kreft et al. 2005). Its regeneration can be restored within as little as one day following injury (Khandelwal et al. 2009). The precise repair mechanisms are complex and only partly understood.

Primarily, in response to an acute injury, the urothelium desquamates, and local necrosis and/or apoptosis may occur (Kreft et al. 2005). Secondly the remaining basal cells begin to proliferate, which decreases in the final stage, during which suprabasal cells start to differentiate (Kreft et. Al 2005). Urothelium can regenerate by cell division within any three - umbrella, intermediate and basal - cell layers (Apodaca 2004). The intermediate and basal cell layers in particular serve as a reservoir for rapid umbrella cell regeneration, but what triggers the intermediate cells to rapidly differentiate is unknown (Hickling et al. 2015). It has been hypothesized that this response is related to growth factors, urine exposure, or due to loss of cell-cell contact (Khandelwal et al. 2009). Urethral strictures, a remarkable clinical dilemma, is an injury in which fibrosis occurs and normal epithelium becomes replaced with squamous metaplasia (Simsek et al. 2018). Considering the smooth muscle layer, it generally has the capability to respond to an injury by undergoing mitosis (Ross et al. 2010). The literature of urethral regeneration is focused on the regeneration of urothelium, mainly bypassing other structural layers.

2.4.2 Etiologies

Congenital defects, traumas and infections may cause urethral defects. Urethral traumas vary from penetrating or blunt injuries caused by severe pelvic fractures, or iatrogenic traumas, such as catheter placement or radiotherapy, for instance (Bryk & Zhao 2016).

Hypospadias is a male congenital malformation of the external genitalia, where abnormal development of the urethral fold and ventral foreskin causes the urethral

opening to exist in an abnormal position (Donaire & Mendez 2018). Hypospadias is the second most common congenital disorder of the male reproductive system after cryptorchidism, which is the absence of at least one testicle from the scrotum (Donaire & Mendez 2018, Leslie & Villanueva 2018). The etiology of hypospadias remains unknown, although genetic, endocrine and environmental factors, such as *in utero* exposure to estrogen-containing pesticides and plastic lining cause hypospadias, where the main pathophysiological event is anomalous or partial urethral closure during first weeks of embryonal development (Donaire & Mendez 2018). About one hundred hypospadias are diagnosed yearly among newborns in Finland (Jalanko 2017). Hypospadias can be classified as distal, midshaft or proximal (Figure 10), distal type being the ruling (60-70%) type (Donaire & Mendez 2018).

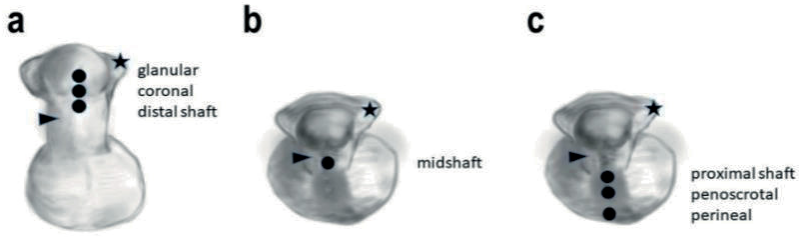

Figure 10. Hypospadias can be divided into distal (a), midshaft (b) or proximal (c) location. Dots mark the location of urethral opening (i.e. meatus), asterisk ventral foreskin and arrows urethral folds. Image modified from van der Horst & Wall 2017.

Epispadias is a rare congenital malformation seen in both males and females. Dorsal failure of urethral plate tubularization is characteristic to epispadias, where the defect can range from glandular to peno-pubic locations (Frimberger 2011). Most commonly it is a part of bladder exstrophy complex, which is an anomaly in which a pair of scissors have dorsally cut the urethra open to the bladder, as a simplified description (K.V. et al. 2015).

2.4.3 Treatment of urethral defects

The management of hypospadias is surgical and it aims to achieve straight penis with correct sized slit-shaped meatus at the apex of the glans, a cone-shaped glans, circumcised or reconstructed foreskin, and acceptable cosmetic outcome (Keays & Dave 2017). There are several surgical repair techniques and the correct technique depends whether the hypospadias under repair is distal or proximal, but also the

amount of penile curvature matters (Snodgrass & Bush 2016). The most common complications after hypospadias repair are (Keays & Dave 2017):

- Fistulas
- Meatal stenosis
- Dehiscence of the glans
- Urethrocele or urethral diverticulum
- Cosmetic issues such as excess skin, skin tags, cysts or suture tracts
- Hair-bearing urethra
- Penile curvature
- Spraying or misdirected urinary stream
- Erectile dysfunction
- Balanitis xerotica obliterans leading to strictures

The management of epispadias is surgical and especially in female patients the urethral continuity from the bladder is pronounced, whereas only penile reconstruction among male patients might be sufficient if the defect does not extend to the bladder neck (Frimberger 2011).

Among adults, penile or urethral reconstructive surgery might be necessary in conditions such as urethral stricture disease, urethral dysfunction, erectile dysfunction and subsequent to oncological procedures (Kiechle et al. 2018). Urethral stricture disease is defined as abnormal narrowing due to urethral fibrosis of the surrounding corpus cavernosum, which is caused by idiopathic, iatrogenic (transurethral resection, catherization or prostate cancer treatments, previous hypospadias surgery), traumatic or inflammatory reasons (Bayne et al. 2017, Simsek et al. 2018). Strictures can be evaluated clinically by symptoms such as decreased urinary stream, incomplete emptying, dysuria, urinary tract infection and/or rising void residual, radiologically (retrograde urethrography, cystourethrography or ultrasound) or endoscopically (Bayne et al. 2017). On the cellular level, pathologically the normal epithelium is replaced with squamous metaplasia. (Simsek et al. 2018). The location of the stricture defines the correct treatment (Callegos & Santucci 2016). Anterior urethra (i.e. fossa navicularis, pendulous and bulbar urethra) is mainly treated by urethroplasty or minimally invasive techniques such as dilatation, visual internal urethrotomy, or stenting, the latter tending to be less successful and potentially more costly (Stein & DeSouza 2013). Posterior urethra (i.e. bladder neck, prostate and membranous urethra) strictures are recommended to be managed by excisional urethroplasty via perineal approach (Gelman & Wisenbauch 2015).

Panurethral strictures are surgically challenging because of tissue shortage to cover long segments, leading to poorer outcome, and thus there is no recognized superior reconstructive technique available (Goel et al. 2011).

Problems, such as limited supply of autologous grafts or flaps, donor site morbidity, long-term deteriorating of grafts or flaps and failure of buccal autologous grafts, might be resolved by tissue engineering and regenerative medicine (Orabi et al. 2013). The reconstructive techniques also have high complication rates and demand high expertise (Abbas et al. 2018). Tissue engineered techniques of urethral replacement can be generalized to acellular matrix, which serves as a patch graft, or cell-seeded scaffolds, which serve as circumferential tubular grafts or partial urethral patch grafts (Orabi et al. 2013).

2.5 Biomaterials

The definition of biomaterials has changed from the first more widely admitted definition from 1987: "A non-viable material used in a medical device, intended to interact with biological systems" (Williams 2009). The current definition of the word biomaterial according to the well-established Merriam-Webster™ dictionary reads as follows: "A natural or synthetic material that is suitable for introduction into living tissue especially as part of a medical device". Biomaterials from a healthcare perspective can be classified as synthetic (metals, polymers, ceramics and composites), naturally derived (animal- and plant-derived) or semi-synthetic or hybrid materials (Bhat & Kumar 2013). In donor-based transplants, an often used classification, considering the donors relation to the recipient, is autografts (same individual), allografts (different individual, same species) or xenografts (other species).

Whether of natural or synthetic origin, an optimal biomaterial should support cell attachment, maintenance, proliferation and differentiation, and provide structural and mechanical support but also importantly support host response (Keane & Badylak 2014). Availability, ethical matters and costs are also remarkable attributes. In tissue engineering, biocompatibility, porosity, controlled biodegradability, favorable surface chemistries, optimal mechanical properties, low toxicity and ECM simulation are stated as the base qualities for a biomaterial (Patel et al. 2011). Mechanical properties, thermoregulation, ultra-violence barrier, aesthetic function and altogether a conventional treatment against skin defects are the main goals when treating skin lesions and injuries (Ahsan et l. 2017).

In this thesis, the focus was on AM, CM, PLCL and PTMC, which are reviewed in the following chapters.

2.5.1 Amniotic membrane

Structure and function

AM is the inner placental membrane that lines the fetus and its surrounding amniotic fluid inside the amniotic sac formed by the amniochorionic membrane (Figure 11). The AM appears approximately 7–8 days after conception and is formed from separation from the epiblast layer of the inner cell mass (Dua et al. 2004, al Sadler 2012). These originally epiblast cells line the amniotic cavity and are thus called amnioblasts (Sadler 2012). The amniotic cavity continues to enlarge due to mitotic activity of amnioblasts. The AM fuses with the surrounding chorion during approximately the 12th week of gestation, obliterating the yolk sac between them, and forming the amniochorionic membrane (Dua et al 2004). The amniochorionic membrane is entirely composed of fetal tissue (Bourne 1962, Insausti et al. 2010).

The AM is 0.02–0.5 millimeters thick and consists of five layers: epithelium, basement membrane, compact layer, fibroblast layer and spongy layer (Bourne 1962). Some literature describes AM as being three-layered, where compact, fibroblast and spongy layers are together referred to as the mesenchymal layer or stroma (Mamede et al. 2012, Malhotra & Jain 2014). Some literature distinguishes a reticular layer just above the chorion (Liu et al 2010). The epithelium consists of a single layer of cells, which vary in shape from flat to cuboidal, and are covered by microvilli structures on their free surface (Bourne 1962, Dua et al. 2004). The epithelium is attached to the basement membrane formed by reticular fibers (Dua et al 2004). There are also large amounts of proteoglycans in the basement membrane, which affects the permeability of AM (Mamede et al. 2012). The amniotic epithelial cells and mesenchymal stromal cells have been under investigation as a promising source of stem cells without ethical barriers and with low immunogenicity and non-tumorigenicity (Niknejad et al. 2008, Insausti et al. 2010). The compact layer almost completely lacks cells, and is composed of a complex network of reticular fibers (mostly collagen type III), and has been described as the strongest layer of AM (Bourne 1962, Mamede et al. 2012). Respectively, the fibroblast layer is the thickest layer and it is composed of a loose fibroblast network (Bourne 1962). The spongy

layer contains a few isolated fibroblasts and wavy bundles of reticulin covered in mucin (Bourne 1962). The spongy layer is attached to the underlying chorion.

AM does not contain blood vessels and the necessary supply of nutrition and oxygen are derived from chorionic fluid, amniotic fluid and fetal surface blood vessels. (Bourne 1962, Dua et al. 2004). AM also lacks lymphatic vessels, muscles and nerves (Bourne 1966, Mamede et al. 2012).

AM maintains amniotic fluid homeostasis (Dua et al. 2004). The amniotic fluid serves as a cushion, absorbs jolts, prevents adherence of the embryo to the AM and allows fetal movements (Sadler 2012). It is uncertain whether the role of AM is secretive or absorptive, maintaining amniotic fluid homeostasis (Dua et al 2004). AM also has metabolic functions, in addition to its protective role for the embryo and amniotic fluid. AM transports water and soluble materials and produces bioactive factors, such as vasoactive peptides, growth factors and cytokines (Mamede et al. 2012).

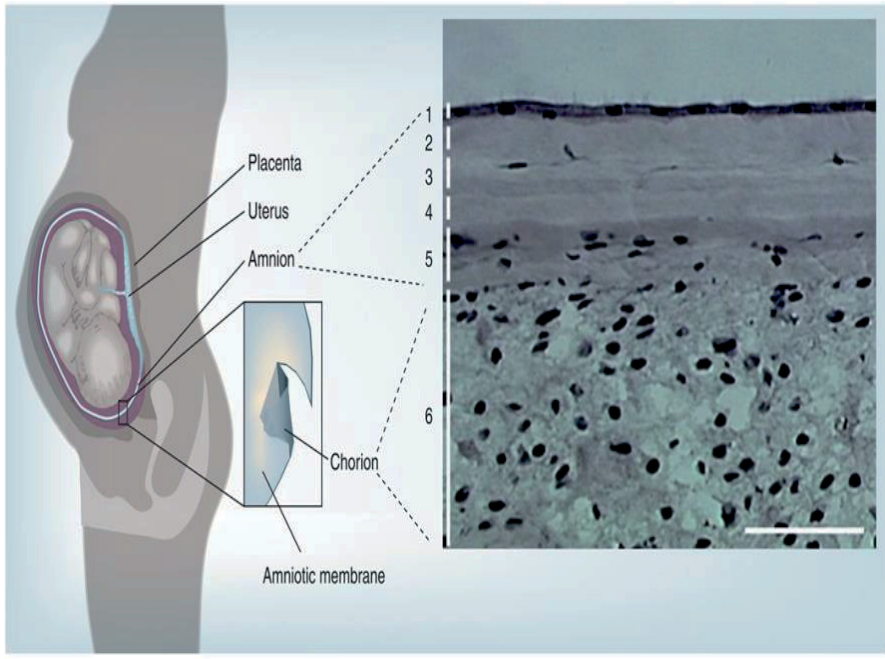

Figure 11. The amniotic sac (i.e. the placental membrane) is formed of amnion and chorion (6). Histologically AM is composed of five distinctive layers: epithelium and its basement membrane (1), compact layer (2), fibroblast layer (3), spongy layer (4) and reticular layer (5) (Liu et al 2010).

Preservation and safety

AM can be preserved fresh (stored at 4 °C), frozen (stored at -80 °C) or dried. Adds et al. concluded that both fresh and frozen preservation methods are applicable, but due to logistical, safety and cost benefits, frozen should be favored (Adds et al. 2001, Mermet et al. 2007). Long-term cryopreservation has been shown to be a practical and economical method, even maintaining an "amnion bank" (Ravishanker et al. 2003, Hopkinson et al. 2008). Dried AM is prepared by low heat and air vacuum, and can be stored at room temperature for up to five years, but it needs to be rehydrated before use (Malhotra & Jain 2014). Dry storage is an applicable method to tissue bank AM as well (Malhotra & Jain 2014).

AM has been preserved and used with or without its epithelial cells. The epithelial layer can be removed using ethylenediaminetetraacetic acid (EDTA), dispase or trypsin/EDTA (Lim et al. 2009). Previous results indicate that intact epithelial layer retards migration and differentiation of cultivated cells, although processing AM with EDTA or dispase might affect its basement membrane (Lim et al. 2009).

The possibility of blood transmitting diseases needs to be retained using AM. Placentas only from cesarean sections are accepted for AM harvesting due to bacterial contamination in vaginal deliveries (Adds et al. 2001). In addition to bacterial contamination of AM, also other transmitting pathogens need to be tested and therefore human immunodeficiency virus, hepatitis B and C, *Treponema pallidum* and human transmissible spongiform encephalopathies (i.e. prion diseases) are recommended to be screened from the donors (Kesting et al. 2008).

The epithelial cells of AM lack expression of human leukocyte antigen class A, B, DR and molecules CD-40, CD-80 and CD-86, and thus AM is considered to be non-immunogenic (Fairbarn et al 2014). In clinical use, no immune rejections have been reported using fresh AM, and glycerol and cryopreservation may even reduce antigenicity due to decreased viability of epithelial cells (Lo & Pope 2006).

Applications in ophthalmology

Most of the studies considering AM are nowadays from the field of ophthalmology. De Rötth was the first to use AM for conjunctival defects in 1940, after which AM was overlooked for almost five decades (Dua et al. 2004, Fernandes et al. 2005). The understanding of cryopreservation as a preservation method led to the revival of AM in ophthalmology (Fernandes et al. 2005). Ever since, AM has been found to adapt well for ocular surgery because it promotes epithelialization, inhibits fibrosis, and has anti-inflammatory, antiangiogenic, antimicrobial and

antiviral properties (Dua et al. 2004, Fernandes et al. 2005). Koizumi et al. showed that preserved AM expresses several growth factors and proteins that might promote corneal epithelialization (Koizumi et al. 2000). Due to its suppressive effect on the transforming growth factor-beta signaling system, deoxyribonucleic acid (DNA) synthesis and subsequent myofibroblast differentiation AM has anti-scarring qualities, which is important in ocular healing (Tseng et al. 1999). AM also gives the ocular surface mechanical cover as a biological bandage (Malhotra & Jain 2014). Beside ocular surgery, with its variety of applications, AM has been used in glaucoma surgery and in oculoplastic procedures (i.e. surgery around the eye) (Dua et al. 2004). In ocular surgery, AM can be used as a patch or as a graft, but a layered technique is also used (Dua et al. 2004, Rahman et al. 2008). As a patch, AM is removed or falls eventually off from the transplanted site after desired epithelialization occurs beneath AM. If AM is used as a graft, it integrates into the ocular surface and epithelialization occurs on the membrane. When AM is used as a graft, AM is usually transplanted the epithelial side up, and vice versa when used as a patch (Dua et al. 2004).

Although AM is widely used in ophthalmology, there are very few well-documented complications. Failure of epithelialization, risk of infections, hematoma formation and the risk of hypopyon (i.e. inflammatory cells in the anterior chamber) are the main complications reported (Dua et al. 2004). However, it has also been reported that different indications for ophthalmological AM treatments makes the evaluation difficult to estimate and the rates vary: success 22-58%, partial success 6–34% and failure 33–44% (Rahman et al. 2008). Success rates, combined with the fact that a clear minority of the studies considering ophthalmological AM transplantation are randomized controlled trials, make some of the results controversial (Gomes et al. 2005). Appropriate patient selection and considered use of AM are important for achieving the best outcome (Malhotra & Jain 2014).

Wounds and skin

John Staige Davis was the first to use AM at Johns Hopkins Hospital in 1910, as part of a study consisting of 550 skin transplantation cases (Davis 1910). In wound healing studies, AM is reported to enhance wound healing by promoting epithelialization, which for the most part relies on uncontrolled studies from the 1970s (Ganatra 2003). The majority of the references on AM promoting epithelialization are from the field of ophthalmology or burns, although its epithelialization-promoting feature is often mentioned in a wound healing context.

The epithelium of AM itself might even impair wound re-epithelialization, because it retards cultivated cell migration and differentiation, but as mentioned, the epithelium can be removed (Lim et al. 2009, Tauzin et al. 2014). It has been found that the basement membrane of AM affects keratinocyte and fibroblast migration, cell attachment, proliferation and differentiation (Lo & Pope 2006). One of the potential functions of AM in wound healing might be providing an ECM in tissue repair (Cornwell et al. 2009, Zelen et al. 2013). The precise mechanisms, however, remain unclear.

AM has been discovered to reduce pain due to the coverage of free nerve endings at the wound site (Ganatra 2003, Lo & Pope 2006). AM has been found to be suitable for chronic wounds, as well promote epithelialization and suppress fibrosis (Mermet et al. 2007, Zelen et al. 2013). In a recent randomized clinical trial for the treatment of chronic pressure wounds, partial and complete healing of the wounds (n = 24) was shown to be significantly faster and without complications in wounds treated with AM compared to local Dilantin (phenytoin) powder treatment (Dehghani et al. 2017). The results considering angiogenetic qualities of AM are controversial. In ophthalmology, AM is often considered to be anti-angiogenic, which is desirable in the surface of the eye. On the contrary, in wound healing sufficient blood supply is crucial. Niknejad et al. concluded that the angiogenic qualities are side-dependent in wound healing: facing the AM the epithelial side up, significant neovascularization is increased, and vice versa it is decreased (Niknejad et al. 2013).

AM has been shown *in vitro* to possess antimicrobial effects, the mechanism of which has been suggested to relate to AM's close adherence to the wound surface (Talmi et al. 1991). The antimicrobial effect is surely favorable considering wound healing applications. In the uterus, the fetal membranes serve as a source of antimicrobials and can even upregulate the expression of selective natural antimicrobials, such as human B-defensins and elafin, which innate immune system and possess anti-bacterial, anti-viral and anti-fungal properties (King et al. 2007).

In burns, AM has been used for skin graft donor sites, partial-thickness and full-thickness burns (Kesting et al. 2008). Systematic validation of results considering epithelialization, dressing changes and antimicrobial effects were heterogeneous when AM was compared to other dressing materials in burns (Kesting et al. 2008). Encouraging but mainly uncontrolled results in burns reveal that safety, usability, costs, re-epithelialization, antimicrobial effects, fluid loss, pain relief, scar and contracture reduction are all qualities associated with AM (Kesting et al. 2008, Lo & Pope 2006).

AM has also been used as a dermatological application in epidermolysis bullosa, an inherited bullous skin disorder, and Stevens-Johnson syndrome characterized by cutaneous erythema, blister formation and hemorrhagic erosions of mucous membranes (Lo & Pope 2006, Mockenhaupt 2011).

Other applications

Beside dermatology and ophthalmology, the AM has been under investigation for several other purposes. In gynecology it has been used for cervical reconstruction, against intrauterine adhesions, vaginal repair, as an intra-abdominal barrier to prevent adhesions, and as a biological dressing following radical vulvectomies and groin dissections (Mhaskar 2005, Amer & Abd-El-Maeboud 2006, Mamede et al. 2012). AM has also been used for abdominal wall repair in gastroschisis and omphaloceles (Gharib et al. 1996, Fernendes et al. 2005). For reconstructive purposes AM has been used in oral cavity, bladder, tympanic membrane, tendon and joint surgery (Fernendes et al. 2005, Coban et al. 2009).

2.5.2 Chitosan membrane

Chitin is the world's second most common natural polysaccharide after cellulose (Jayakumar et al. 2010). Chitin was first identified in 1884 (Younes & Rinaudo 2015). In nature, chitin occurs in the exoskeleton of arthropods, and in the cell walls of fungi and yeast, where it is organized as crystalline microfibrils (Younes & Rinaudo 2015). Chitin can be found in three different polymorphs: α-, β- and γ-chitin, α-type being the most common (Muxika et al. 2017). Chitin has been found to be biocompatible, bioactive, biodegradable and mechanically strong, but it has poor solubility (Muxika et al. 2017).

Poor solubility impedes the use of chitin, and to achieve better solubility, chitin has to be converted to chitosan. Chitosan is rarely found on its own in nature, although it can be identified from fungal cell wall as free chitosan and combined with glycan (Liaqat & Eltem 2018). Chitosan was discovered by French chemist Henri Braconnot in mushrooms in 1811 (Dodane & Vilivalam 1998). Shrimp and crab shells are the main commercial source of chitin for manufacturing chitosan (Younes & Rinaudo 2015). First the shells are demineralized and deproteinized (Nwe et al. 2014). Chitin can be converted into chitosan through chemical processing, or enzymatically by deacetylation (Figure 12) (Synowiecki & Al-Khateeb 2003). The

deacetylation degree of chitin and chitosan is defined according to the molar fraction of N-acetylated units (Younes & Rinaudo 2015). Chemical processing is favored due to lower costs and larger processing volumes (Muxika et al. 2017). The chemical process varies, depending on hydrochloric acid and sodium hydroxide (NaOH) concentrations, treatment time and temperature, whether chitosan is derived from crab shell, shrimp shell or squid plate chitin (Nwe et al. 2014). Basically, 10–15 M NaOH treatment at 40–105 °C from hours to days deacetylates chitin into chitosan (Nwe et al. 2014). Chemical concentrations, especially NaOH, used temperature, and time influence the deacetylation degree, molecular weight, molecular weight distribution and deacetylation distribution, which reflect the applicability of chitosan (Synowiecki & Al-Khateeb 2003). In particular, the degree of deacetylation affects solubility, viscosity and biological activity. The other important quality defining chitosan's physical and chemical properties is molecular mass. Lower molecular mass molecules possess promising properties in the pharmaceutical field, which can be prepared from high molecular weight chitosan by depolymerization using enzymatic, oxidative or ultrasonic degradation (Mao et al. 2004). Chitin and chitosan can be processed into gels, membranes, nanofibers, beads, nanoparticles, scaffolds and sponges (Jayakumar et al. 2010). It has been estimated that 150,000 tons of chitin-derived chitosan is produced annually, which is mostly used in cosmetics, organic fertilizers and dietary supplements (Liaqat & Eltem 2018).

Chitosan's potential as a biomaterial is based on structural similarity to ECM glycosaminoglycans, its ability to be molded, suitable mechanical properties with controllable pore size when used as a scaffold, and alterable degradation rate (Ahsan et al. 2017). In chitosan studies there is great diversity, depending on which kind of chitosan is researched. Desired structure can vary from membranes to nanofibers and gels and its deacetylation degree has a major impact on its qualities, which makes it challenging to state a clear consensus how chitosan should be applied (Ribeiro et al. 2017). Chitosan-based structures are also relatively easy to prepare and can be used for cytokine/growth modulator release (Ahsan et al. 2017). Thus, chitosan has a variety of tissue engineering applications.

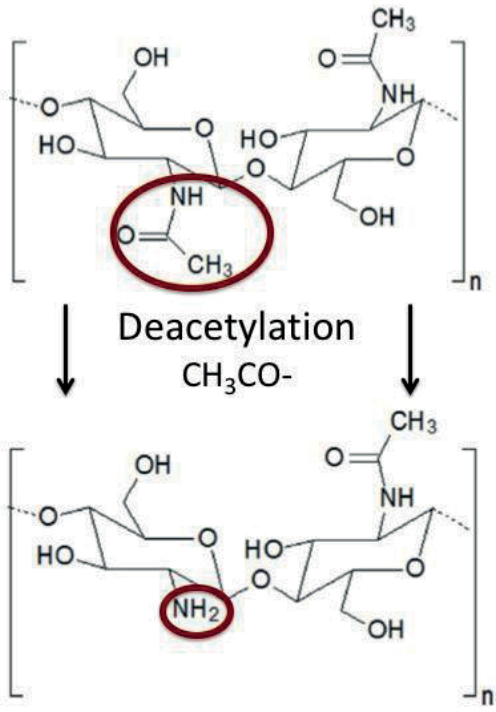

Figure 12. The deacetylation of chitin to chitosan. Image modified from Muxika et al. 2017.

Chitosan in wound healing

It has been suggested that chitosan is implicated in multiple cellular processes during wound healing with minimal side effects, has near nonexistent encapsulation, promotes polymorphonuclear neutrophils and granulation, has hemostatic properties, promotes infiltration and migration of neutrophils, macrophages and epithelial cells, and decreases scar tissue, but the mechanisms must still be investigated in more depth (Patrulea et al. 2015). Chitosan is thought to be a suppressive biomaterial, regarding the inflammation stage of wound healing (Farhadihosseinabadi et al. 2019). Chitosan's hemostatic properties might be due to positive charged amino groups interacting with negatively charged red blood cell surfaces, and especially higher deacetylation degree has a considerable effect on chitosan's erythrocyte aggregation and platelet binding properties (Bano et al. 2017). Chitosan-treated wounds have shown increased infiltration of polymorphonuclear cells, neutrophils, eosinophils and basophils, to the wound site leading to thick fibrin layer that directs fibroblasts, macrophages and type III collagen production (Ueno et al. 1999, Oryan & Sahvieh 2017). Chitosan's depolymerization is thought to initiate

fibroblast proliferation and collagen deposition (Bano et al. 2107). Promotion of wound contraction and epithelialization has been suggested in a mouse model using chitosan hydrogel (Ishihara et al. 2002). Some studies suggest that CM has angiogenetic features due to mesenchymal and endothelial cell proliferation (Oryan & Sahvieh 2017). In burn wounds, chitosan gel combined with silver sulfadiazine resulted in improved angiogenesis and fibroblast and endothelial cell proliferation Oryan & Sahvieh 2017). As a dressing, chitosan has also a strong adhesive property and might possess analgesic qualities (Bano et al. 2017).

Chitosan has shown antimicrobial activity in wound healing against bacteria, fungi and viruses. Low molecular weight increases chitosan's antimicrobial properties, and its efficacy depends on various factors such as concentration, microorganism species, hydrophilic/hydrophobic characteristics and solubility (Bano et al. 2017). The interaction between bacterial cell anionic groups and chitosan's cationic (NH3+) groups and interference with messenger ribonucleic acid (RNA) and protein synthesis are stated as the two main mechanisms behind its antibacterial efficacy (Bano et al. 2017). There is no clear evidence how chitosan's deacetylation degree effects antimicrobial activity. Chitosan-based dressings have been investigated, with promising results against wound infections causing high local concentrations of gentamycin, silver sulfadiazine and chlorhexidine (Ahsan et al. 2017). Selenium and silver-loaded chitosan scaffolds have been shown *in vitro* to enhance antibacterial activity as a potential novel antimicrobial dressing (Biswas et al. 2018). Chitosan hydrogel combined with fibroblast growth factor-2 showed accelerated wound closure and contraction in the first two days in a diabetic mice model (Obara et al. 2003).

Until now, there are only few clinical publications of chitosan on diabetic wounds/ulcers in relatively small and uncontrolled studies with variable patient characteristics (Escárcega-Galaz AA et al. 2018). In a small (n = 20) uncontrolled clinical pilot, chitosan gel was successfully used to treat pressure ulcers, and in 90% of the patients, the treatment was effective considering wound size reduction (Campani et al 2018). Azad et al. used meshed or non-meshed CM as a dressing on skin-graft donor sites and found CM to enhance healing, with a positive effect on re-epithelialization and granular layer regeneration after 10 days compared to the Bactigras control (Azad et al 2004). CM has promoted normal skin coloration on skin-graft donor sites (Stone et al. 2000). Heparin combined with CM stimulated *in vitro* re-epithelialization, possibly due to increased wound area growth factors, and was shown to shorten re-epithelialization time in a clinical (n = 10) study on skin-graft donor sites (Kratz et al. 1998).

Other applications

Chitosan has not been studied extensively in urological applications. In one report, it has been found to serve as a potential conduit for renal proximal tubule tissue engineering with cultivated cells (Chiang et al. 2018). An *in vitro* study demonstrated that human renal proximal tubule cells cultivated on chitosan showed better differentiation status and functional active transportation compared to collagen surface. Besides wound healing and urology, chitosan has been researched in a variety of purposes, which are summarized in Table 3.

Chitosan has also been examined as a vaccine adjuvant. Chitosan has shown to promote cell-mediated immune response by inducing T helper 1 cell capacity (Moran et al. 2018). T lymphocytes, especially T helper $CD4^+$ cells, and B lymphocytes are the main cells involved in adaptive immunity. Interestingly, IL-4, a cytokine related to wound healing, is produced by activated T helper $CD4^+$ cells (Wills-Karp & Finkelman 2015). There is some contradictory joint evidence between chitosan and IL-4 in vaccine related studies. In porcine spleen cells, chitosan did not increase IL-4 expression, but when adjuvanted to *Helicobacter pylori* vaccine, chitosan increased IL-4 cytokine levels (Farhadihosseinabadi et al. 2019). Chitosan as a vaccine adjuvant has particularly shown significant evidence for nasal vaccine, where it has reached clinical investigation as an adjuvant on norovirus vaccine (Smith et al. 2014).

Table 3. Summary of other chitosan applications.

Purpose	Major considerations	Reference
Bone	Chitosan might be appropriate bioimplant for bone fracture and cartilage healing but the results are partially controversial	Oryan & Sahvieh 2017
Bone	Chitosan combined to calcium phosphate hydroxyapatite is characterized by good osteoconductivity and stimulation of osteogenesis and researchers are aiming to develop scaffolds with adequate mechanical properties	Stepniewski et al. 2018
Dentistry	Chitosan has been used as an antimicrobial, adhesive, scaffold, cariostatic and oral drug deliverer	Husain et al. 2017
Drug delivery	Chitosan-based micro/nanoparticulate systems have researched as drug delivery systems where its solubility, mucoadhesive nature, ability to transiently open epithelial junctions and biodegradability induced by lysozyme (mucosal surfaces) and chitinase (intestinal flora)	Ahsan et al. 2017
Neuro	Chitosan has shown neuroprotective activity and researched for Alzheimer´s disease	Ouyang QQ et al. 2017
Neuro	Chitosan oligosaccharides possess protective effects against neuronal disorders	Hao et al. 2017
Other	In cancer therapy chitosan has showed applicability in chemotherapeutic delivery and in healthcare as an adjuvant in vaccine immunotherapy and as a nasal absorption enhancer	Babu & Ramesh 2017
Other	Chitosan could potentially be used for insulin delivery, antimicrobial objectives and targeting cancer cells	Tabasum et al. 2017
Other	Chitosan has antioxidative, hypocholesterolemic, antimicrobial and anti-inflammatory benefits	Je & Kim 2012
Other	Chitosans anti-inflammatory mechanism is explained by downregulation of inflammatory chemokine messenger RNA expression, selectin blockage, immune induction and inflammatory cytokine decrease	Lee et al. 2017
Other	Chitosan dressing has showed promising results decreasing edema and improving hemostasis in sinus surgery	Zhou et al. 2017

2.5.3 Polycaprolactone and poly(L-lactide-co-ε-caprolactone)

PCL is one of the most used aliphatic polyesters in regenerative medical science, along with polylactide (PLA), polyglycolide (PGA) and polyethylene glycol (PEG) (Fernandez et al. 2012). PCL can be prepared by condensation of 6-hydroxycapric or ring-opening polymerization of ε-caprolactone, the latter being the main route (Labet & Thielemans 2009). Ring-opening polymerization is a chemical reaction in polymer chemistry, in which the terminal end of a polymer reacts with cyclic monomers, opening them to allow further chaining (Figure 13) (Nuyken & Pask 2013).

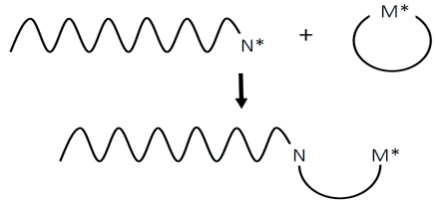

Figure 13. Schematic simplification of ring-opening polymerization.

PCL is soluble in chloroform, benzene, toluene, cyclohexanone, 2-nitropropane, acetone, 2-butanone, ethyl acetate, dimethylformamide and acetonitrile, but insoluble in alcohols, petroleum ether, diethyl ether and water at room temperature (Sinha et al. 2004). PCL has a low melting point (60 °C) and low viscosity, and it can be easily processed thermally (Gross & Kalra 2002). The low -60 °C glass transition temperature of PCL widens its potential use as a biomaterial compared to most absorbable polymers, which are inflexible due to higher glass-transition temperature, have low elongation break values, high crystallinity and thus possess unfavorable qualities for numerous clinical purposes (Fernandez et al. 2012).

Degradation conditions, molecular weight and crystallinity degree determines PCLs hydrolytic degradation, which takes several months to years (Labet & Thielemans 2009). The human body is incapable of enzymatically degrading PCL, but multiple microbes are capable of enzymatic degradation (Gross & Kalra 2002). The degradation of PCL is thought to be three-tiered (Labet & Thielemans 2009):

1. Amorphous structure degradation, where crystallinity degree increases and molecular weight remains constant,
2. Mass decrease, due to ester bond cleavage,
3. Carboxylic acid autocatalytic degradation by end chain scission (high temperatures) or random chain scission (low temperatures)

PCL's crystallinity degree decreases upon copolymerization with lactide (PLCL), leading to higher water absorption and higher degradation rate, making it more appropriate for tissue engineering (Garkhal et al. 2007). Thus, lactide copolymerization is a suitable method to control PCL's mechanical properties, shape-memory, degradation and drug-releasing properties (Fernandez et al. 2012). Higher lactide amount increases PLCL's glass transition temperature, leading to a harder texture, whereas PCL amount increase causes higher flexibility, and a rubberier construction (Burks et al. 2006). PLCL's glass transition temperature is 9 °C, but at body temperature PLCL remains elastic (Zhu et al. 2007).

Applications of PLCL

PLCL has been studied in a variety of applications, such as vascular, nerve and musculoskeletal disorders (Table 4).

In this thesis, the focus was on urethral regeneration. PLCL has not been studied extensively in urological applications. Human urothelial cells attach, proliferate and maintain their viability and phenotype on PLCL membrane (Sartoneva et al. 2011). Thus, PLCL has significant further potential for urothelial tissue engineering. Smooth or textured PLCL membranes are more suitable for urothelial tissue engineering in terms of human urothelial cell cultivation and mechanical properties than compression-molded PLCL membranes (Sartoneva et al 2012). PLCL blended 70:30 with poly-(1,1-lactide-co-glycolic acid) has been reported to be suitable as a stent-like connector between the blabber neck and urethra, due to tunable degradation rate and alterable mechanical properties (Ang et al. 2018). PLCL has been found *in vivo* to be more suitable for ureter regeneration than acellular aortic arch (Kloskowski et al. 2014). Vaginal epithelial and stromal cells also attached and retained their viability on a novel CO_2 foamed PLCL scaffold, demonstrating PLCL's potential for vaginal epithelial tissue engineering (Sartoneva et al 2018).

For dermal application, finger-shaped porous PLCL scaffolds were 3D printed and seeded with human dermal fibroblasts *in vitro*, combined with peptide hydrogel coupled with neuropeptide substance P to accelerate angiogenesis and recruit mesenchymal stem cells (Im et al. 2018). The results of these *in vivo* implanted scaffolds suggested that PLCL combined with substance P containing peptide hydrogel might be a good future treatment modality for skin defects.

Table 4. Summary of other PLCL applications (+ = combined, vs. = compared).

Purpose	Material	Major considerations	Ref.
Bone	PLCL + Tween 80	PLCL blended with Tween 80 (a nonionic surfactant) improved PLCLs hydrophilicity and osteogenicity	Yassin et al. 2016
Bone	PLCL vs. others	Tyrosine-derived polycarbonate and poly(propylene fumarate) scaffolds showed better osteoconductivity compared to poly(L-lactide-co-glycolide) and PLCL scaffolds for bone defect treatment in vivo but mineralized cancellous allograft was found superior	Luang-phakdy et al. 2013
Cartilage	PLCL	In vitro and in vivo results suggest that PLCL could be promote chondrogenic differentiation and chondral ECM deposition	Jung et al. 2008
Cartilage	PLCL	Chitosan modification might enhance PLCLs cell compatibility towards better cartilage tissue regeneration without altering mechanical properties	Yang et al. 2012
Esophagus	PLCL + fibronectin	Electrospun PLCL scaffold surface grafted with fibronectin and seeded with porcine esophageal epithelial cells has in vitro been suggested as a potential functional esophagus substitute	Zhu et al. 2007
Nerve	PLCL + silk fibroin	In peripheral nerve regeneration, silk fibroin blended to PLCL conduits promoted fibroblast proliferation and VEGF release leading to enhanced vascularization and better axonal regeneration	Wang et al. 2018
Other	PLCL	Biodegradable tissue separation balloons were prepared from PLCL and used as prostate-rectum separators and in rotator cuff tear	Basu et al. 2016
Tendon	PLCL	PLCL for rotator cuff tears in a preclinical in vivo study were found to have a favorable host response upon long-term exposure	Ramot et al. 2015
Tendon	PLCL vs. poly(L/D)lactide	In tendon construct, braided poly(L/D)lactide scaffolds were found superior compared to PLCL scaffolds	Vuornos et al. 2016
Vascular	PLCL	Smooth muscle cells were seeded on PLCL scaffolds and in vivo the scaffolds showed excellent tissue compatibility	Jeaong et al. 2004
Vascular	PLCL + substance P	Substance P was conjugated to PLCL meshes and compared to the nonconjugated mesh and in vitro it promoted angiogenesis and recruited more human mesenchymal stem cells	Shafig et al. 2015
Vascular	PLCL	Mechanical properties and degradation rate of PLCL films had sufficient strength towards aortic pressure and lifespan to allow adipose-derived stem cells growth for aortic regeneration	Burks et al. 2006
Vascular	PLCL	PLCL scaffolds without cell seeding enhanced in vivo endothelial coverage and reduced thrombosis as an aortic vascular graft	Mun et al. 2013

2.5.4 Poly(1,3 trimethylene carbonate)

PTMC is a rubbery amorphous cyclic aliphatic polycarbonate ester (Shi et al. 2009). Aliphatic polycarbonates can be prepared by three methods: condensation polymerization using diols and carbonates; copolymerization of epoxides and carbon dioxide (CO_2); or ring-opening of cyclic carbonates with nucleophilic or cationic initiators (Figure 13) (Zhu et al. 1991). In broad terms, PTMC can also be described as a biodegradable elastomer: a specific biological setting with good biocompatibility, glass transition beneath body temperature, and in a certain manner it maintains its length and form if stretched (Shi et al 2009). PTMC's glass transition temperature (-14 °C) is clearly below body temperature and it becomes extremely soft at about 40–60 °C (Engelberg & Kohn 1991).

The mechanical properties, flexibility and tensile strength of PTMC enhance in correlation with its molecular weight, and 100,000 g/mol has determined as a critical value for PTMC in soft tissue engineering purposes (Pêgo et al. 2003). PTMC's elasticity makes it a potential biomaterial in practice in comparison to other synthetic biodegradable biomaterials, such as PLA and PGA, which can be stiff and possess unfavorable degradation profiles (Papenburg et al. 2009). PTMC can be alternatively synthesized with other polymers, such as aforementioned PLA or PCL, in order to adjust its properties (Papenburg et al. 2009). Gamma irradiation may be used for PTMC crosslinking, which simultaneously further stabilizes and sterilizes it (Bat et al. 2013).

PTMC is soluble in chloroform, methylene chloride, benzene and tetrahydrofuran, and insoluble in water, alcohols and ether (Zhu et al 1991). PTMC's degradation increases *in vivo*, which suggests an enzymatic degradation process, and its degradation does not produce acidic end products (Zhu et al 1991, Zhang et al. 2006). High molecular weight PTMC does not degrade in Dulbecco's phosphate-buffered Saline (DPBS) within two years, but when implanted subcutaneously it degrades nearly completely within three weeks by surface erosion process (Pêgo et al. 2003). Cellular phagocytosis has been suggested to be partly responsible for the rapid *in vivo* degradation process (Pêgo et al. 2003). Later, macrophage-mediated erosion due to cholesterol esterase and superoxide anion radicals has been discovered to be behind the *in vivo* degradation process (Bat et al. 2009). PTMC's fast *in vivo* degradation creates a challenge to obtain proper biomechanics and favorable degradation rate for biomedical applications (Shi et al. 2009). In turn, PTMC's tunable degradation and stabile form offer prospective for biomedical applications, especially for short-term purposes.

Applications of PTMC

PTMC has been studied in a variety of applications (Table 5). Specifically, in urological applications, PTMC has not yet been studied. As a preliminary study, however, rat adipose-derived stem cells were seeded on electrospun PLA and poly(L-lactide)-trimethylene carbonate-glycolide polymers for pelvic organ prolapse and urinary incontinence (Wang et al. 2018). Successful cell seeding increased their biomechanical properties, but the application has not yet been tested *in vivo*.

Recently, PTMC was incorporated with poly(L-co-D,L lactic acid) and handled with aloe vera powder, to create a wound dressing possessing aloe vera's anti-inflammatory, antiseptic and antimicrobial properties (Komatsu et al. 2017). Fibroblast attachment and proliferation *in vitro* and the mechanical features seemed suitable for further *in vivo* studies aiming for skin healing and curative application. Electrospun PCL/PTMC fiber mats were blended *in vitro* with shikonin, a natural bioactive with anti-tumor, antioxidative, antibacterial and anti-inflammatory properties, where the mats showed rapid alterable drug release, and were discussed as a potential treatment against wound or other dermal bacterial infections (Han et al. 2009).

Table 5. Summarization of other PTMC applications (+ = combined, vs. = compared).

Purpose	Material	Major considerations	Ref.
Abdominal	PTMC + PLA	PLA/PTMC (50/50%) membranes significantly decreased postoperative intra-abdominal adhesions after intestine surgery and revealed good biocompatibility	Qin et al. 2006
Abdominal	PTMC	PTMC membrane without combination to PLA, has shown good results as an antiadhesive intra-abdominally	Vogels et al. 2015
Bone	PTMC	PTMC assists bone regeneration degrading 12 weeks after implantation in critical sized mandibular defects	Van Leeuwen et al. 2012
Bone	PTMC vs. PTMC + $Ca_3(PO_4)_2$	PTMC was found suitable for cranial bone defect reconstruction in vivo, although it revealed no differences compared to unfilled defects or PTMC-calcium phosphate	Zeng et al. 2017
Bone	PTMC	PTMC based drug delivery (gentamycin and vancomycin) showed promising results for osteomyelitis	Kluin et al. 2009
Cardio	PTMC + D,L-lactide	PTMC copolymerized with D,L-lactide has shown to be noncytotoxic allowing cardiomyocyte adhesion and proliferation with suitable mechanical properties	Pêgo et al. 2003
Neuro	PTMC	Human Schwann cells attached and proliferated on PTMC films in vitro on an artificial nerve graft	Pêgo et al. 2003
Neuro	PTMC	PTMC combined to high caprolactone content has been in vitro shown to promote axonal regeneration and prompting neurons into a regenerative state	Rocha et al. 2014
Ophthalmology	PTMC	In vivo histopathology showed that PTMC was suitable as a drainage device in glaucoma surgery	Rönkkö et al. 2009
Ophthalmology	PTMC + poly(ethylene glycol)	PTMC crosslinked to poly(ethylene glycol) has been investigated as an intravitreal corticosteroid delivery system	Amsden & Marecak 2016
Vascular	PTMC	Tubular PTMCs were shown in vitro to be highly biocompatible for human umbilical vein endothelial cells, smooth muscle cells and mesenchymal stem cells with excellent mechanical properties for vascular engineering	Song et al. 2010, Song et al. 2011
Vascular	PTMC + L-lactide	PTMC copolymerized with L-lactide showed good cytocompatibility and hemocompatibility as a cardiovascular stent in vitro	Shen et al. 2015

3 AIMS OF THE STUDY

The general aim of this thesis was to discover biocompatible solutions for epithelial repair for full-thickness skin and urothelial defects. AM, CM, PLCL and PTMC were studied with *in vivo* and *in vitro* models.

The specific aims were:

1. To evaluate the effect of AM on wound healing, considering wound size, histology and systemic IL-4 levels, using a rat model (I).

2. To investigate how CM suits wound healing, in terms of wound size, contraction, histology and systemic IL-4 levels, with a rat model (II).

3. To evaluate the suitability of PLCL and PTMC for urethral defect reconstruction, with *in vitro* and *in vivo* rabbit models (III).

4 MATERIALS AND METHODS

4.1 Animals (I-III)

The Sprague-Dawley rat was chosen for wound studies, whereas New Zealand White rabbits were used for the urethral regeneration model. The animals underwent the surgical procedures and sample collection under general anesthesia. Postoperative pain was relieved. The animals were individually caged on an *ad libitum* diet, and followed by professional animal care personnel. The animals were euthanized after sample collection using CO_2 (I, II) or intravenous pentobarbital (III). The animal experiments are summarized in Table 6.

Table 6. Summary of the animal experiments (a = five control animals, b = only control animals, c = only two control animals for 2- and 4-week histology).

Publication	Groups	Follow-up	Animals per group	Analysis
I	AM Control	0[a], 3, 7, 14 or 21 days	Rat n=6 (total 53)	Wound size Serum sample (IL-4) Histology
II	CM Control	0[b], 3, 7, 14 or 21 days	Rat n=6 (total 54)	Wound size and contraction Serum sample (IL-4) Histology
III	PLCL PTMC Control[c]	2, 4 or 16 weeks	Rabbit n=5 (total 34)	Urethrography Histology Immunohistochemistry

The National Research Council's guide for the care and use of laboratory animals was followed during the studies (I–III). The Animal Care and Use Committee of the respective Provincial Committee for Animal Experiments admitted the permits for animal experiments (ESLH-2008-04691/Ym-23, ESLH-2009-06718/Ym-23). Researchers attending to animal experiments had licenses to perform animal experiments. The collection of placentas, and thereby AM (R06045), and human urothelial tissue (R07160) samples from volunteer donors were conducted in accordance with the guidelines of the Ethics Committee of the Pirkanmaa Hospital District, Tampere, Finland. The studies followed the Helsinki declaration.

4.2 Amniotic membrane (I)

Placentas, including the chorion-amnion sacs and umbilical cords, were received from volunteer donors undergoing elective caesarean section. Donors were tested for syphilis, human immunodeficiency virus, hepatitis B and C prior to placental donation. The caesarean sections took place in Tampere University Hospital. After tissue donation, the placentas were stored at -80 °C until further use.

The placentas were thawed overnight at room temperature to prepare the AM needed. Chorion-amnion sacs were sharply detached from the placentas. AM was separated from chorion membrane using blunt dissection and AM was rinsed ten times with 0.9% weight/volume (w/v) sodium chloride (NaCl) (Baxter Healthcare Ltd., Newbury, United Kingdom) to remove blood clots and chorion remnants. AM was then cut into appropriately sized pieces to handle and incubated overnight in 10% antibiotic solution in DPBS (Lonza Group Ltd., Basel, Switzerland) at 4 °C. The antibiotic solution contained amphotericin B (2.5 µg/mL, Invitrogen Inc., Carlsbad, USA), penicillin (5.0 µg/mL Invitrogen Inc.), streptomycin (50 µg/mL, Invitrogen Inc.) and neomycin (100 µg/mL, Aldrich Inc., St. Louis, USA). On the following day, processed AM was restored in plastic containers of DPBS with antibiotics and glycerol at a ratio of 1:1 (Merck & Co. Inc., New Jersey, USA.) and cryopreserved at -80 °C.

Cryopreserved AM was thawed at 37 °C in a water bath and rinsed three times with DPBS to remove DPBS-glycerol (Lonza Group Ltd.) solution. AM was then spread on a Petri dish and incubated overnight at 4 °C in dispase-solution (1 mg/mL, Invitrogen Inc.) in Dulbecco's Modified Eagle Medium with nutrient mixture F-12 (Thermo Fisher Scientific, MA, USA) containing penicillin (5.0 µg/mL Invitrogen Inc.), streptomycin (100 µg/mL, Invitrogen Inc.) and amphotericin B (2.5 µg/mL,

Invitrogen Inc.). Dispase incubation was conducted to remove epithelial layer of AM and reveal the basement membrane. After the overnight incubation, gentle scraping (Corning® cell scraper, Sigma Aldrich Inc., St. Louis, USA) ensured the removal of the epithelial layer, which was verified by microscopic (Nikon Zoom Stereomicroscope SMZ800) inspection. To remove dispase remnants, AM was rinsed 10 times with DPBS (Lonza Group Ltd.). Processed AM was cut in approximately 20 mm diameter round pieces and spread on CellCrown6-rings (Scaffdex Oy, Tampere, Finland) to ease the application process (Figure 14).

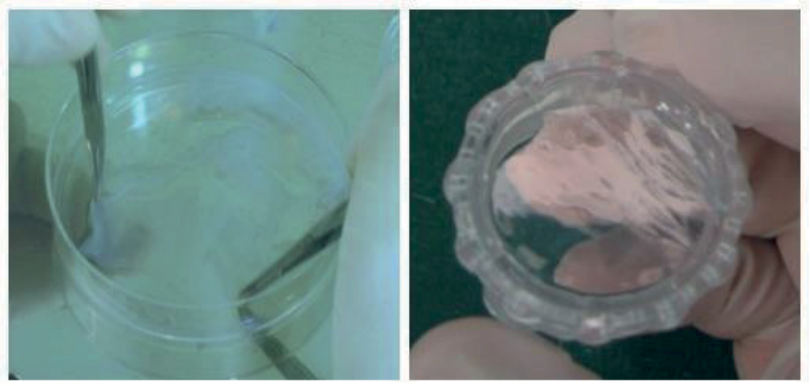

Figure 14. CellCrown6-rings (Scaffdex Oy) were utilized for AM wound site application.

4.3 Chitosan membrane (II)

Chitosan was received from Novasso Oy (Novasso Oy, Tampere, Finland), whereof the membranes were manufactured in the Department of Electronics and Communications Engineering of Tampere University. 73% deacetylated microcrystalline chitosan was used to manufacture CMs. The molecular weight of chitosan was 240 kDa. Chitosan was dissolved in a solution containing deionized water and acetic acid (Sigma Aldrich Inc.). The composed solution contained chitosan and solvent in a 1:1 w/v ratio, and achieved 1.5 wt% chitosan. The chitosan solution was then poured into polytetrafluoroethylene molds. Molds containing chitosan solution were dried in a laminar flow cabinet for 48 h and then additionally for one week in a vacuum at room temperature. Manufactured CMs were approximately 120 μm thick.

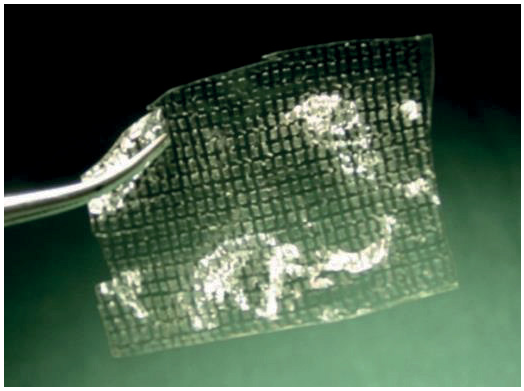

Figure 15. Prepared CM, ready to be tailored and applied.

Due to acetic manufacturing process that the use of acetic acid caused, CMs had to be neutralized before use, to enhance biocompatibility. CMs were first incubated in 5 M NaOH (Baxter Healthcare Ltd.) for 30 min at room temperature. After NaOH incubation, the CMs were rinsed ten times with 0.9% NaCl (Baxter Healthcare Ltd.), and five times with DPBS (Lonza Group Ltd.). The neutralization (pH 7.0) was ensured with pH indicator paper (Merck & Co. Inc.). The CMs were then ready to be applied to the wound surface (Figure 15). The definitive size and shape were tailored immediately prior to application.

4.4 Poly(L-lactide-co-ε-caprolactone) (III)

Proxy Biomedical (Proxy Biomedical Ltd, Galway, Ireland) provided medical grade PLCL membranes for the study. PLCL membranes were manufactured with film molding and the membranes were 200 μm thick. The surface of the membranes was textured using a micromachining device and the samples were sterilized using gamma irradiation at 25 kGys. X-ray microtomography (Zeiss Xradia MicroXCT-400, Zeiss, Pleasanton, USA) was used to image the surface structure of PLCL membrane, and the image stacks were reconstructed to three-dimensional images using special software (Figure 16) (Xradia XRMreconstructor software, Zeiss). The PLCL membranes were tailored before use to precisely cover the urothelial defects.

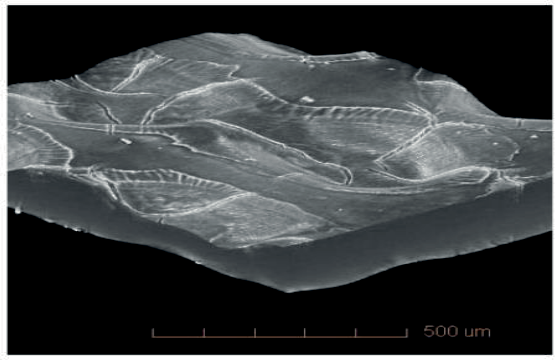

Figure 16. Microtomography image of PLCL membrane used in the study.

4.5 Poly(1,3 trimethylene carbonate) (III)

The Department of Biomaterial Science and Technology of Twente University provided PTMC membranes for the study. High molecular weight poly(1,3 trimethylene carbonate) membranes were synthesized under nitrogen blankets at 150 °C by 6 h ring opening polymerization of trimethylene carbonate (Boehringer Ingelheim, Ingelheim am Rhein, Germany). In the synthesis process, stannous octoate (Sigma Aldrich, St. Louis, USA) was used as a catalyst, and water as an initiator. The complete polymer tube was melted at 160 °C and compressed with up to 100 kN compression in a molder (Fontijne laboratory press THB400, The Netherlands). The first compression was followed by a two-step compression cycle, with the first cycle under 30 kN force for 1 min, followed rapidly by 300 kN force for 1 min. In the final synthesis step, 30 kN force was applied for 2.5 min, and raised to a final force of 350 kN for 1.5 minutes. The produced membranes were 250 μm thick and their molecular weight was approximately 275 kg/mol. Produced PTMC membrane was also imaged using μCT (Zeiss), as mentioned regarding the PLCL membrane (Figure 17). PTMC membranes were then cut, packed, vacuum-sealed and sterilized using 25 kGy Cobalt-60 sourced gamma irradiation (Synergy Health, Ede, The Netherlands). The PTMC membranes were cut to size immediately prior to application.

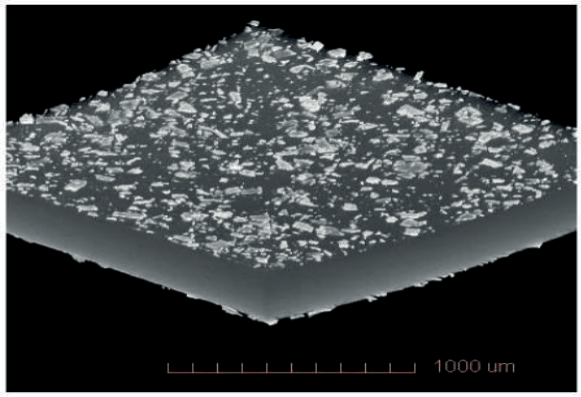

Figure 17. Microtomography image of PTMC membrane used in the study.

4.6 Wound healing model (I-II)

Healthy adult male Sprague-Dawley rats (Harlan laboratories, Horst, Netherlands) were selected for the experiments. The animals were held on an *ad libitum* diet, caged individually and housed in the Animal Laboratory of University of Tampere throughout the studies. The National Research Council's Guide for the Care and Use of Laboratory animals was followed.

4.6.1 Experiments

The rats were weighed and anesthetized by intraperitoneal medetomidine-ketamine (Domitor 0.05 mg/100 g; Orion Oyj, Espoo, Finland and Ketalar 7.5 mg/100 g; Parke-Davis Inc., Caringbah, Australia) injections. Under anesthesia, the area of surgery was cleansed with ethanol (Etax A, Altia Oyj, Helsinki, Finland) and shaved (I-III). Moistened Aquacel® wound dressing was selected due to pilot results before the actual studies were executed.

Round areas ~15 mm in diameter were marked on rat scalps (I, II). Along these marks, skin defects were excised on the scalps of rats using surgical scissors (Figure 18). The defects were then measured from two directions perpendicular to each other. The formed wound was defined using the mathematical formula of an ellipse: Awound = $\pi \times A \times B$, where A and B are semi-major and minor axes of an ellipse, to define wound area as mm^2.

The wound sites were additionally tattooed with dot-like marks to detect contraction in the study concerning CM (II). The area which the dot-like tattoo marks outlined, was also measured and defined as an ellipse, as mentioned above. After the excision, tattooed marks (II) and areal measurements were performed, the rats were randomized into groups: AM (I) or CM (II) and control groups. In the AM or CM groups the wounds were covered with AM or CM and Aquacel® (ConvaTec Oy, Espoo, Finland), whereas in the control group the wounds were covered with Aquacel® (ConvaTec Oy) alone. Aquacel® (ConvaTec Oy) was moistened before use with 0.9% NaCl (Baxter Healthcare Ltd.). In the AM (I) group, the enzymatically revealed basement membrane side of AM faced the wound site and the spongy layer up against Aquacel® (ConvaTec Oy). In the CM (II) group, the processed CM pieces were tailored to fit the wounds precisely, immediately prior to application. In primary anesthesia, all animals were given subcutaneous buprenorphine (0.002 mg/100 g, Schering-Plough Europe Inc., Brussels, Belgium) injections for postoperative pain relief. Buprenorphine (Schering-Plough Europe Inc.) injections were repeated daily if the rats exhibited pain under supervision of professional animal care personnel.

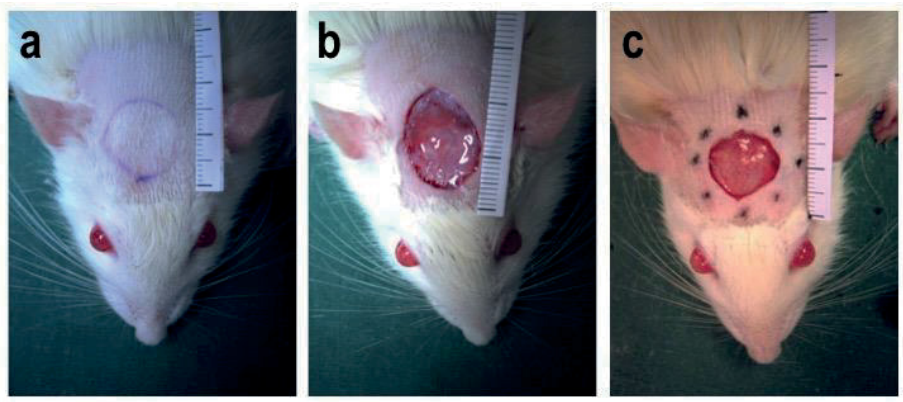

Figure 18. Wounds were measured, marked, excised (a) and covered with tailored AM (b) or CM (c) and Aquacel® in the study group. Control animal wounds were treated alone with Aquacel®. In the CM study (II) the wound sites were additionally tattooed (c).

4.6.2 Follow-up

The rats were subdivided within AM, CM and control groups into follow-up groups and followed up for 0, 3, 7, 14 or 21 days. At the end of each time-point, rats were anesthetized again with intraperitoneal medetomidine-ketamine (Orion Oyj,

Parke-Davis Inc.) injections with dosages described above, similar to primary anesthesia. The anesthetized rats then underwent a final examination, including wound area measurements, tattooed area measurements (II), blood sample withdrawal via heart puncture for systemic IL-4 analysis, wound site excision for histological analysis, and CO_2 euthanasia. Wound areas were defined as mentioned above, without knowing the group, and represented as percentages from the original wound area. The day zero follow-up group contained only control rats. Time-points - expect the day zero control group in the AM study (n = 5) - contained 6 control rats and 6 study rats (I, II). Day zero group rats underwent the final examination under primary anesthesia.

4.7 Urethral regeneration model (III)

New Zealand White rabbits (Harlan laboratories, Horst, Netherlands) were selected for the experiments, caged individually on an *ad libitum* diet, and housed in the Animal Laboratory of University of Tampere. The National Research Council's Guide for the Care and Use of Laboratory animals was followed.

4.7.1 Experiments

The rabbits were anesthetized using medetomidine-ketamine (0.3 mg/kg Domitor, Orion Oyj and 0.3 mg/kg Ketalar, Parke Davis Inc), which were given intramuscularly. The rabbits also received preoperative intramuscular prophylactic antibiotic (2.5 mg/kg enrofloxacin, Baytril Vet, Bayer Animal Health, Leverkusen, Germany).

A longitudinal incision of 2 cm was made from the inguinal region to penile region of disinfected rabbit skin (III). After the anterior urethra was exposed, an oval 2 x 1 cm defect was created and four 6/0 nonabsorbent holding sutures (Figure 19) (Ethilon, Ethicon Inc., New Jersey, US) were placed into each quarter of the defect. The defect site was covered with a tailored on-lay PLCL or PTMC membrane, which was sutured onto the free edges of the urothelial mucosa using an absorbable 6/0 suture (PDS II, Ethicon, New Jersey, US). The attached membrane was then tubularized around a transurethral catheter (Mediplast AB, Malmö, Sweden) and 4/0 absorbable sutures (Vicryl, Ethicon Inc, New Jersey, US) were used for wound closure. After the operation the catheter was removed. Two rabbits underwent sham

surgery, where the defect was created in similar manner, but the excised tissue was sutured back as a graft to investigate whether the operation caused inflammation. The animals received subcutaneous carprofen (4 mg/kg Norocarp Vet, Norbrook Laboratories Ltd, Newry, Northern Ireland) and buprenorphine (0.05 mg/kg, Schering-Plough Europe Inc.) injections under primary anesthesia for postoperative analgesia. Buprenorphine (Schering-Plough Europe Inc.) injections were repeated regularly on the first postoperative day, where carprofen (Norbrook Laboratories Ltd) injections were given daily until the second postoperative day, and continued daily if necessary.

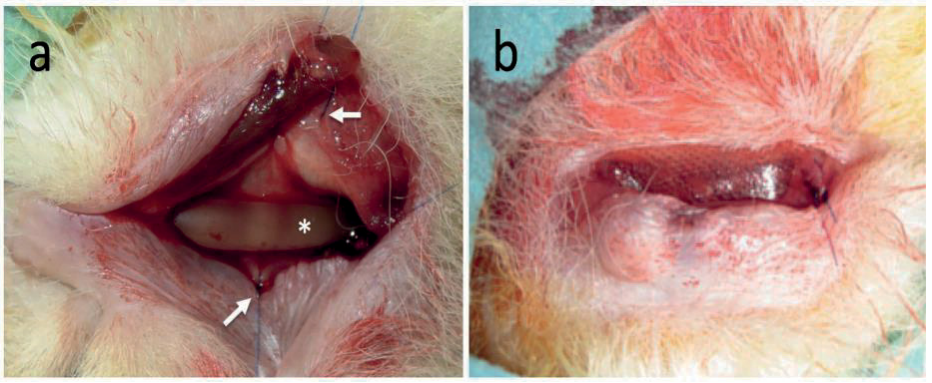

Figure 19. An oval urethral defect (a) was excised from a longitudinal incision and covered with tailored PLCL or PTMC (b), which was fixed using nonabsorbent sutures. The transurethral catheter is marked with an asterisk, whereas the arrows indicate the defect edge holding sutures.

4.7.2 Follow-up

Both PLCL and PTMC membrane treated groups were followed up for 2, 4 or 16 weeks, and both groups and all time points contained 5 animals. After follow-up, the animals were weighed and anesthetized similarly to the previously described primary anesthesia. Then the animals were catheterized (Mediplast AB) distally to the defect area, and the catheter was fixed with an encircling holding suture (Ethicon Inc.) to the distal end of the penis. Iohexol radiocontrast agent (Omnipaque, GE Healtcare AS, Oslo, Norway) was injected through the catheter and simultaneous X-ray pictures (Philips Oralix, Amsterdam, Holland) were taken to examine the operation site. After the urethrographic examination, the animals were euthanized

with intravenous pentobarbital (1 mg/kg, Orion Oyj). The defect area was excised instantly after euthanasia and stored in 4% paraformaldehyde (PFA) (Sigma-Aldrich Inc.) for histological analysis and immunohistochemistry. The operation sites of the sham operated rabbits (n = 2) were respectively excised for further histological analysis.

4.8 Histological analysis (I-III)

In the histological analysis, the harvested tissue samples were PFA fixed, paraffin embedded and stained. A light microscope (Nikon Corporation) was used to analyze the histological finding in the following manner.

Wound histology

The wound sites (I, II) were collected including the rat skull underneath, cross-sectioned in paraffin, and stained with hematoxylin-eosin (HE) (Histola Oy, Tampere, Finland). In the second study, the remaining half of the sample was further cross-sectioned, forming a perpendicular half-view of the first section to cover more information from the wound site. The histological analysis was performed without knowing the group or follow-up. Epithelialization, edema, fibrin, necrosis, hemorrhage, angiogenesis and leukocytosis were analyzed (I, II). Epithelialization was calculated from the wound sites using a microscopical ten-grid and represented as percentages covering the estimated size of the original wound. Edema and fibrin were scored from 0–3, from five different views, using 4X magnification. Necrosis, hemorrhage and angiogenesis were likewise scored from 0–3, but viewed from nine different views, using 25X magnification. Score zero corresponded to normal, score one mild, score two moderate and score three severe incidence of each parameter. The final score was an average of the views analyzed. Leucocytes were represented as cell count average from nine different views, using 25X magnification. The presence of AM and CM were also observed.

Urethra histology

In the urothelial study (III), the defect areas were collected after controlled euthanasia at end time-points. Samples were stained with HE (Reagena Oy, Toivala, Finland) and Masson's trichrome (Sigma-Aldrich Inc.) stain. The histological examination was performed without knowing the group using 40X magnification.

The examined parameters from HE stained samples were edema, inflammatory cell appearance, epithelial integrity, and epithelial structure. Edema was scored from zero to three, where zero represented no edema, one mild, two moderate and three severe edema (Sayeg et al. 2013). Inflammatory cell appearance was also scored, where zero represented normal cell appearance, one <25%, two 25–50% and three >50% of all cells. Epithelial integrity was categorized as discontinuous or continuous. Epithelial structure was respectively categorized as no structure, monolayer or layered, i.e. stratified normal urothelial structure (Villoldo et al. 2013). Fibrosis was defined from the samples stained with Masson's trichrome stain and scored. Score zero indicated no fibrosis, one mild (<25%), two moderate (25–50%) and three severe (>50%) (Uyeturk et al. 2014). The sham operated rabbit samples were respectively analyzed at 2- and 4-week time-points. The membranes were also observed from the defect site.

4.9 Interleukin 4 analysis (I-II)

Serum IL-4 levels were analyzed regarding wound healing studies in support of the thorough histological analysis. At the end time points, ~5 mL blood samples from each rat via transthoracic heart puncture were collected in serum tubes (BD Inc., Franklin Lakes, USA). Serum tubes were cooled down for >1 h at 4 °C before being centrifuged for 10 min at 1,000 g. The separated serum was pipetted into separate vials. Serum samples were stored at -80 °C. When all the samples had been harvested, they were thawed at room temperature. Three parallel samples from each rat were measured using Rat IL-4 ELISA kit (Diaclone / Gen-Probe Life Sciences Inc., Besancon, France) to detect IL-4 levels according to manufacturer's instructions. Results were analyzed on a multilabel counter with 450 nm wavelength (Wallac Victor 1420 Multilabel Counter, Waltham, USA).

4.10 Immunohistochemistry (III)

Pancytokeratin AE1/AE3 staining was used to detect the urothelium from the samples. For the analysis, the samples were PFA-fixed and embedded into paraffin (Sigma-Aldrich Inc.). The samples were then microwaved in 10 mM EDTA buffer (Sigma-Aldrich Inc.) and blocked in 3% hydrogen peroxide (Sigma-Aldrich Inc.) for antigen retrieval. After this, the samples were incubated in primary 1:100 antibody

dilution (Thermo Fisher Scientific Inc.) overnight and conjugated with 1:200 secondary antibody dilution (Goat anti-mouse IgG, Thermo Fisher Scientific). The samples were then analyzed microscopically (Nikon Corporation).

4.11 Urothelial cell culture on PLCL and PTMC membranes (III)

4.11.1 Cell culture

The suitability of PLCL and PTMC for urothelial cells was tested *in vitro*. Human urothelial cells were harvested from tissue samples that were received from three volunteer child donors undergoing ureter surgery conducted for clinical indications. The tissue samples were cleansed, pieced and incubated in a solution containing 0.01% of 1 M HEPES buffer (Sigma-Aldrich Inc.), 4 x 10–3% of kIU aprotin (Sigma-Aldrich Inc.), 0.1% EDTA (Sigma-Aldrich Inc.) and 0.01% penicillin-streptomycin (Lonza Group Ltd.) in Hanks' balanced salt solution without Ca^{2+} or Mg^{2+} (Invitrogen Inc., MA, USA). After the incubation process, urothelial sheets were separated from the tissue samples and incubated in 0.1% trypsin solution (Lonza Group Ltd.). The enzymatic activity of trypsin was inactivated using 10% human serum (PAA Laboratories Inc., Pashing, Austria), which was added with Hanks' balanced solution (Invitrogen Inc.). The solution was then centrifuged, and the resulting urothelial cell containing pellet was suspended in urothelium medium (Invitrogen Inc.). The isolated human urothelial cells were then cultured in cell bind T75 flasks (Sigma-Aldrich Inc.) at 37 °C in an air atmosphere containing 5% CO_2. Isolated human urothelial cells were expanded for further use. The isolation followed the protocol Southgate et al. has represented (Southgate et al. 2002), which has been executed by our group previously (Sartoneva et al. 2011).

4.11.2 Live/dead and CyQuant analysis

The PLCL and PTMC membranes were attached to CellCrown48 (Scaffdex Oy) culture devices. The membranes were then incubated for 24 h in urothelium medium (Epilife, Invitrogen Inc.) prior to actual cultivation. 30,000 cells/cm^2 on each membrane were seeded in 30 μL of urothelium medium (Invitrogen Inc.), allowed to attach for 2 h, added with 500 μL of urothelium medium (Invitrogen Inc.) and

cultivated for 7 and 14 days at 37 °C. The urothelium medium (Invitrogen Inc.) was changed twice a week. The viability of the cultivated urothelial cells was verified using live/dead staining. For the staining, the cultivated cells were incubated for 30 min at room temperature in a solution containing 0.25 μM calcein-AM (Molecular Probes, Waltham, USA) and 0.3 μM ethidium homodimer-1 (Molecular Probes). After staining the cultures, a fluorescence microscope (Olympus, IX51S8F-2, camera DP71, Tokyo, Japan) was used to estimate the amount of viable living cells, which stained green. Non-viable cells stained red.

In addition, cell attachment of the urothelial cells on the PLCL and PTMC membranes was verified by determining the amount of total DNA. The DNA amount was determined using CyQUANT Cell Proliferation Assay kit (Invitrogen). Three parallel cultivations on PLCL and PTMC membranes were cultured for 24 h. Urothelial cells were extracted from the same patient sample, and 20,000 urothelial cells were seeded into each well. Cultivated cells were lysed using 0.1% Triton-X-100 buffer (Sigma-Aldrich), stored at -70 °C and then thawed for analysis, where 20 μL of each sample was mixed with 180 μL of working solution, which contained CyQUANT GR dye and lysis buffer (Invitrogen). A multiplate reader was then used to measure the fluorescence levels at 480/520 nm (Wallac).

4.11.3 Real-time reverse transcription polymerase chain reaction

After culturing urothelial cells on PLCL or PTMC membranes for 14 days, the relative expression of urothelium marker genes were studied using qRT-PCR. 50,0000 urothelial cells/cm^2 were seeded and cultured on PLCL, PTMC or cell culture plastic (polystyrene) surface, which served as a control material. The total RNA was isolated from the cultures with Nucleospin kit reagent (Macherey-Nagel GmbH & Co. KG, Düren, Germany). High-Capacity cDNA Reverse Transcriptase Kit (Thermo Fisher Inc.) was used to reverse transcribe the isolated RNA to complementary DNA (cDNA) and the expression of CK7, CK8, CK19, UPIa, UPIb and UPIII was analyzed. The collected expression data were normalized to the expression of housekeeping gene, which was the ribosomal protein lateral stalk subunit P0. The sequences for the qRT-PCR primers are given in the original publication (Sartoneva & Nordback et al. 2018). The reactions between cDNA, forward and reverse primers and SYBR Green PCR Master Mix (Thermo Fisher Inc.) were conducted with AbiPrism 7000 Sequence Detection System (Thermo Fisher Inc.) with enzyme activation for 10 min at 95 °C, which was followed by 45

cycles for 15 s at 95 °C and 60 s at 60 °C. A previously published mathematical model was used to calculate the relative expression of the above-mentioned markers (Pfaffl 2001).

4.12 Statistical analysis (I-III)

SPSS version 16 and 22 for Windows program (SPSS Inc., Chicago, USA) was used to compose the statistical analysis. Unpaired student's t-test was used for numeric parameters. Numeric parameters were: wound size (I,II), contraction (II), epithelialization (I,II), leucocyte counts (I,II) and IL-4 concentrations (I,II). Mann-Whitney test was used for scored parameters. Scored parameters were inflammation cells (III), edema (I-III), fibrosis (I-III), hemorrhage (I-II), angiogenesis (I-II) and epithelial structure (III). Fisher's test was used to analyze epithelial integrity (III). The statistically significant difference between the groups was set at $p < 0.05$. A statistician was consulted for the statistical analysis.

5 RESULTS

5.1 The use of biomaterials (I-III)

AM and CM were studied on wound surfaces, whereas PLCL and PTMC membranes were studied on urethral defects. AM was found to be challenging to handle due to its slick consistency, but it tolerated tension well during the handling process (I). CellCrown6-rings (Scaffdex Inc.) were discovered to be helpful in handling AM during the application process, and enabled the desired positioning of AMs' basement side towards the wound surface. In practice, CM was found to be more easily handled, and to be tailored to correct shape and size to the wound surface than AM (II). PLCL membranes consistency was harder than PTMC membranes and was thus more laborious to suture in position and mold into the desired shape (III).

Our methods and biomaterials seemed to be tolerable to the animals. There was no need for extra pain medication after the second postoperative day in our wound studies (I-II). Most of the rabbits (III) started to eat, drink and urinate within three days after the surgery. Only one rabbit recovered from surgery on the fourth day instead of the third. Two rabbits from the PTMC group died postoperatively and were excluded from the study after autopsies revealed that the causes of death did not relate to the presence of biomaterials.

5.2 Wound size and contraction (I-II)

Wound size median (± SD) was significantly smaller in the AM group on day three compared to the control group ($p = 0.009$ (I). On day three, the AM group wound area was 60 ± 11% of the original size, whereas the control group wound size was respectively 81 ± 13%. The result considering wound area was similar in the CM group (II), where the CM group wound area median (60 ± 6%) was also

significantly ($p = 0.048$) smaller than the control group wound area median (78 ± 19%). At the final 21-day time-point, the wound areas were 6 ± 3% in the AM group, compared to the 7 ± 6% of the original wound area in the control group (I). In the CM study, the respective percentages were 4 ± 2% in the CM group and 5 ± 3% in the control group (II). The wounds were not significantly different in area between AM or CM groups compared to the control groups at the 7, 14 or 21-day time-points. Throughout the CM study (II), there were no statistically significant differences between the groups in wound contraction, as defined from the tattoo marks.

5.3 Wound histology (I-II)

Wound epithelialization increased from day 3 to 21 in our wound healing studies in the study groups and control groups. Wounds treated with AM seemed to develop faster epithelial coverage on days 3, 7 and 14, but the differences were not statistically significant. At the final time-point (21 days), epithelial coverage had proceeded well, without significant differences ($p = 0.359$). Our observations considering epithelialization in CM treated wounds were analogous. Epithelialization seemed to be faster on days 3, 7 and 14 in the CM group, and on 21-day time point in the control group, without statistically significant differences.

In the AM study, peak scores for edema were observed on day 3 in the AM group, and on days 3 and 7 in the control group. Respectively in the CM study, peak edema scores were observed on day 3 in both groups. Edema decreased to the day 0 score level at the end point of our follow-up in both studies. Wound fibrin scores peaked on day 7 in all groups, but seemed to remain higher than day 0 at the end time-point of 21 days, without significant differences.

Vascular changes in the wound healing studies were examined according to two parameters: hemorrhage and angiogenesis. The highest hemorrhage score in the AM and its control group was on day 3, when it was 1.0 (0.8–1.3). Hemorrhage scores remained stable in the CM group throughout days 3, 7 and 14, when the control group's highest score was observed on day 7. Angiogenesis developed towards the end time-point in the studies in the AM and CM groups. In the control groups, the highest angiogenesis scores where at the 14-day time-point in both studies. The vascular changes were insignificant between the groups.

The leucocyte count remained higher than on day 0 (17 ± 5) in both groups in the AM study. The 21-day leucocyte counts were 42 ± 15 in the AM group, and 38

± 12 in the control group. In the CM group, the leucocyte count was significantly lower ($p = 0.0031$) in the CM group (55 ± 10) on day 7 than in the control group (75 ± 16). Otherwise, there were no significant differences between the groups (Tables 7 & 8).

AM was undetectable from the samples. CM was microscopically visible on days 3 and 7. On days 14 and 21, however, there were no observations of CM anymore.

Table 7. Summary of the histological results of the AM study (I). Necrosis was not present and thus is excluded from the table. Scored parameters are given as median and range. Epithelialization and leukocytes are given as mean ± SD.

	Parameter	AM	Control	p-value
Day 0	Epithelialization (%)	-	0.0	-
	Edema (score)	-	0.5 [0.0 - 0.8]	-
	Fibrin (score)	-	0.0 [0.0 - 0.7]	-
	Hemorrhage (score)	-	0.4 [0.3 - 0.8]	-
	Angiogenesis (score)	-	0.0 [0.0 - 0.5]	-
	Leukocytes (n)		24 ± 9	-
Day 3	Epithelialization (%)	9.5 ± 3.0	6.7 ± 2.3	0.101
	Edema (score)	0.5 [0.0 - 0.8]	1.8 [1.3 - 2.0]	0.310
	Fibrin (score)	1.2 [0.7 - 1.7]	1.2 [1.0 - 1.7]	0.937
	Hemorrhage (score)	1.0 [0.8 - 1.3]	1.2 [1.0 - 1.7]	0.937
	Angiogenesis (score)	0.2 [0.0 - 0.5]	0.3 [0.0 - 0.7]	0.589
	Leukocytes (n)	68 ± 23	72 ± 30	0.834
Day 7	Epithelialization (%)	19 ± 10	15 ± 6.5	0.385
	Edema (score)	1.8 [0.7 - 2.7]	1.8 [0.8 - 2.8]	0.937
	Fibrin (score)	2.0 [0.2 - 3.0]	1.8 [1.3 - 2.5]	1.000
	Hemorrhage (score)	0.7 [0.2 - 0.8]	0.9 [0.6 - 0.9]	0.093
	Angiogenesis (score)	0.3 [0.0 - 1.1]	0.7 [0.3 - 1.3]	0.310
	Leukocytes (n)	68 ± 40	60 ± 17	0.649
Day 14	Epithelialization (%)	45 ± 31	34 ± 15	0.470
	Edema (score)	1.2 [0.3 - 1.5]	1.0 [0.2 - 1.5]	0.589
	Fibrin (score)	1.5 [0.3 - 2.5]	0.8 [0.7 - 1.8]	0.589
	Hemorrhage (score)	0.5 [0.3 - 1.1]	0.6 [0.2 - 0.8]	0.937
	Angiogenesis (score)	1.3 [0.6 - 2.3]	1.5 [0.8 - 2.3]	0.589
	Leukocytes (n)	57 ± 23	68 ± 26	0.422
Day 21	Epithelialization (%)	60 ± 14	72 ± 26	0.359
	Edema (score)	0.3 [0.0 - 0.5]	0.3 [0.0 - 0.7]	0.818
	Fibrin (score)	0.9 [0.0 - 1.3]	1.0 [0.3 - 3.0]	0.699
	Hemorrhage (score)	0.5 [0.3 - 0.6]	0.5 [0.2 - 0.8]	0.937
	Angiogenesis (score)	1.6 [0.3 - 2.1]	1.2 [0.7 - 1.5]	0.240
	Leukocytes (n)	62 ± 15	55 ± 26	0.595

Table 8. Summary of the histological results of the CM study (II). Necrosis was examined but not discovered and thus is excluded from the table. Scored parameters are given as median and range. Epithelialization and leukocytes are given as mean ± SD. * $p < 0.05$

	Parameter	CM	Control	p-value
Day 0	Epithelialization (%)	-	0.0	-
	Edema (score)	-	0.5 [0 - 1]	-
	Fibrin (score)	-	0.0 [0 - 1]	-
	Hemorrhage (score)	-	1.0 [1 - 1]	-
	Angiogenesis (score)	-	0.0 [0 - 0]	-
	Leukocytes (n)		17 ± 5	-
Day 3	Epithelialization (%)	15 ± 4	14 ± 8	0.641
	Edema (score)	2.0 [2 - 2]	2.0 [1 - 2]	0.138
	Fibrin (score)	1.8 [1 - 2]	1.3 [1 - 2]	0.093
	Hemorrhage (score)	1.0 [1 - 1]	1.0 [1 - 2]	0.138
	Angiogenesis (score)	0.3 [0 - 2]	0.2 [0 - 1]	0.902
	Leukocytes (n)	72 ± 12	75 ± 21	0.809
Day 7	Epithelialization (%)	34 ± 7	32 ± 9	0.397
	Edema (score)	1.8 [1 - 2]	2.0 [1 - 2]	1.000
	Fibrin (score)	2.3 [2 - 3]	2.0 [2 - 3]	0.523
	Hemorrhage (score)	1.0 [1 - 1]	1.0 [1 - 2]	0.317
	Angiogenesis (score)	1.0. [1 - 2]	1.5 [0 - 2]	0.523
	Leukocytes (n)	55 ± 10	75 ± 16	**0.031***
Day 14	Epithelialization (%)	41 ± 21	40 ± 15	0.897
	Edema (score)	1.0 [0 - 2]	1.0 [1 - 1]	0.317
	Fibrin (score)	1.0 [0 - 2]	1.5 [1 - 2]	0.116
	Hemorrhage (score)	1.0 [1 - 1]	1.6 [0 - 1]	0.317
	Angiogenesis (score)	1.0 [0 - 2]	2.0 [1 - 2]	0.162
	Leukocytes (n)	58 ± 15	71 ± 29	0.334
Day 21	Epithelialization (%)	88 ± 15	96 ± 11	0.361
	Edema (score)	0.5 [0 - 1]	0.0 [0 - 1]	0.241
	Fibrin (score)	0.5 [0 - 1]	0.0 [0 - 1]	0.575
	Hemorrhage (score)	1.0 [0 - 2]	0.0 [0 - 1]	0.212
	Angiogenesis (score)	1.0 [1 - 2]	1.0 [0 - 3]	0.445
	Leukocytes (n)	42 ± 15	38 ± 12	0.673

5.4 Serum IL-4 levels (I-II)

As a wound-healing transmitter, IL-4 was analyzed from rat serum at the follow-up time-points in the studies. IL-4 levels seemed to decrease in the AM and its control group until day 21. There were no significant differences between the groups within the time-points (I). In the CM group, the difference on days 7 and 14 was statistically significant ($p = 0.007$ and $p = 0.003$, respectively) when it was compared to the control group (II). The IL-4 level was higher in the CM group at these time points (Figure 20). The difference evened out on day 21, without significant differences (II). The highest level of IL-4 in the AM and CM groups were at day 7 in wound healing studies (I-II).

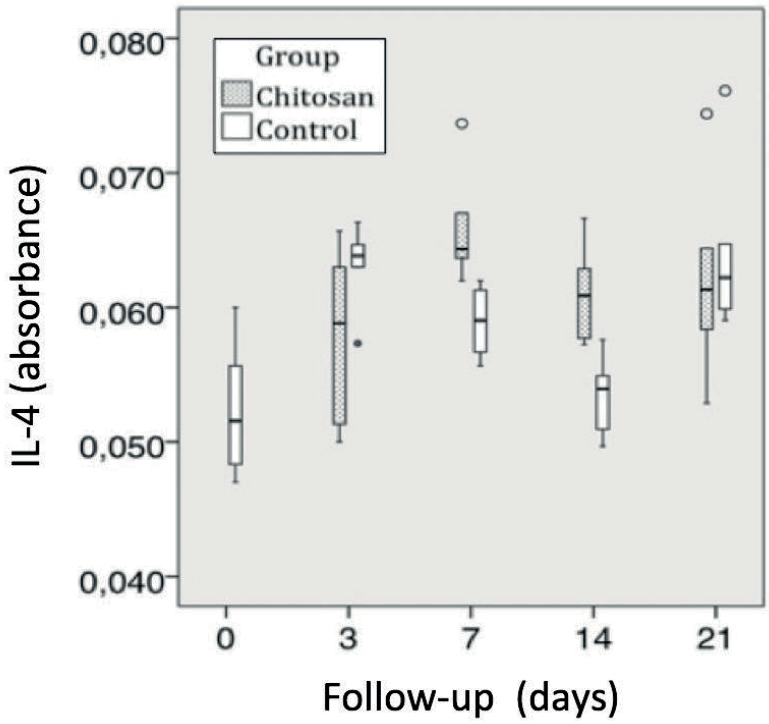

Figure 20. IL-4 (absorbance) levels between the CM and control groups (II) in different time-points. The difference on days 7 and 14 was significantly higher in the CM group ($p < 0.05$). IL-4 levels are given as mean ± SD. Range and dispersion are visualized in the boxplot chart.

5.5 Urethrographic examination (III)

Urethrographic examination was performed on all rabbits, 2, 4 or 16 weeks after primary surgery, when urethral reconstruction using PLCL and PTMC membranes was performed. In the examination, the radiocontrast agent injected to the urethra and bladder revealed no signs of major urethral strictures (Figure 21). No contrast agent leakage to extra urethral tissue was discovered. The return of spontaneous postoperative urination also supported the finding of urethrographic examination.

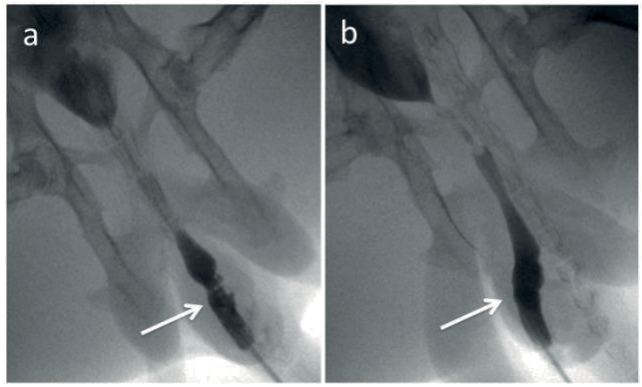

Figure 21. Images from the urethrographic examination 16 weeks after the operation using PLCL (a) and PTMC (b). White arrow marks the reconstruction site. The injected radiocontrast agent is visible in the urethra and bladder as a dark shadow in the images. The examination thus supported the return of spontaneous urination.

5.6 Urethra histology and immunohistochemistry (III)

Inflammation, which was analyzed with edema and inflammation cell appearance, altered from none to moderate in PLCL and PTMC treated urethral defects. At the 16-week time point, the edema score median was zero (= none) in the PLCL group, and one (mild) in the PTMC group. The difference was statistically insignificant ($p = 0.548$). Inflammation cell appearance scores at the 16-week time point were zero [range 0–1] and zero [0–2], respectively, without significant differences ($p = 0.841$). Throughout the study, the highest inflammation cell appearance score was observed at the 4-week time-point in the PTMC group (2 [0–3]).

The urothelium was evaluated with two parameters: epithelial integrity (discontinuous or continuous) and structure (no structure, monolayered or layered

structure). The epithelial structure developed normal, continuous structure, in both groups during the follow-up. In all samples, epithelial structure was continuous at the 16-week time-point. At the 16-week time-point, 60% in the PLCL and 80% in the PTMC group was already layered stratified epithelium. Within the PTMC group, the difference between 2- and 16-week time-points was statistically significant ($p = 0.048$), where 20% of the samples were layered at the 2-week time-point, compared to the 16-week time point (80%).

Fibrosis scores varied from mild to moderate in both groups. There were no statistically significant differences between the groups. Fibrosis scores were highest at the 16-week time point, considering both groups in similar manner being moderate and ranging from mild (score 1) to moderate (score 2). The results of the control samples are given in Table 9.

PLCL and PTMC perished from the defects after the 4-week time period onwards (i.e. 16-week time point).

In our immunohistochemistry analysis, we stained successfully the tissue samples with AE1/AE3 cytokeratin marker. The analysis demonstrated *de novo* formation of urothelium in both groups. There were no visual differences between the groups at any time-point. The *de novo* urothelium seemed to develop towards stratified epithelium, which is characteristic of normal or mature urothelium.

Table 9. Summary of the histological results of the urothelial study (III).

	Parameter		Control	PLCL	PTMC	p-value
2 weeks	Inflammation	Cells	1	1 [0-2]	1 [1-2]	0.310
		Edema	1	1 [0-2]	0 [0-1]	0.222
	Epithelial integrity	Discontinuous	100 % (1)	60 % (3)	80 % (4)	1.000
		Continuous	0 % (0)	40 % (2)	20 % (1)	
	Epithelial structure	None	0 % (0)	20 % (1)	20 % (1)	1.000
		Monolayer	100 % (1)	60 % (3)	60 % (3)	
		Layered	0 % (0)	20 % (1)	20 % (1)	
	Fibrosis		1	1 [1-2]	1 [1-2]	1.000
4 weeks	Inflammation	Cells	0	1 [0-2]	2 [0-3]	0.310
		Edema	0	1 [0-1]	0 [0-1]	0.690
	Epithelial integrity	Discontinuous	0 % (0)	60 % (3)	100 % (5)	0.444
		Continuous	100 % (1)	40 % (2)	0 % (0)	
	Epithelial structure	None	0 % (0)	20 % (1)	40 % (2)	0.348
		Monolayer	0 % (0)	60 % (3)	60 % (3)	
		Layered	100 % (1)	20 % (1)	0 % (0)	
	Fibrosis		0	1 [1-2]	2 [1-2]	0.067
16 weeks	Inflammation	Cells	-	0 [0-1]	0 [0-2]	0.841
		Edema	-	0 [0-1]	1 [0-2]	0.548
	Epithelial integrity	Discontinuous	-	0 % (0)	0 % (0)	1.000
		Continuous	-	100 % (5)	100 % (5)	
	Epithelial structure	None	-	0 % (0)	0 % (0)	0.545
		Monolayer	-	40 % (2)	20 % (1)	
		Layered	-	60 % (3)	80 % (4)	
	Fibrosis		-	2 [1-2]	2 [1-2]	0.545

5.7 Urothelial cell culture (III)

Urothelial cell viability was confirmed with live/dead staining, in which viable cells cultivated on PLCL and PTMC membranes stained green. The majority of cultivated urothelial cells were viable on both membranes (Figure 22). The amount of dead (i.e. red) cells was minimal after one and two weeks of cultivation.

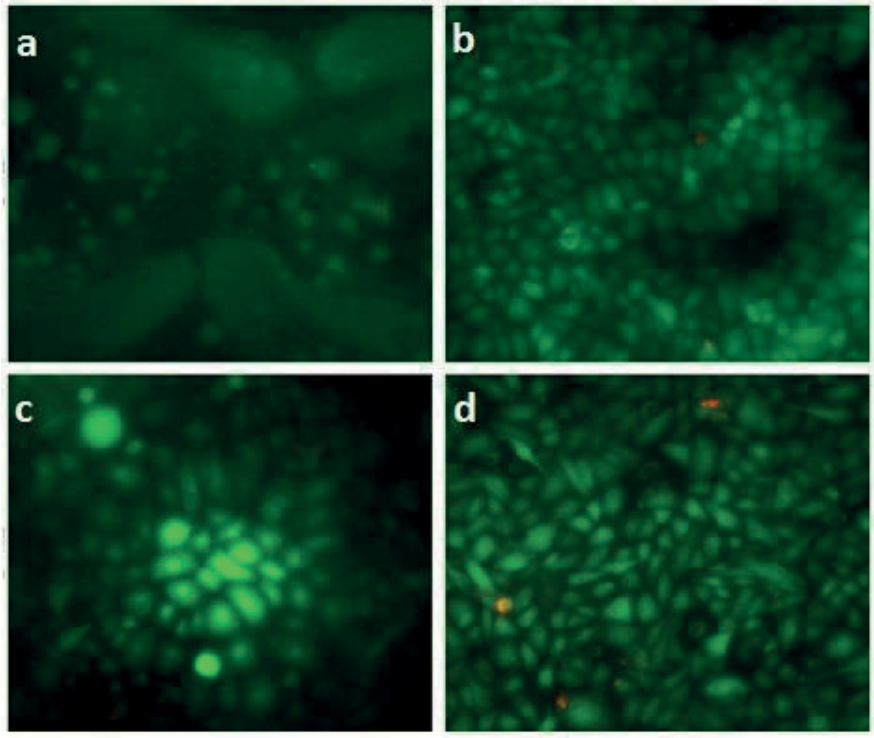

Figure 22. Images a and c represent highly viable urothelial cell cultivation on PLCL membrane after 1 week (a) and 2 weeks (c), whereas images b and d respectively on PTMC membrane. Viable cells stained fluorescent green and dead fluorescent red in live/dead staining.

The CyQUANT assay supported the finding of good cellular attachment but revealed that more urothelial cells attached to the PLCL membrane compared to PTMC one day after cell implantation with a statistically significant difference ($p < 0.05$). The qualitative analysis revealed that the number of urothelial cells was lower on PLCL membrane than PTMC membrane. The difference was clear, especially after the first week of cultivation.

Using qRT-PCR, the expression of different urothelial markers was studied 14 days after cell culture on PLCL, PTMC and polystyrene, which served as a control.

Cultured urothelial cells expressed CK7, CK8 and CK19 on all three materials, whereas the expression of CK7 and CK8 was significantly ($p < 0.05$) higher among PLCL cultured cells, compared to PTMC or the control. However, CK19 expression was significantly ($p < 0.05$) lower on PLCL cultivated cells, compared to the control. From the uroplakins, only UPIa and UPIb were expressed from PLCL cultivated cells, whereas PTMC cultivated cells also expressed UPIII. The expression of UPIb and UPIII was significantly ($p < 0.05$) lower among the PLCL compared to PTMC cultivated human urothelial cells. UPIa expression was significantly ($p < 0.05$) higher in the control compared to PLCL.

6 DISCUSSION

6.1 Wound healing

The application dictates what kind of biomaterial should be considered as "optimal". Particularly in skin wound healing, pain relief, hemostasis, fluid loss prevention, protection and wound healing promotion in general are the most remarkable attributes. Some general qualifications, such as supporting cell viability, attachment, maintenance, proliferation and differentiation, but also structural and mechanical properties are of course important (Keane & Badylak 2014). Costs and ethical issues often play major practical roles as well. One of the advantages of AM and CM is their good availability, although transmitting diseases must be screened considering AM. Thus, the bacterial contamination risk limits AM harvesting to cesarean sections (Adds et al. 2001, Kesting et al. 2008). Chitin, the source of chitosan, is the world's second most common polysaccharide with no such limitations (Younes & Rinaudo 2015). Both AM and CM require processing prior to use. AM must be manually separated from the placenta. Also, the preparation of CM with chitin extraction, deproteinization and demineralization, deacetylation and molding of the desired solution demands resources. CM has better availability as the processing could be refined to reach larger volumes, if necessary.

AM and CM can both be preserved after processing, which makes their use more practical when one can withdraw biomaterial deposit when need occurs. AM can be preserved as fresh, cryopreserved or dried (Adds et al. 2001, Mermet et al. 2007, Malhotra & Jain 2014). In this thesis, AM was cryopreserved. AM was noted to be more challenging to handle compared to CM, due to its silky consistency. CellCrown6-rings (Scaffdex Oy) eased the transplantation in the desired orientation, which was the denuded basement membrane side towards the wound site. Probably dry AM moistened at the wound site would make the handling easier without additional support. CM's self-supporting structure was easily tailored to the correct size and shape.

Epithelial cells of AM can be removed or left attached already prior to preservation. Epithelial cell removal can be executed enzymatically using EDTA, dispase or trypsin/EDTA, but the denudation process might affect AM (Lim et al.

2009). Prolonged enzymatic incubation has been suspected to enhance the degradation of AM due to basement membrane alteration. Overnight denudation process with dispase was fairly long, but the temperature was only 4°C, decreasing enzymatic activity. Also, the dispase concentration was low (1 mg/mL). Previous results support denudation, since the intact epithelial cell layer has been shown to retard cell migration and differentiation (Lim et. al 2009).

CMs had to be neutralized prior to use, because of the acetic manufacturing process. Neutralization was simpler compared to AMs' denudation containing only 30 min NaOH incubation and careful DPBS rinsing. In the chitosan study, the deacetylation degree was 73%. The deacetylation degree has a major impact on the qualities of chitosan (Ribeiro et al. 2017). 73% deacetylation degree can be considered to be average. The molecular mass of the chitosan was 240 kDa, which can be considered to be low, and may be more suitable in the pharmaceutical field (Mao et al. 2004). Chitosan can be manufactured as gels, membranes, scaffolds and sponges (Pillai et al. 2009, Jayakumar et al. 2011). The versatility can be seen as high potential for various purposes. Varying deacetylation degree and form make it challenging to state a clear consensus how chitosan should be applied.

Wound healing is a complex process and the use of a wound healing model is necessary. An ideal animal model would replicate the etiology and pathogenesis of a wound and illustrate the clinical situation, but unfortunately there is no model that would comprehensively fulfil these requirements (Gottrup et al. 2000). After all, for understandable ethical reasons, human models for wound healing are available only in a small and restricted manner. Skin wound healing experiments were studied on a Sprague-Dawley rat model. Rodents are commonly used in wound healing studies, male Sprague-Dawley rats being the preferred rodent. The major anatomical difference compared to humans is the panniculus carnosus muscle, which is common to loose-skinned species, and is involved in wound contraction (Naldaiz-Gastesi et al. 2016). Anatomically, human and pig skin would be closer to each other, but availability, small size, short gestation and lifespan with well-known health and genetics support the use of rat in wound healing studies (Dorsett-Martin 2004).

The method used seemed to be tolerable to the animals, and the excisional wound model was selected based on pilot tests. The animals needed minimal extra pain medication, and regained their minor post-operative weight lost fast. AM and CM have been reported to reduce pain at wound site (Ganatra 2003, Lo & Pope 2006, Bano et al. 2017).

Wounds were placed on the scalps of rats near their ears and other facial parts, where the skin is somewhat fixed in otherwise loose-skinned rats, for better

resemblance to human skin. The most-used wound placement in rat wound studies is the dorsal region (Dorsett-Martin 2004). Among wound placement, pilot tests were also used to determine wound dressing. Moisturized Aquacel® (ConvaTec Oy) was found to be most suitable, as the animals seemed to habituate better to a lighter dressing.

Wound areas were significantly smaller at day three in AM and CM groups, compared to their controls. Other time-points revealed no differences. It can be discussed that the membranes' positive effect limits early wound healing mechanisms and/or the membranes degrade from the wound surfaces, so that the effect does not last. According to previous literature, the mechanisms of AM and CM in wound healing are not clear, due to heterogenic study design and biomaterial-related properties. If they affect early wound healing mechanisms, hemostatic, inflammatory or proliferative factors should be considered, instead of factors affecting maturation and remodeling.

Wound healing starts with hemostasis, when fibrin clot formation, platelet aggregation and local vasoconstriction occur immediately after the injury (Janis et al. 2010). These events could be reflected as decreased hemorrhage and increased fibrin formation from wound histology. The differences between the groups during the experiments were insignificant. Higher deacetylation degree of CM has been connected to enhanced erythrocyte aggregation and platelet binding properties (Bano et al. 2017). The CMs average deacetylation degree could thus decrease the affect. The excisional wounds also bled minimally, and required no additional hemostatic maneuvers, such as bipolar coagulation or ligature sutures. The effect of vasoconstriction could not be estimated in the histological analysis, but it is unlikely that increased vasocontraction, certainly not on its own, could explain the noted significant wound size differences.

The hemostasis stage is followed by the inflammation stage, in which tissue macrophages, leukocytes, fibroblasts and endothelial cells activate and invade the wound site (Janis & Harrison 2016). The leucocyte count was significantly lower in the CM group on day seven compared to the control group. This suggests that either CM actually reduced inflammation, or the inflammation stage progressed faster in the CM group. Interestingly serum IL-4 levels were significantly higher in the CM group, compared to the control at 7- and 14-day time-points. IL-4 generally enhances anti-inflammatory and reduces pro-inflammatory cytokines (Varin & Gordon 2009). Thus, based on these results, we suggest that CM affects via IL-4 pathway, reducing inflammation. Obviously, IL-4 is only one of the many signal pathways in the complexity of wound heling. Previously the anti-inflammatory mechanism of

chitosan has been explained by downregulation of inflammatory chemokine expression, selectin, immune induction and inflammatory cytokine release (Lee et al. 2017). In this context, the finding considering IL-4 levels is remarkable and that even systemic IL-4 level changes gave significant results. The results suggest that CM affects as an active dressing modulating the pro-/anti-inflammatory balance. Suppression of inflammation stage is crucial that wound healing proceeds to the proliferation stage (Janis et al. 2010). If this transition phase is impaired, it might lead to a chronic wound. IL-4 levels in the AM study compared to the control were insignificant and therefore the effects of AM seem not to be IL-4 related. IL-4 has not previously been investigated in context of AM or CM in wound healing. Edema, which could also represent inflammation, was insignificant between the study and control groups at all time-points.

In the proliferation stage, epithelialization, angiogenesis and granulation tissue and provisional matrix formation develop (Buchanan et al. 2016). The results revealed no significant differences between the groups, concerning epithelialization. In the context of skin wound healing studies, AM is often stated to promote epithelialization, although most results concern the field of ophthalmology. Corneal epithelialization does not only differ anatomically from skin wound healing, but the entire healing process is also different, having three distinctive components to corneal epithelialization: cell migration, cell proliferation and cell adhesion (Dua et al. 1994). On day three, when wound area was smaller in favor of AM- and CM-treated wounds, can be thought to be a transition phase between inflammation and proliferation stages. Regarding epithelialization, dispase denudation of AM is also somewhat contradictory. On the other hand, the epithelium of AM might impair re-epithelialization retarding cell migration and differentiation, but also the denudation process itself might negatively affect the basement membrane of AM (Lim et al. 2009, Tauzin et al. 2014). Dispase remnants after denudation can be hypothesized to be repelling to re-epithelization and thus AM needs to be carefully rinsed afterwards. In a previous study, chitosan hydrogel has shown to promote epithelialization, but during these experiments, no such impact in membrane form was revealed (Ishihara et al. 2012).

The results revealed no significant angiogenic properties of AM or CM. Regarding AM, the study supported previous findings that AM's angiogenetic qualities decrease when it is positioned with the epithelial surface towards the wound surface (Niknejad et al. 2013). CM has been hypothesized to possess angiogenic qualities (Oryan & Sahvieh 2017). In our studies, however, angiogenic effects were not observed.

During proliferation stage, myofibroblasts also differentiate, causing wound contraction (Janis et al. 2010). In an excisional wound healing model, the wounds heal from the edges but also by contraction, where the panniculus carnosus has a role in rats (Gottrup et al. 2004). Wound contraction might partly be responsible for wound size reduction in the AM study. After the AM study, the study design was altered so that the wound edges were tattooed to measure contraction in the CM study. Although the result considering wound size reduction was similar to AM with CM, contraction did not seem to explain the difference between CM and its control group. Chitosan hydrogel has been suggested to promote contraction, but our CM results did not support the finding, although the different form of material might have an influence on the effect (Ishihara et al. 2012).

To study the degradation rates of AM and CM, it was attempted to see the membranes from the wound surface in the histological analysis. Unfortunately, AM was not detected from wound surfaces, and previous literature reveals no consensus on how fast AM degrades in an *in vivo* wound environment. Interestingly, CM was visible on days three and seven, but not at the later time-points. On this basis, CM degraded from the wound surface after the first week. The degradation from the wound surface could be the major reason for the limited early stage positive impact on wound size of CM, but it can be hypothesized considering AM as well. Thus, as an important finding, AM and CM should probably be reapplied to the wound surface around the first week from the start. As a noteworthy observation, such a recommendation cannot be recognized from previously published AM or CM literature.

Several limitations of the wound healing studies can also be discussed. Unfortunately, the available resources are not limitless. As brought up in the literature review, there are differences between rodent and human wounds. A pig wound healing model would probably be more comparable to humans. From wound histology, one must remember that even though the given results were analyzed from different views in our method, the analysis focuses to a local area of the general wound. In the future it would be more than interesting to study the local effect of CM considering IL-4 levels, now that the systemic analysis gave such interesting results. The local effect could be hypothesized to be even more evident.

6.2 Urethral regeneration

Urethral reconstruction of severe defects is complicated, requires special expertise, and has a possibility of disadvantageous tissue effects and complications (Keays & Dave 2017, Abbas et al. 2018). Well-established use of autologous grafts is not simple, due to limited supply and donor site morbidity (Orabi et al. 2013). Thus, there is a need for additional nonurological grafts that should overcome today's standards in outcome and complication rates. The demand is versatile, from biocompatibility to structure-related properties.

Previous studies have shown PLCL's suitability as a growth surface for human urothelial cells with promising results (Sartoneva et al. 2011). PLCL has already been studied for various purposes such as a vascular, musculoskeletal and dermal application (Mun et al. 2013, Yassin et al. 2016, Jung et al. 2018, Im et al 2018). For ureter segment regeneration PLCL was more suitable than acellular aortic arch (Kloskowski et al. 2014), but to a larger extent, PLCL has not yet been studied. A recent preliminary *in vitro* study with mechanical characterization revealed that PLCL has potential as a stent material for connecting the bladder and urethra (Ang et al. 2018). Similar to PLCL, PTMC has also been studied in a variety of applications, but in urological applications there are no *in vivo* or clinical stage publications. The suitability of PLCL and PTMC for urethral regeneration has not been previously compared. In general, previous literature reveals that there is a clear lack of comparative studies. The manufacturing methods are also suitable for broad use.

In our study, rapid postoperative appetite and spontaneous urination indicated that the urethral regeneration model seemed to be tolerable for the rabbits. Unfortunately, one rabbit from the PLCL group had slight delay recovering and two rabbits from the PTMC group died on the second postoperative day. The deceased rabbits underwent autopsy that revealed no obvious cause of death although the other one had a hematoma at the operation site. Because both of them urinated postoperatively but neglected food and water, it is unlikely that the deaths were biomaterial-related.

Spontaneous urination and urethrographic examinations ensured that the all postoperative urethras were open. Some narrowing was seen in the urethrographic examination, which might be due to single-plane X-ray pictures or lower flexibility of the used biomaterials compared to natural urethra, when syringed with radiocontrast agent. One of the primary reasons for urethrographic examination was to discover whether there are remarkable strictures. Overall, fistulas and strictures remain some of the main problems in urethral reconstruction (Keays & Dave 2017,

Bayne et al. 2017). At the 16-week time-point the examination revealed no severe strictures, although some mild narrowing in the PLCL group's proximal defect site was observed. No fistulas were discovered in the examination.

Simultaneously to defect site excision for histological analysis, the reconstruction area was also visually inspected. Based on visual inspection, at the 4-week time-point both of the membranes were still present, but they had visually degraded by the 16-week time-point. The results of the histological analysis supported visual inspection results and the membranes degraded after the 4-week time-point. The result is in line with previous degradation data (Pêgo et al. 2003, Zhang et al. 2006, Sartoneva et al. 2012). The PLCL membranes seemed to be more uneven compared to PTMC membranes. PLCL membranes were also more rigid at 2- and 4-week time-points. Also, in practice, PTMC seemed to be easier to mold and suture into the correct tubular size and shape compared to PLCL. Both PLCL and PTMC have been previously used for tubular reconstructive purposes in vascular contexts (Son et al. 2011, Mun et al. 2013). PTMC's elasticity has been stated one of the beneficial properties of PTMC as a biomaterial (Papenburg et al. 2009). In addition to biomaterial degradation, the 16-week time-point inspection revealed no obvious strictures or differences considering the urothelium.

The hypothesis was that urothelial cells are likely to migrate from the defect edges on the membranes, and eventually form continuous urothelium. The HE stained samples revealed that epithelial integrity and structure developed toward normal urothelium in both groups. Also, the cytokeratin staining supported the finding. After 2 weeks, the defect edge was still detectable in both groups. The epithelial integrity of the PTMC group at 2- and 16-week time-points was significantly better compared to PLCL. The defect edge perished and the *de novo* epithelium showed characteristic stratification at the 16-week time-point.

The histological analysis revealed that the fibrotic changes varied from mild to moderate. Urinary retention or remarkable strictures were not detected clinically or in the X-ray pictures, which thus supported the histological findings. After all, all forms of invasive treatment cause fibrotic changes at some degree. On the basis of these findings, both biomaterials showed potential to at least partly resolve one of the major challenges in urethral reconstruction.

The possibility of inflammation should always be evaluated when using foreign reconstructive materials. It has been stated that in delicate urothelial tissue engineering, biomaterials should not cause severe inflammatory responses (Orabi et al. 2013). PLCL's slow degradation might partly be responsible for its mild inflammatory response (Taira et al. 2003). PTMC implanted to the mandible has

previously showed mild histological tissue reaction (Van Leeuwen et al. 2012). There is no reasonable previous literature on urethral tissue responses considering PLCL or PTMC. The histological analysis revealed low inflammatory cell counts and edema, suggesting mild inflammatory responses in both groups.

Human urothelial cell attachment was significantly higher on PTMC than PLCL. The attached cells were found vital on both biomaterials and were proven biocompatible for the purpose. Cytokeratins CK7, CK8 and CK 19 were analyzed because they are expressed in multilayered epithelium and urothelium in general. Also, uroplakins Ia, Ib and III were analyzed, as they are specific markers for superficial urothelial cells (Southgate et al. 2002, de Graaf et al. 2016). The phenotype of cultivated urothelial cells were evaluated with these markers and both biomaterials supported the phenotype of urothelial cells confirming their biocompatibility for urethral regeneration. Interestingly, PTMC seemed to support the expression of uroplakin markers superior compared to PLCL.

The histological analysis is local, considering the total urethral defect in the same manner as in the wound healing studies. Stricture development being one of the key clinical problems, a urethrography based on computed tomography would probably have given a more precise visual perspective of the urethral lumen compared to accomplished native X-ray imaging. As usual, the available resources set boundaries for the chosen methods, which should be considered planning future studies for urethral regeneration.

6.3 Future perspectives

AM and CM both promoted wound healing, and although the effect was limited to the early stage, in this way they fulfilled one major quality of an optimal wound dressing. They also protected the wound and were found to be tolerable for their selected purpose. Some future perspectives can be stated based on these finding and experiences. From a productive perspective, the processing methods of AM could probably be developed towards a more efficient direction, from the slow and thus costly current process. Dried AM may be easier to handle as a wound dressing than fresh or frozen AM. Denudation of the epithelial layer seems justified, but special attention should be paid to keep the incubation mild or moderate, and rinse dispase remnants with care. The optimal form and deacetylation degree still demand further studies optimizing chitosan for wound healing purposes. IL-4 levels were significantly higher in the CM study compared to the controls, but the mechanisms

behind both membranes are likely far more complex and require further investigation. The IL-4 results should be further investigated with local quantitative measurements from the wound site, where the result could be hypothesized to be even more evident.

Mentioned limitations should be taken under consideration for the future studies to achieve the optimal biomaterial for wound healing in clinical practice. These results encourage the study of AM and CM as complex cell seeded membranes with sophisticated wound models, developing the optimal wound healing method in a cost-effective manner. In particular, models for chronic wound healing should be improved.

In urethral regeneration, both PLCL and PTMC demonstrated true potential and suitability in urethral regeneration. Practical handling, positive phenotype marker findings and epithelial integrity development revealed PTMC's potential, in particular. As this was the first time PTMC was investigated in this manner, it can be stated as a small breakthrough. Hopefully, in the future, PLCL and PTMC could overcome the current notable reconstructive problems, such as limited autologous supply and donor site morbidity, with high success rates, as a true clinical solution. Using cell seeded PLCL and PTMC for urethral regeneration seems to be the next obvious evolutionary step. Cell seeding might also have an effect in the mechanical properties of the biomaterials (Wang et al. 2018). PLCL and PTMC could also be combined with other polymers, such as PLA, to adjust the degradation rate for instance. At least, PLCL and PTMC should be compared with other biomaterials, and with buccal autologous flaps, as they are used today.

7 CONCLUSIONS

Based on these studies, all four biomaterials were found to have potential as biocompatible solutions for epithelial repair (I-III). It is concluded that:

1. AM was found to enhance early stage wound healing in terms of wound size. The effect decreased in later phases and did not influence IL-4 levels. (I)

2. CM promoted early stage wound healing, reduced inflammation and affected the IL-4 pathway. CM was found to degrade from the wound surface after day 7. (II)

3. PLCL and PTMC were both suitable for urethral reconstruction. PTMC was found to be more suitable considering flexibility, ease to shape and suture, and developing epithelial integrity. (III)

8 ACKNOWLEDGEMENTS

First, I would like to express my most sincere gratitude to my supervisors Associate Professor Susanna Miettinen and Adjunct Professor Minna Kääriäinen. You both always shared your expertise and kept me motivated with this thesis. I enjoyed the atmosphere we had during this project. It is evident that without your endless support and guidance, this thesis would not have been completed.

I also express my deep gratitude towards the members of my follow-up committee - Professor Riitta Seppänen-Kaijansinkko and Adjunct Professor Hannu Kuokkanen - for their valuable comments on the manuscripts. Your support, especially at the beginning of the project, was crucial.

Further, the official examiners of this thesis earn my sincere expression of gratitude. The constructive comments and professional review of Adjunct Professor Ilkka Koskivuo and Adjunct Professor Esko Kankuri enhanced the scientific value of the thesis.

I warmly express my thanks to all co-authors - Professor Markku Pelto-Huikko, Dr. Anne-Marie Haaparanta, Professor Minna Kellomäki, Dr. Reetta Sartoneva, Dr. Suvi Haimi, Professor Dirk W. Grijpma, Mr. Kalle Lehto, Dr. Niall Rooney and Adjunct Professor Tuija Lahdes-Vasama - for their contribution to the manuscripts composing this thesis. I also thank pathologist Marita Laurila for her expertise, and Heini Huhtala for her valuable statistical support.

All members of the "Mese Group" deserve my deep gratitude for their support and delightful companionship. In particular, I want to thank Minna Salomäki, Sari Kalliokoski, Miia Juntunen and Anna-Maija Honkala for their excellent technical assistance in the laboratory. I am thankful towards all collaborators at BioMediTech, Pirkanmaa Hospital District and University of Twente. The practical guidance of animal laboratory personnel at Tampere University was also crucial throughout the project. I also want to thank all my supportive colleagues during these years.

During these years and within this project, we have had many laughs with my friends on a vast variety of occasions at home and abroad. It's hard to say no, when it's time to go, and I (usually) know how it goes…

My parents Seija and Isto Nordback have always encouraged and supported me throughout my life, this project being no exception. My brother Tatu earns my

honest gratitude for his support. I collectively thank my other relatives and in-laws, as well.

My deepest gratitude sincerely goes to my lovely wife Emma who believed in me when I had doubts and kept me going. Your understanding goes beyond belief. Certainly, without your support I could not have done this. Our son Hugo's assistance was surely sufficient and although a bit different, he should almost be stated as a co-author.

This thesis was financially supported by the competitive research funding of Pirkanmaa Hospital District, Finnish Cultural Foundation (Lempi Rinteen -rahasto), Emil Aaltonen Foundation, City of Tampere Science Fund and The Finnish Research Foundation of Children's Diseases.

9 REFERENCES

Abbas TO, Mahdi E, Hasan A, AlAnsari A, Pennisi CP. Current Status of Tissue Engineering in the Management of Severe Hypospadias. Front Pediatr. 2018 Jan 22;5:283.

Adds PJ, Hunt C, Hartley S. Bacterial contamination of amniotic membrane. Br J Ophthalmol. 2001; 85: 2, 228–230.

Adds PJ, Hunt CJ, Dart JK. Amniotic membrane grafts, "fresh" or frozen? A clinical and *in vitro* comparison. Br J Ophthalmol. 2001 Aug;85(8):905-7.

Ahsan SM, Thomas M, Reddy KK, Sooraparaju SG, Asthana A, Bhatnagar I. Chitosan as biomaterial in drug delivery and tissue engineering. Int J Biol Macromol. 2017 Sep 1. pii: S0141-8130(17)31884-6.

Ali N, Rosenblum MD. Regulatory T cells in skin. Immunology. 2017 Nov;152(3):372-381.

Amer MI, Abd-El-Maeboud KH. Amnion graft following hysteroscopic lysis of intrauterine adhesions. J Obstet Gynaecol Res. 2006 Dec;32(6):559-66.

Amsden BG, Marecak D. Long-Term Sustained Release from a Biodegradable Photo-Cross-Linked Network for Intraocular Corticosteroid Delivery. Mol Pharm. 2016 Sep 6;13(9):2004-12.

Ang HY, Chan J, Toong D, Venkatraman SS, Chia SJ, Huang YY. Tailoring the mechanical and biodegradable properties of binary blends of biomedical thermoplastic elastomer. J Mech Behav Biomed Mater. 2018 Mar;79:64-72.

Apodaca G. The uroepithelium: not just a passive barrier. Traffic. 2004 Mar;5(3):117-28.

Armstrong DG, Boulton AJM, Bus SA. Diabetic Foot Ulcers and Their Recurrence. N Engl J Med. 2017 Jun 15;376(24):2367-2375.

Aro A, Mutanen M, Uusitupa U. Ravitsemustiede. 3rd edition. Kustannus Oy Duodecim. 2007;2:217.

Azad AK, Sermsintham N, Chandrkrachang S, Stevens WF. Chitosan membrane as a wound-healing dressing: characterization and clinical application. J Biomed Mater Res B Appl Biomater. 2004 May 15;69(2):216-22.

Babu A, Ramesh R. Multifaceted Applications of Chitosan in Cancer Drug Delivery and Therapy. Mar Drugs. 2017 Mar 27;15(4).

Bąk M, Gutkowska ON, Wagner E, Gosk J. The role of chitin and chitosan in peripheral nerve reconstruction. Polim Med. 2017 Jan-Jun;47(1):43-47.

Bano I, Arshad M, Yasin T, Ghauri MA, Younus M. Chitosan: A potential biopolymer for wound management. Int J Biol Macromol. 2017 Sep;102:380-383.

Basu A, Haim-Zada M, Domb AJ. Biodegradable inflatable balloons for tissue separation. Biomaterials. 2016 Oct;105:109-116.

Bat E, van Kooten TG, Feijen J, Grijpma DW. Macrophage-mediated erosion of gamma irradiated poly(trimethylene carbonate) films. Biomaterials. 2009 Aug;30(22):3652-61.

Bat E, van Kooten TG, Harmsen MC, Plantinga JA, van Luyn MJ, Feijen J, Grijpma DW. Physical properties and erosion behavior of poly(trimethylene carbonate-co-ε-caprolactone) networks. Macromol Biosci. 2013 May;13(5):573-83.

Bayne DB, Gaither TW, Awad MA, Murphy GP, Osterberg EC, Breyer BN. Guidelines of guidelines: a review of urethral stricture evaluation, management, and follow-up. Transl Androl Urol. 2017 Apr;6(2):288-294.

Bezuhly M, Fish JS. Acute burn care. Plast Reconstr Surg. 2012 Aug;130(2):349e-358e.

Betts JG, DeSaix P, Johnson JE, Kruse DH, Wise JA. Anatomy and Physiology. OpenStax College. Jul 13, 2018.

Bhat S, Kumar A. Biomaterials and bioengineering tomorrow's healthcare. Biomatter. 2013 Jul-Sep;3(3).

Biswas DP, O'Brien-Simpson NM, Reynolds EC, O'Connor AJ, Tran PA. Comparative study of novel in situ decorated porous chitosan-selenium scaffolds and porous chitosan-silver scaffolds towards antimicrobial wound dressing application. J Colloid Interface Sci. 2018 Apr 1;515:78-91.

Bourne G. The foetal membranes. A review of the anatomy of normal amnion and chorion and some aspects of their function. Postgrad Med J. 1962 Apr;38:193-201.

Bourne GL. The anatomy of the human amnion and chorion. Proc R Soc Med. 1966 Nov;59(11 Part 1):1127-8.

Britto EJ, Morrison CA. Wound, Dressings. StatPearls [Internet]. Treasure Island (FL): StatPearls Publishing; 2017 Jun-.2017 Nov 7.

Bryk DJ, Zhao LC. Guideline of guidelines: a review of urological trauma guidelines. BJU Int. 2016 Feb;117(2):226-34.

Buchanan PJ, Kung TA, Cederna PS. Evidence-Based Medicine: Wound Closure. Plast Reconstr Surg. 2016 Sep;138(3 Suppl):257S-70S.

Burks CA, Bundy K, Fotuhi P, Alt E. Characterization of 75:25 poly(l-lactide-co-epsilon-caprolactone) thin films for the endoluminal delivery of adipose-derived stem cells to abdominal aortic aneurysms. Tissue Eng. 2006 Sep;12(9):2591-600.

Burns T, Breathnach S, Cox N, Griffths C. Rook´s Textbook of Dermatology. Blackwell Publishing. 2008; 7th Edition.

Campani V, Pagnozzi E, Mataro I, Mayol L, Perna A, D'Urso F, Carillo A, Cammarota M, Maiuri MC, De Rosa G. Chitosan Gel to Treat Pressure Ulcers: A Clinical Pilot Study. Pharmaceutics. 2018 Jan 17;10(1).

Cheung C. Older Adults, Falls, and Skin Integrity. Adv Skin Wound Care. 2017 Jan;30(1):40-46.

Chiang IN, Huang WC, Huang CY, Pu YS, Young TH. Development of a chitosan-based tissue-engineered renal proximal tubule conduit. J Biomed Mater Res B Appl Biomater. 2018 Jan;106(1):9-20.

Coban I, Satoğlu IS, Gültekin A, Tuna B, Tatari H, Fidan M. Effects of human amniotic fluid and membrane in the treatment of Achilles tendon ruptures in locally corticosteroid-induced Achilles tendinosis: an experimental study on rats. Foot Ankle Surg. 2009;15(1):22-7.

Cornwell KG, Landsman A, James KS. Extracellular matrix biomaterials for soft tissue repair. Clin Podiatr Med Surg. 2009 Oct;26(4):507-23.

Davis, J.W. Skin transplantation with a review of 550 cases at the Johns Hopkins hospital. Johns Hopkins Med J. 1910;15: 307–396.

de Graaf P, van der Linde EM, Peter FWM, Rosier PF, Izeta A, Sievert KD, Bosch JLH, de Kort, LM. Systematic review to compare urothelium differentiation with urethral epithelium differentiation in fetal development, as a basis of tissue engineering of the male urethra. Tissue Eng Part B Rev 23, 257, 2016.

Dehghani M, Azarpira N, Mohammad Karimi V, Mossayebi H, Esfandiari E. Grafting with Cryopreserved Amniotic Membrane versus Conservative Wound Care in Treatment of Pressure Ulcers: A Randomized Clinical Trial. Bull Emerg Trauma. 2017 Oct;5(4):249-258.

Dodane V, Vilivalam VD. Pharmaceutical applications of chitosan. Pharmaceutical Science & Technology Today. 1. 246-253. 10.1016/S1461-5347(98)00059-5. 1998.

Donaire AE, Mendez MD. Hypospadias. StatPearls [Internet]. Treasure Island (FL): StatPearls Publishing; 2018-. 2018 Jan 11.

Dorsett-Martin WA. Rat models of skin wound healing: a review. Wound Repair Regen. 2004 Nov-Dec;12(6):591-9.

Dua HS, Gomes JAP, King AJ, Maharajan VS. The amniotic membrane in ophthalmology. Surv Ophthalmol. 2004 Jan-Feb;49(1):51-77.

Dua HS, Gomes JA, Singh A. Corneal epithelial wound healing. Br J Ophthalmol. 1994 May;78(5):401-8.

Engelberg I, Kohn J. Physico-mechanical properties of degradable polymers used in medical applications: a comparative study. Biomaterials. 1991 Apr;12(3):292-304.

Escárcega-Galaz AA, Cruz-Mercado JL, López-Cervantes J, Sánchez-Machado DI, Brito-Zurita OR, Ornelas-Aguirre JM. Chitosan treatment for skin ulcers associated with diabetes. Saudi J Biol Sci. 2018 Jan;25(1):130-135.

Fairbairn NG, Randolph MA, Redmond RW. The clinical applications of human amnion in plastic surgery. J Plast Reconstr Aesthet Surg. 2014 May;67(5):662-75.

Farhadihosseinabadi B, Zarebkohan A, Eftekhary M, Heiat M, Moosazadeh Moghaddam M, Gholipourmalekabadi M. Crosstalk between chitosan and cell signaling pathways. Cell Mol Life Sci. 2019 Apr 27.

Fernandes M, Sridhar MS, Sangwan VS, Rao GN. Amniotic membrane transplantation for ocular surface reconstruction. Cornea. 2005 Aug;24(6):643-53.

Fernández J, Etxeberria A, Sarasua JR. Synthesis, structure and properties of poly(L-lactide-co-ε-caprolactone) statistical copolymers. J Mech Behav Biomed Mater. 2012 May;9:100-12.

Fife CE, Farrow W, Hebert AA, Armer NC, Stewart BR, Cormier JN, Armer JM. Skin and Wound Care in Lymphedema Patients: A Taxonomy, Primer, and Literature Review. Adv Skin Wound Care. 2017 Jul;30(7):305-318.

Gallegos MA, Santucci RA. Advances in urethral stricture management. F1000Res. 2016 Dec 23;5:2913.

Ganatra MA. Amniotic membrane in surgery. J Pak Med Assoc. 2003 Jan;53(1):29-32.

Garkhal K, Verma S, Jonnalagadda S, Kumar N. Fast degradable poly (L-lactide-co-ε-caprolactone) microspheres for tissue engineering: Synthesis, characterization, and degradation behavior. 2007. J Pol Sci Part A: 45 (13), 2755-2764

Gelman J, Wisenbaugh ES. Posterior Urethral Strictures. Adv Urol. 2015;2015:628107.

Gharib M , Ure BM, Klose M. Use of amniotic grafts in the repair of gastroschisis. Pediatr Surg Int. 1996 Mar;11(2-3):96-9.

Gomes JA, Romano A, Santos MS, Dua HS. Amniotic membrane use in ophthalmology. Curr Opin Ophthalmol. 2005 Aug;16(4):233-40.

Gottrup F, Agren MS, Karlsmark T. Models for use in wound healing research: a survey focusing on *in vitro* and *in vivo* adult soft tissue. Wound Repair Regen. 2000 Mar-Apr;8(2):83-96.

Grey JE, Harding KG, Enoch S. Venous and arterial leg ulcers. BMJ. 2006 Feb 11;332(7537):347-50.
Grigoropoulou P, Eleftheriadou I, Jude EB, Tentolouris N. Diabetic Foot Infections: An Update in Diagnosis and Management. Curr Diab Rep. 2017 Jan;17(1):3.
Gross RA, Kalra B. Biodegradable polymers for the environment. Science. 2002 Aug 2;297(5582):803-7.
Grunwald TB, Garner WL. Acute Burns. Plast Reconstr Surg. 2008 May;121(5):311e-319e.
Han J, Chen TX, Branford-White CJ, Zhu LM. Electrospun shikonin-loaded PCL/PTMC composite fiber mats with potential biomedical applications. Int J Pharm. 2009 Dec 1;382(1-2):215-21.
Hao C, Wang W, Wang S, Zhang L, Guo Y. An Overview of the Protective Effects of Chitosan and Acetylated Chitosan Oligosaccharides against Neuronal Disorders. Mar Drugs. 2017 Mar 23;15(4).
Hickling DR, Sun TT, Wu XR. Anatomy and Physiology of the Urinary Tract: Relation to Host Defense and Microbial Infection. Microbiol Spectr. 2015 Aug;3(4).
Holstein AF, Davidoff MS, Breucker H, Countouris N, Orlandini G. Different epithelia in the distal human male urethra. Cell Tissue Res. 1991 Apr;264(1):23-32.
Hopkinson A, Shanmuganathan VA, Gray T, Yeung AM, Lowe J, James DK, Dua HS. Optimization of amniotic membrane (AM) denuding for tissue engineering. Tissue Eng Part C Methods. 2008 Dec;14(4):371-81.
Hsiao T, Council M. Wound, Closure Techniques. StatPearls [Internet]. Treasure Island (FL): StatPearls Publishing; 2017 Jun-.2017 Nov 6.
Husain S, Al-Samadani KH, Najeeb S, Zafar MS, Khurshid Z, Zohaib S, Qasim SB. Chitosan Biomaterials for Current and Potential Dental Applications. Materials (Basel). 2017 May 31;10(6).
Ikada Y, Tsuji H. Biodegradable polyesters for medical and ecological applications. Macromol. Rapid Commun. 21, 117–132 (2000).
Im H, Kim SH, Kim SH, Jung Y. Skin Regeneration with a Scaffold of Predefined Shape and Bioactive Peptide Hydrogels. Tissue Eng Part A. 2018 Jul 30.
Insausti CL, Blanquer M, Bleda P, Iniesta P, Majado MJ, Castellanos G, Moraleda JM. The amniotic membrane as a source of stem cells. Histol Histopathol. 2010 Jan;25(1):91-8.
Ishihara M, Nakanishi K, Ono K, Sato M, Kikuchi M, Saito Y, Yura H, Matsui T, Hattori H, Uenoyama M, Kurita A. Photocrosslinkable chitosan as a dressing for wound occlusion and accelerator in healing process. Biomaterials. 2002 Feb;23(3):833-40.
Ito M, Azuma Y, Ohta T, Komoriya K. Effects of ultrasound and 1,25-dihydroxyvitamin D3 on growth factor secretion in co-cultures of osteoblasts and endothelial cells. Ultrasound Med Biol. 2000 Jan;26(1):161-6.
Jalanko H. Tietoa potilaalle: Virtsateiden ongelmat lapsilla. Lääkärikirja Duodecim. 02.12.2017.
Janis JE, Harrison B. Wound Healing: Part I. Basic Science. Plast Reconstr Surg. 2016 Sep;138(3 Suppl):9S-17S.
Janis JE, Kwon RK, Lalonde DH. A practical guide to wound healing. Plast Reconstr Surg. 2010 Jun;125(6):230e-44e.
Jayakumar R, Prabaharan M, Nair SV, Tamura H. Novel chitin and chitosan nanofibers in biomedical applications. Biotechnol Adv. 2010 Jan-Feb;28(1):142-50.

Jayakumar R, Prabaharan M, Sudheesh Kumar PT, Nair SV, Tamura H. Biomaterials based on chitin and chitosan in wound dressing applications. Biotechnol Adv. 2011 May-Jun;29(3):322-37.

Je JY, Kim SK. Chitosan as potential marine nutraceutical. Adv Food Nutr Res. 2012;65:121-35.

Jeong SI, Kim BS, Kang SW, Kwon JH, Lee YM, Kim SH, Kim YH. *In vivo* biocompatibilty and degradation behavior of elastic poly(L-lactide-co-epsilon-caprolactone) scaffolds. Biomaterials. 2004 Dec;25(28):5939-46.

Jeschke M, Rogers AD. Managing severe burn injuries: challenges and solutions in complex and chronic wound care. Chronic Wound Care Management and Research. 2016. 59. 10.2147/CWCMR.S86762.

Jokinen JJ, Sipponen A, Lohi J, Salo H. Haavanhoidon uusia ja vanhoja tuulia. Suomen Lääkärilehti 2009;64(24):2187-2193

Jung Y, Park MS, Lee JW, Kim YH, Kim SH, Kim SH. Cartilage regeneration with highly-elastic three-dimensional scaffolds prepared from biodegradable poly(L-lactide-co-epsilon-caprolactone). Biomaterials. 2008 Dec;29(35):4630-6.

Keane TJ, Badylak SF. Biomaterials for tissue engineering applications. Semin Pediatr Surg. 2014 Jun;23(3):112-8.

Keays MA, Dave S. Current hypospadias management: Diagnosis, surgical management, and long-term patient-centred outcomes. Can Urol Assoc J. 2017 Jan-Feb;11(1-2Suppl1):S48-S53.

Kesting MR, Wolff KD, Hohlweg-Majert B, Steinstraesser L. The role of allogenic amniotic membrane in burn treatment. J Burn Care Res. 2008 Nov-Dec;29(6):907-16.

Khandelwal P, Abraham SN, Apodaca G. Cell biology and physiology of the uroepithelium. Am J Physiol Renal Physiol. 2009 Dec;297(6):F1477-501

Kiechle JE, Chertack N, Gonzalez CM. Penile and Urethral Reconstructive Surgery. Med Clin North Am. 2018 Mar;102(2):325-335.

King AE, Paltoo A, Kelly RW, Sallenave JM, Bocking AD, Challis JR. Expression of natural antimicrobials by human placenta and fetal membranes. Placenta. 2007 Feb-Mar;28(2-3):161-9.

Kloskowski T, Jundziłł A, Kowalczyk T, Nowacki M, Bodnar M, Marszałek A, Pokrywczyńska M, Frontczak-Baniewicz M, Kowalewski TA, Chłosta P, Drewa T. Ureter regeneration-the proper scaffold has to be defined. PLoS One. 2014 Aug 27;9(8):e106023

Kluin OS, van der Mei HC, Busscher HJ, Neut D. A surface-eroding antibiotic delivery system based on poly-(trimethylene carbonate). Biomaterials. 2009 Sep;30(27):4738-42.

Koizumi NJ, Inatomi TJ, Sotozono CJ, Fullwood NJ, Quantock AJ, Kinoshita S. Growth factor mRNA and protein in preserved human amniotic membrane. Curr Eye Res. 2000 Mar;20(3):173-7.

Komatsu D, Mistura DV, Motta A, Domingues JA, Hausen MA, Duek E. Development of a membrane of poly (L-co-D,L lactic acid-co-trimethylene carbonate) with aloe vera: An alternative biomaterial designed to improve skin healing. J Biomater Appl. 2017 Sep;32(3):311-320.

Kratz G, Back M, Arnander C, Larm O. Immobilised heparin accelerates the healing of human wounds *in vivo*. Scand J Plast Reconstr Surg Hand Surg. 1998 Dec;32(4):381-5.

Kreft ME, Sterle M, Veranic P, Jezernik K. Urothelial injuries and the early wound healing response: tight junctions and urothelial cytodifferentiation. Histochem Cell Biol. 2005 Jun;123(4-5):529-39.
K V SK, Mammen A, Varma KK. Pathogenesis of bladder exstrophy: A new hypothesis. J Pediatr Urol. 2015 Dec;11(6):314-8.
Labet M, Thielemans W. Synthesis of polycaprolactone: a review. Chem Soc Rev. 2009 Dec;38(12):3484-504.
Lammers G, Verhaegen PD, Ulrich MM, Schalkwijk J, Middelkoop E, Weiland D, Nillesen ST, Van Kuppevelt TH, Daamen WF. An overview of methods for the *in vivo* evaluation of tissue-engineered skin constructs. Tissue Eng Part B Rev. 2011 Feb;17(1):33-55.
Leaper DJ. Traumatic and surgical wounds. BMJ. 2006 Mar 4;332(7540):532-5.
Lenselink EA. Role of fibronectin in normal wound healing. Int Wound J. 2015 Jun;12(3):313-6.
Lee CK, Hansen SL. Management of acute wounds. Surg Clin North Am. 2009 Jun;89(3):659-76.
Lee YE, Kim H, Seo C, Park T, Lee KB, Yoo SY, Hong SC, Kim JT, Lee J. Marine polysaccharides: therapeutic efficacy and biomedical applications. Arch Pharm Res. 2017 Sep;40(9):1006-1020.
Leslie SW, Villanueva CA. Cryptorchidism. StatPearls [Internet]. Treasure Island (FL): StatPearls Publishing; 2018-.2018 Jan 6.
Li J, Lin F. Microfluidic devices for studying chemotaxis and electrotaxis. Trends Cell Biol. 2011 Aug;21(8):489-97.
Liaqat F, Eltem R. Chitooligosaccharides and their biological activities: A comprehensive review. Carbohydr Polym. 2018 Mar 15;184:243-259.
Lim LS, Riau A, Poh R, Tan DT, Beuerman RW, Mehta JS. Effect of dispase denudation on amniotic membrane. Mol Vis. 2009 Sep 25;15:1962-70.
Liu J, Sheha H, Fu Y, Liang L, Tseng SC. Update on amniotic membrane transplantation. Expert Rev Ophthalmol. 2010 Oct;5(5):645-661.
Lo V, Pope E. Amniotic membrane use in dermatology. Int J Dermatol. 2009 Sep;48(9):935-40.
Luangphakdy V, Walker E, Shinohara K, Pan H, Hefferan T, Bauer TW, Stockdale L, Saini S, Dadsetan M, Runge MB, Vasanji A, Griffith L, Yaszemski M, Muschler GF. Evaluation of osteoconductive scaffolds in the canine femoral multi-defect model. Tissue Eng Part A. 2013 Mar;19(5-6):634-48.
Makrantonaki E, Ganceviciene R, Zouboulis C. An update on the role of the sebaceous gland in the pathogenesis of acne. Dermatoendocrinol. 2011 Jan;3(1):41-9.
Malhotra C, Jain AK. Human amniotic membrane transplantation: Different modalities of its use in ophthalmology. World J Transplant. 2014 Jun 24;4(2):111-21.
Mamede AC, Carvalho MJ, Abrantes AM, Laranjo M, Maia CJ, Botelho MF. Amniotic membrane: from structure and functions to clinical applications. Cell Tissue Res. 2012 Aug;349(2):447-58.
Mao S, Shuai X, Unger F, Simon M, Bi D, Kissel T. The depolymerization of chitosan: effects on physicochemical and biological properties. Int J Pharm. 2004 Aug 20;281(1-2):45-54.
Martin NA, Falder S. A review of the evidence for threshold of burn injury. Burns. 2017 May 20. pii: S0305-4179(17)30215-2.

Martin P. Wound healing - aiming for perfect skin regeneration. Science. 1997 Apr 4;276(5309):75-81.
Mermet I, Pottier N, Sainthillier JM, Malugani C, Cairey-Remonnay S, Maddens S, Riethmuller D, Tiberghien P, Humbert P, Aubin F. Use of amniotic membrane transplantation in the treatment of venous leg ulcers. Wound Repair Regen. 2007 Jul-Aug;15(4):459-64.
Mhaskar R. Amniotic membrane for cervical reconstruction. Int J Gynaecol Obstet. 2005 Aug;90(2):123-7.
Mockenhaupt M. The current understanding of Stevens-Johnson syndrome and toxic epidermal necrolysis. Expert Rev Clin Immunol. 2011 Nov;7(6):803-13.
Moran HBT, Turley JL, Andersson M, Lavelle EC. Immunomodulatory properties of chitosan polymers. Biomaterials. 2018 Nov;184:1-9.
Mun CH, Kim SH, Jung Y, Kim SH, Kim AK, Kim DI, Kim SH. Elastic, double-layered poly (l-lactide-co-ϵ-caprolactone) scaffold for long-term vascular reconstruction. J Bioactive Compatible Polym. 2013, 28(3), 233-246.
Muralidharan S, Gu J, Laub GW: A new biological membrane for pericardial closure. J Biomed Mater Res. 1991 Oct;25(10):1201-9.
Mustoe TA, O'Shaughnessy K, Kloeters O. Chronic wound pathogenesis and current treatment strategies: a unifying hypothesis. Plast Reconstr Surg. 2006 Jun;117(7 Suppl):35S-41S.
Muxika A, Etxabide A, Uranga J, Guerrero P, de la Caba K. Chitosan as a bioactive polymer: Processing, properties and applications. Int J Biol Macromol. 2017 Dec;105(Pt 2):1358-1368.
Muzzarelli RAA. Chitin and chitosans for the repair of wounded skin, nerve, cartilage and bone. Carbohydr Polym 2009;76:167–82.
Myers WT, Leong M, Phillips LG. Optimizing the patient for surgical treatment of the wound. Clin Plast Surg. 2007 Oct;34(4):607-20.
Naldaiz-Gastesi N, Goicoechea M, Alonso-Martín S, Aiastui A, López-Mayorga M, García-Belda P, Lacalle J, San José C, Araúzo-Bravo MJ, Trouilh L, Anton-Leberre V, Herrero D, Matheu A, Bernad A, García-Verdugo JM, Carvajal JJ, Relaix F, Lopez de Munain A, García-Parra P, Izeta A. Identification and Characterization of the Dermal Panniculus Carnosus Muscle Stem Cells. Stem Cell Reports. 2016 Sep 13;7(3):411-24.
Neville RF, Kayssi A, Buescher T, Stempel MS. The diabetic foot. Curr Probl Surg. 2016 Sep;53(9):408-37.
Niknejad H, Peirovi H, Jorjani M, Ahmadiani A, Ghanavi J, Seifalian AM. Properties of the amniotic membrane for potential use in tissue engineering. Eur Cell Mater. 2008 Apr 29;15:88-99.
Niknejad H, Paeini-Vayghan G, Tehrani FA, Khayat-Khoei M, Peirovi H. Side dependent effects of the human amnion on angiogenesis. Placenta. 2013 Apr;34(4):340-5.
Nuyken O, Pask SD. Ring-Opening Polymerization - An Introductory Review. Polymers 2013, 5, 361-403;
Nwe N, Furuike T, Tamura H. Isolation and characterization of chitin and chitosan from marine origin. Adv Food Nutr Res. 2014;72:1-15.
Obara K, Ishihara M, Ishizuka T, Fujita M, Ozeki Y, Maehara T, Saito Y, Yura H, Matsui T, Hattori H, Kikuchi M, Kurita A. Photocrosslinkable chitosan hydrogel containing fibroblast growth factor-2 stimulates wound healing in healing-impaired db/db mice. Biomaterials. 2003 Sep;24(20):3437-44.

OECD (2004), Test No. 428: Skin Absorption: *In Vitro* Method, OECD Guidelines for the Testing of Chemicals, Section 4, OECD Publishing, Paris.
OECD (2015), Test No. 439: *In Vitro* Skin Irritation: Reconstructed Human Epidermis Test Method, OECD Guidelines for the Testing of Chemicals, Section 4, OECD Publishing, Paris.
Orabi H, Bouhout S, Morissette A, Rousseau A, Chabaud S, Bolduc S. Tissue engineering of urinary bladder and urethra: advances from bench to patients. ScientificWorldJournal. 2013 Dec 24;2013:154564.
Oryan A, Sahvieh S. Effectiveness of chitosan scaffold in skin, bone and cartilage healing. Int J Biol Macromol. 2017 Nov;104(Pt A):1003-1011.
Ouyang QQ, Zhao S, Li SD, Song. Application of Chitosan, Chitooligosaccharide, and Their Derivatives in the Treatment of Alzheimer's Disease. Mar Drugs. 2017 Nov 7;15(11).
Papenburg BJ, Schüller-Ravoo S, Bolhuis-Versteeg LA, Hartsuiker L, Grijpma DW, Feijen J, Wessling M, Stamatialis D. Designing porosity and topography of poly(1,3-trimethylene carbonate) scaffolds. Acta Biomater. 2009 Nov;5(9):3281-94.
Patrulea V, Ostafe V, Borchard G, Jordan O. Chitosan as a starting material for wound healing applications. Eur J Pharm Biopharm. 2015 Nov;97(Pt B):417-26.
Pfaffl MW. A new mathematical model for relative quantification in real-time RT-PCR. Nucleic Acids Res. 2001 May 1;29(9):e45.
Paul W, Sharma CP. Chitin and alginates wound dressings: a short review. Trends Biomater Artif Organs 2004;18:18–23.
Patel H, Bonde M, Srinivasan G. Biodegradable Polymer Scaffold for Tissue Engineering. Trends Biomater. Artif. Organs, 25(1), 20-29 (2011).
Pêgo AP, Grijpma DW, Feijen J. Enhanced mechanical properties of 1,3-trimethylene carbonate polymers and networks. Polymer. 2003;44(21):6495—504. 8.
Pêgo AP, Siebum B, Van Luyn MJ, Gallego Y, Van Seijen XJ, Poot AA, Grijpma DW, Feijen J. Preparation of degradable porous structures based on 1,3-trimethylene carbonate and D,L-lactide (co)polymers for heart tissue engineering. Tissue Eng 9, 981, 2003.
Pêgo AP, Van Luyn MJ, Brouwer LA, van Wachem PB, Poot AA, Grijpma DW, Feijen J. *In vivo* behavior of poly(1,3-trimethylene carbonate) and copolymers of 1,3-trimethylene carbonate with D,L-lactide or epsilon-caprolactone: Degradation and tissue response. J Biomed Mater Res A. 2003 Dec 1;67(3):1044-54.
Pêgo AP, Vleggeert-Lankamp CL, Deenen M, Lakke EA, Grijpma DW, Poot AA, Marani E, Feijen J. Adhesion and growth of human Schwann cells on trimethylene carbonate (co)polymers. J Biomed Mater Res A. 2003 Dec 1;67(3):876-85.
Pence BD, Woods JA. Exercise, Obesity, and Cutaneous Wound Healing: Evidence from Rodent and Human Studies. Adv Wound Care (New Rochelle). 2014 Jan 1;3(1):71-79.
Pillai CKS, Paul W, Sharma CP. Chitin and chitosan polymers: chemistry, solubility and fiber formation. Prog Polym Sci. 2009 Jul;34:641–78.
Posnett J, Gottrup F, Lundgren H, Saal G. The resource impact of wounds on health-care providers in Europe. J Wound Care. 2009 Apr;18(4):154-161.
Proksch E, Brandner JM, Jensen JM. The skin: an indispensable barrier. Exp Dermatol. 2008 Dec;17(12):1063-72.
Qin Y, Yuan M, Li L, Guo S, Yuan M, Li W, Xue J. Use of polylactic acid/polytrimethylene carbonate blends membrane to prevent postoperative adhesions. J Biomed Mater Res B Appl Biomater. 2006 Nov;79(2):312-9.

Rahman I, Said DG, Maharajan VS, Dua HS. Amniotic membrane in ophthalmology: indications and limitations. Eye (Lond). 2009 Oct;23(10):1954-61.

Ramot Y, Nyska A, Markovitz E, Dekel A, Klaiman G, Zada MH, Domb AJ, Maronpot RR. Long-term Local and Systemic Safety of Poly(L-lactide-co-epsilon-caprolactone) after Subcutaneous and Intra-articular Implantation in Rats. Toxicol Pathol. 2015 Dec;43(8):1127-40.

Ravishanker R, Bath AS, Roy R. "Amnion Bank"--the use of long term glycerol preserved amniotic membranes in the management of superficial and superficial partial thickness burns. Burns. 2003 Jun;29(4):369-74.

Rocha DN, Brites P, Fonseca C, Pêgo AP. Poly(trimethylene carbonate-co-ε-caprolactone) promotes axonal growth. PLoS One. 2014 Feb 27;9(2):e88593.

Ross MH, Pawlina W. Histology – A Text and Atlas. 6th edition. Lippincott Williams & Wilkins 2010.

Rönkkö S, Rekonen P, Sihvola R, Kaarniranta K, Puustjärvi T, Teräsvirta M, Uusitalo H. Histopathology of the three implanted degradable biopolymers in rabbit eye. J Biomed Mater Res A. 2009 Mar 1;88(3):717-24.

Sadler TW. Langman´s Medical Embryology. 12th edition. Editor Taylor C. Lippincott Williams & Wilkins 2012;21:339-344.

Sartoneva R, Haaparanta AM, Lahdes-Vasama T, Mannerström B, Kellomäki M, Salomäki M, Sándor G, Seppänen R, Miettinen S, Haimi S. Characterizing and optimizing poly-L-lactide-co-ε-caprolactone membranes for urothelial tissue engineering. J R Soc Interface. 2012 Dec 7;9(77):3444-54.

Sartoneva R, Haimi S, Miettinen S, Mannerström B, Haaparanta A-M Sándor G, Kellomäki M, Suuronen R, Lahdes-Vasama T. Comparison of poly(lactide-ε-caprolactone) membrane and amniotic membrane for urothelium tissue engineering applications. J R Soc Interface. 2011 8: 671-7.

Sartoneva R, Kuismanen K, Juntunen M, Karjalainen S, Hannula M, Kyllönen L, Hyttinen J, Huhtala H, Paakinaho K, Miettinen S. Porous poly-l-lactide-co-ε-caprolactone scaffold: a novel biomaterial for vaginal tissue engineering. R Soc Open Sci. 2018 Aug 15;5(8):180811.

Sartoneva R, Nordback PH, Haimi S, Grijpma DW, Lehto K, Rooney N, Seppänen-Kaijansinkko R, Miettinen S, Lahdes-Vasama T. Comparison of poly(L-lactide-co-ε-caprolactone) and poly(trimethylene carbonate) membranes for urethral regeneration: an *in vitro* and *in vivo* study. Tissue Eng Part A. 2018 Jan;24(1-2):117-127.

Sato T, Kirimura Y, Mori Y. The co-culture of dermal fibroblasts with human epidermal keratinocytes induces increased prostaglandin E2 production and cyclooxygenase 2 activity in fibroblasts. J Invest Dermatol. 1997 Sep;109(3):334-9.

Sayeg K, Freitas-Filho LG, Waitzberg AF, Arias VE, Laks M, Egydio FM, Oliveira AS. Integration of collagen matrices into the urethra when implanted as onlay graft, Int Braz J Urol, 2013 39: 414-23.

Seaton M, Hocking A, Gibran NS. Porcine models of cutaneous wound healing. ILAR J. 2015;56(1):127-38.

Serezani APM, Bozdogan G, Sehra S, Walsh D, Krishnamurthy P, Sierra Potchanant EA, Nalepa G, Goenka S, Turner MJ, Spandau DF, Kaplan MH. IL-4 impairs wound healing potential in the skin by repressing fibronectin expression. J Allergy Clin Immunol. 2017 Jan;139(1):142-151.e5.

Shafiq M, Jung Y, Kim SH. Stem cell recruitment, angiogenesis, and tissue regeneration in substance P-conjugated poly(l-lactide-co-ε-caprolactone) nonwoven meshes. J Biomed Mater Res A. 2015 Aug;103(8):2673-88.

Shen X, Su F, Dong J, Fan Z, Duan Y, Li S. *In vitro* biocompatibility evaluation of bioresorbable copolymers prepared from L-lactide, 1, 3-trimethylene carbonate, and glycolide for cardiovascular applications. J Biomater Sci Polym Ed. 2015;26(8):497-514.

Shi R, Chen D, Liu Q, Wu Y, Xu X, Zhang L, Tian W. Recent advances in synthetic bioelastomers. Int J Mol Sci. 2009 Nov 20;10(10):4223-56.

Shimizu R, Kishi K. Skin graft. Plast Surg Int. 2012;2012:563493.

Simsek A, Aldamanhori R, Chapple CR, MacNeil S. Overcoming scarring in the urethra: Challenges for tissue engineering. Asian J Urol. 2018 Apr;5(2):69-77.

Sinha VR, Bansal K, Kaushik R, Kumria R, Trehan A. Poly-epsilon-caprolactone microspheres and nanospheres: an overview. Int J Pharm. 2004 Jun 18;278(1):1-23.

Smith A, Perelman M, Hinchcliffe M. Chitosan: a promising safe and immune-enhancing adjuvant for intranasal vaccines. Hum Vaccin Immunother. 2014;10(3):797-807.

Snodgrass W, Bush N. Primary hypospadias repair techniques: A review of the evidence. Urol Ann. 2016 Oct-Dec;8(4):403-408.

Song Y, Kamphuis MM, Zhang Z, Sterk LM, Vermes I, Poot AA, Feijen J, Grijpma DW. Flexible and elastic porous poly(trimethylene carbonate) structures for use in vascular tissue engineering. Acta Biomater. 2010 Apr;6(4):1269-77.

Song Y, Wennink JW, Kamphuis MM, Sterk LM, Vermes I, Poot AA, Feijen J, Grijpma DW. Dynamic culturing of smooth muscle cells in tubular poly(trimethylene carbonate) scaffolds for vascular tissue engineering. Tissue Eng Part A. 2011 Feb;17(3-4):381-7.

Southgate J, Masters JRW, Trejdosiewicz LK. Culture of human urothelium. In Culture of epithelial cells (eds R. I. Freshney & M. G. Freshney), pp. 381 – 399. New York, NY: John Wiley & Sons. 2002.

Summerfield A, Meurens F, Ricklin ME. The immunology of the porcine skin and its value as a model for human skin. Mol Immunol. 2015 Jul;66(1):14-21.

Chronic leg ulcers. Current Care Guidelines. Working group set up by the Finnish Medical Society Duodecim and the Finnish Dermatology Society. Helsinki: The Finnish Medical Society Duodecim, 2017 (referred March 3, 2014). Available online at: www.kaypahoito.fi

Synowiecki J, Al-Khateeb NA. Production, properties, and some new applications of chitin and its derivatives. Crit Rev Food Sci Nutr. 2003;43(2):145-71.

Stein MJ, DeSouza RA. Anterior urethral stricture review. Transl Androl Urol. 2013 Mar;2(1):32-8.

Stępniewski M, Martynkiewicz J, Gosk J. Chitosan and its composites: Properties for use in bone substitution. Polim Med. 2017 Jan-Jun;47(1):49-53.

Stone CA, Wright H, Clarke T, Powell R, Devaraj VS. Healing at skin graft donor sites dressed with chitosan. Br J Plast Surg. 2000 Oct;53(7):601-6.

Tabasum S, Noreen A, Kanwal A, Zuber M, Anjum MN, Zia KM. Glycoproteins functionalized natural and synthetic polymers for prospective biomedical applications: A review. Int J Biol Macromol. 2017 May;98:748-776.

Taira M, Araki Y, Nakao H, Takahashi J, Hyon SH, Tsutsumi, S. Cellular reactions to polylactide-based sponge and collagen gel in subcutaneous tissue. J Oral Rehabil 30, 106, 2003.

Talmi YP, Sigler L, Inge E, Finkelstein Y, Zohar Y. Antibacterial properties of human amniotic membranes. Placenta. 1991 May-Jun;12(3):285-8.
Tauzin H, Rolin G, Viennet C, Saas P, Humbert P, Muret P. A skin substitute based on human amniotic membrane. Cell Tissue Bank. 2014 Jun;15(2):257-65.
Tenenhaus M, Rennekampff HO. Current Concepts in Tissue Engineering: Skin and Wound. Plast Reconstr Surg. 2016 Sep;138(3 Suppl):42S-50S.
Tran JP, McLaughlin JM, Li RT, Phillips LG. Prevention of Pressure Ulcers in the Acute Care Setting: New Innovations and Technologies. Plast Reconstr Surg. 2016 Sep;138(3 Suppl):232S-40S.
Trelford JD, Trelford-Sauder M. The amnion in surgery, past and present. Am J Obstet Gynecol. 1979 Aug 1;134(7):833-45.
Tseng SC, Li DQ, Ma X. Suppression of transforming growth factor-beta isoforms, TGF-beta receptor type II, and myofibroblast differentiation in cultured human corneal and limbal fibroblasts by amniotic membrane matrix. J Cell Physiol. 1999 Jun;179(3):325-35.
Ueno H, Yamada H, Tanaka I, Kaba N, Matsuura M, Okumura M, Kadosawa T, Fujinaga T. Accelerating effects of chitosan for healing at early phase of experimental open wound in dogs. Biomaterials. 1999 Aug;20(15):1407-14.
Uyeturk U, Gucuk A, Firat T, Kemahli E, Kukner A, Ozyalvacli ME. Effect of mitomycin, bevacizumab, and 5-Fluorouracil to inhibit urethral fibrosis in a rabbit model, J Endourol, 2014 28: 1363-7.
Varin A, Gordon S. Alternative activation of macrophages: immune function and cellular biology. Immunobiology. 2009;214(7):630-41.
van der Horst HJ, de Wall LL. Hypospadias, all there is to know. Eur J Pediatr. 2017 Apr;176(4):435-441.
Van Leeuwen AC, Van Kooten TG, Grijpma DW, Bos RR. *In vivo* behaviour of a biodegradable poly(trimethylene carbonate) barrier membrane: a histological study in rats. J Mater Sci Mater Med. 2012 Aug;23(8):1951-9.
Vidmar J, Chingwaru C, Chingwaru W. Mammalian cell models to advance our understanding of wound healing: a review. J Surg Res. 2017 Apr;210:269-280.
Vig K, Chaudhari A, Tripathi S, Dixit S, Sahu R, Pillai S, Dennis VA, Singh SR. Advances in Skin Regeneration Using Tissue Engineering. Int J Mol Sci. 2017 Apr 7;18(4).
Villoldo GM, Loresi M, Giudice C, Damia O, Moldes JM, DeBadiola F, Barbich M, Argibay P Histologic Changes After Urethroplasty Using Small Intestinal Submucosa Unseeded with Cells in Rabbits with Injured Urethra, Urology. 2013 81: 1380 e1-5.
Vogels RR, Bosmans JW, van Barneveld KW, Verdoold V, van Rijn S, Gijbels MJ, Penders J, Breukink SO, Grijpma DW, Bouvy ND. A new poly(1,3-trimethylene carbonate) film provides effective adhesion reduction after major abdominal surgery in a rat model. Surgery. 2015 Jun;157(6):1113-20.
Vuornos K, Björninen M, Talvitie E, Paakinaho K, Kellomäki M, Huhtala H, Miettinen S, Seppänen-Kaijansinkko R, Haimi S. Human Adipose Stem Cells Differentiated on Braided Polylactide Scaffolds Is a Potential Approach for Tendon Tissue Engineering. Tissue Eng Part A. 2016 Mar;22(5-6):513-23.
Wang C, Jia Y, Yang W, Zhang C, Zhang K, Chai Y. Silk fibroin enhances peripheral nerve regeneration by improving vascularization within nerve conduits. J Biomed Mater Res A. 2018 Jul;106(7):2070-2077.

Wang X, Chen Y, Fan Z, Hua K. Comparing different tissue-engineered repair materials for the treatment of pelvic organ prolapse and urinary incontinence: which material is better? Int Urogynecol J. 2018 Jan;29(1):131-138.
Weiner L, Fu W, Chirico WJ, Brissette JL. Skin as a living coloring book: how epithelial cells create patterns of pigmentation. Pigment Cell Melanoma Res. 2014 Aug 8.
Werdin F, Tennenhaus M, Schaller HE, Rennekampff HO. Evidence-based management strategies for treatment of chronic wounds. Eplasty. 2009 Jun 4;9:e19.
Williams DF. On the nature of biomaterials. Biomaterials. 2009 Oct;30(30):5897-909.
Wills-Karp M, Finkelman FD. Untangling the complex web of IL-4- and IL-13-mediated signaling pathways. Sci Signal. 2008 Dec 23;1(51):pe55.
Wound Healing Society. Guidelines for the best care of chronic wounds. Wound Repair Regen. 2006;14:647–710.
Yamany T, Van Batavia J, Mendelsohn C. Formation and regeneration of the urothelium. Curr Opin Organ Transplant. 2014 Jun;19(3):323-30.
Yang Z, Wu Y, Li C, Zhang T, Zou Y, Hui JH, Ge Z, Lee EH. Improved mesenchymal stem cells attachment and *in vitro* cartilage tissue formation on chitosan-modified poly(L-lactide-co-epsilon-caprolactone) scaffold. Tissue Eng Part A. 2012 Feb;18(3-4):242-51.
Yassin MA, Leknes KN, Sun Y, Lie SA, Finne-Wistrand A, Mustafa K. Surfactant tuning of hydrophilicity of porous degradable copolymer scaffolds promotes cellular proliferation and enhances bone formation. J Biomed Mater Res A. 2016 Aug;104(8):2049-59.
Younes I, Rinaudo M. Chitin and chitosan preparation from marine sources. Structure, properties and applications. Mar Drugs. 2015 Mar 2;13(3):1133-74.
Zelen CM, Serena TE, Denoziere G, Fetterolf DE. A prospective randomized comparative parallel study of amniotic membrane wound graft in the management of diabetic foot ulcers. Int Wound J. 2013 Oct;10(5):502-7.
Zeng N, van Leeuwen AC, Grijpma DW, Bos RR, Kuijer R. Poly(trimethylene carbonate)-based composite materials for reconstruction of critical-sized cranial bone defects in sheep. J Craniomaxillofac Surg. 2017 Feb;45(2):338-346.
Zhang Z, Kuijer R, Bulstra SK, Grijpma DW, Feijen J. The *in vivo* and *in vitro* degradation behavior of poly(trimethylene carbonate). Biomaterials. 2006 Mar;27(9):1741-8.
Zhou JC, Zhang JJ, Zhang W, Ke ZY, Zhang B. Efficacy of chitosan dressing on endoscopic sinus surgery: a systematic review and meta-analysis. Eur Arch Otorhinolaryngol. 2017 Sep;274(9):3269-3274.
Zhu KJ, Hendren RW, Jensen K, Pitt CG. Synthesis, properties, and biodegradation of poly(1,3-trimethylene carbonate). Macromolecules 1991;24(8):1736–40.
Zhu Y, Leong MF, Ong WF, Chan-Park MB, Chian KS. Esophageal epithelium regeneration on fibronectin grafted poly(L-lactide-co-caprolactone) (PLLC) nanofiber scaffold. Biomaterials. 2007 Feb;28(5):861-8.

10 ORIGINAL COMMUNICATIONS

Amniotic membrane reduces wound size in early stages of the healing process

• **Objective:** To investigate the effects of dispase de-epithelialised, glycerol cryopreserved AM on full-thickness skin defects, using a rat model.

• **Method:** Skin defects of 15mm diameter were surgically created and measured on the scalps of 53 male rats. Animals were divided into two groups and followed for 0, 3, 7, 14 or 21 days. AM group wounds were covered with de-epithelialized AM and sodium chloride moistened Aquacel (ConvaTec Inc.); control group wounds were covered with sodium chloride moistened Aquacel alone. After the follow-up, wounds were measured again, serum samples were taken and wound sites were harvested for histological analysis. Systemic interleukin-4 (IL-4) levels were analysed from serum.

• **Results:** On day 3, a statistically significant difference ($p < 0.01$) was observed in mean wound size, with wound size in the AM group smaller than in the control group (60 ± 12 % vs 81 ± 13 % of the original size); other time points showed no significance difference in wound size between the two groups. We could not detect differences between the groups in histological parameters or serum IL-4 levels.

• **Conclusion:** According to this study, AM enhances early stage wound healing considering wound size but its effect decreases in later phases. The IL-4 results provide no clear evidence that IL-4 contributes to the effect of AM on wound healing.

• **Declaration of interest:** This study was financially supported by the Competitive Research Funding of the Tampere University Hospital (Grant 9H041, 9J047). The authors have no additional conflicts of interest to declare.

amnion; amniotic membrane; wound; full-thickness; interleukin-4

Amniotic membrane (AM) is the inner fetal membrane, composed of epithelial cell layer, collagen-rich basement membrane layer and fibroblastic spongy layer.[1] The microscopical structure of AM is interesting because it does not contain blood vessels, lymphatic canals or nerves.[2] AM also does not express HLA-A, B or DR antigens, giving it very low antigenicity and thus potential in tissue engineering.[3] It has been shown that AM can be used both fresh and glycerol preserved, with the latter equivalent to dressings.[4] Gamma-irradiation has also been shown to be an option to preserve AM.[5]

Davis was the first to suggest the use of AM for skin defects, as early as 1910.[6] Ever since, AM has been used in a variety of applications: in gynecological reconstructive surgery,[7,8] intra-abdominal surgery,[9] dural defect repair,[10] mandibular vestibuloplasty[11] and treating burn injuries and ulcers.[12–14] Currently, AM is used primarily in the field of ophthalmology,[15] where it is known to promote corneal epithelialisation,[16] reduce pain,[17] and have anti-microbial and anti-inflammatory properties.[18,19]

A recent study suggests that AM induces epithelialisation, particularly in massive post-traumatic wounds,[20] with AM also shown to reduce scarring.[7] For burn injuries, AM has been suggested to be one of the most effective biological dressings.[12,21] However, it is not clear whether AM induces or inhibits angiogenesis, which is an important part of wound healing.[22,23]

The wound healing process, in general, is directed by several cytokines. One of the crucial mediators is interleukin-4 (IL-4). In addition to the wound healing process, IL-4 has a role in immune regulation, cell growth and leukocyte differentiation.[24,25] Its main effect in wound healing is to induce the expression of extracellular matrix proteins.[26]

The clinical use of AM is largely based on case reports and uncontrolled clinical series. The behaviour of AM and its interaction with tissues have not been well described. Thus, the aim of this study was to investigate the effects of dispase de-epithelialised, glycerol cryo-preserved AM on full-thickness skin defects, using a rat model. The effect of AM on wound size and histological outcome were analysed. The study also measured systemic IL-4 levels.

Method

Amniotic membrane

Chorion-amnion sacs were received from volunteers undergoing elective caesarean section delivery for medical reasons in Tampere University Hospital. AM is less like to be contaminated with potentially pathogenic bacteria in caesarean sections than

P.H. Nordback,[1,2,3] MD;
S. Miettinen,[1,2,3] PhD;
M. Kääriäinen,[4] MD, PhD;
M. Pelto-Huikko,[5] MD, PhD;
H. Kuokkanen,[4] MD, PhD;
R. Suuronen,[1,2,6,7] MD, PhD, DDS;
1 Institute of Biomedical Technology, University of Tampere, Finland;
2 BioMediTech, Tampere, Finland;
3 Science Centre, Tampere University Hospital, Finland;
4 Department of Plastic surgery, Tampere University Hospital, Finland;
5 Department of Anatomy, University of Tampere, Finland;
6 Department of Eye, Ear and Oral Diseases, Tampere University Hospital, Finland;

continued on page 2

7 Department of Biomedical Engineering, Tampere University of Technology, Finland. Email: panu.nordback@uta.fi

vaginal deliveries.[27] Chorion-amnion sacs attached to placentas were stored at –80°C.

Placentas were thawed at room temperature, overnight, before preparation. Chorion-amnion membrane was detached from the placenta using blunt dissection. AM was separated from the chorion and washed 10 times with 0.9% sodium chloride (Baxter Healthcare Ltd.). AMs were then stored at 4°C in 10% Dulbecco's phosphate-buffered saline solution (DPBS; Lonza Inc.), containing antibiotics (2.5µg/ml amphotericin B [Invitrogen Ltd.], 5.0µg/ml penicillin [Invitrogen Ltd.], 50µg/ml streptomycin [Invitrogen Ltd.] and 100µg/ml neomycin [Sigma-Aldrich Inc.]). The next day, pieces of AM were cryopreserved at –80°C in 1:1 DPBS-glycerol solution, in plastic containers.

Before use, AM was thawed, washed three times with DPBS, spread on a Petri dish and incubated overnight with 40mg dispase (Invitrogen Ltd.) in 40ml of DMEM/F-12 (Invitrogen Ltd.) solution containing 100U/ml penicillin, 100µg/ml streptomycin and 250ng/ml amphotericin B, to remove epithelial cells. Overnight incubation of AM was followed by scraping for complete removal of the epithelial layer, which was verified by microscopic inspection.

Dispase-processed AM was washed 10 times with cold DPBS to remove dispase. The AM was difficult to handle due to its consistency; CellCrown6-ring (Scaffdex Inc.) was discovered to be helpful in handling AM during the transplantation process. Approximately 20mm-diameter AM pieces were then cut and spread on CellCrown6-rings for transplantation to the wound surface (Fig 1a). AM was transplanted to the wound, with the revealed basement membrane facings towards the wound surface.

Glycerol has been used as a preservation method for AM in previous studies.[4] Our method to process glycerol-preserved AM differed from the method of Maral et al.,[4] as we stored the placentas at –80°C before processing and washed the membranes with sodium chloride instead of tap water; our antibiotic solution also contained amphotericin, penicillin and streptomycin, and we used only 50% glycerol solution, instead of 85%. This method is thought to be less contaminative, due to a wider spread of antibiotics and the use of sodium chloride, instead of tap water.

The study was conducted in accordance with the guidelines of the Ethics Committee of the Pirkanmaa Hospital District, Tampere, Finland (R06045, 03/2006).

Wound preparation

Healthy adult male Sprague-Dawley rats, weighing 300–500g, were purchased from the Animal Laboratory of Tampere University. Permits for animal experiments were acquired from the Animal Care and Use Committee of the respective Provincial Committee for Animal Experiments (ESLH-2008-04691/Ym-23).

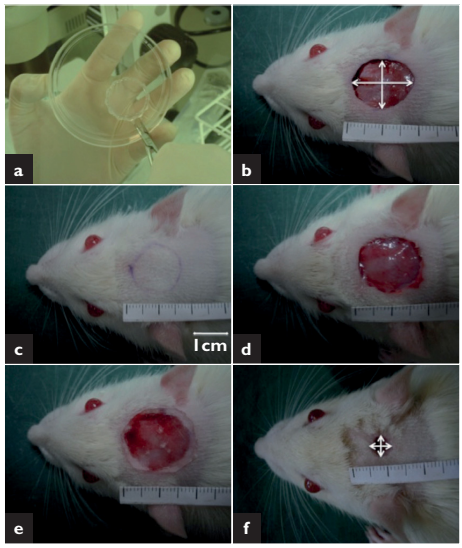

Fig 1. Series of wound preparation and care. AM was cut and spread on CellCrown6-rings for transplantation to the wound surface, (a). The circular full-thickness skin defects were surgically created on the rats scalps, (b,c). Wounds were covered with AM, and moistened Aquacel (d), or moistened Aquacel alone, (e). Wounds were measured in two directions before and after the follow-up to define the wound surface reduction, (b,f)

The National Research Council's guide for the care and use of laboratory animals was followed.

Pilot tests were conducted before the experimental series, considering wound size, location and wound care. In pilot tests, we tested abdominal and dorsal regions, as well as the scalps for sites of the wound. We tested Mepilex (Mölnlycke Health Care), Mepilex Lite (Mölnlycke Health Care) and Aquacel (ConvaTec Inc.) as wound dressings. Mepilex and Mepilex Lite were fixated both with and without sutures.

Rats were anaesthetised by intraperitoneal injection of 0.05mg/100g body weight medetomidine (Domitor; Orion Inc.) and 7.5mg/100g body weight ketamine (Ketalar; Parke Davis Inc.). Rat scalps were shaved and cleansed with 80% ethanol.

Full-thickness (to the bottom of dermis) circular skin defects of approximately 15mm diameter were excised, using surgical scissors, on the scalps of the anaesthetised rats (Fig 1b,c), representing a large wound in relation to the size of the animal.

Defects were then measured along two axes, with a measuring tape (Fig 1c). Measurements were taken from the widest and longest points of the wound. Using these measurements, the wound surface was calculated from the mathematical formula for ellipse area: $A_{wound}=\pi\times a\times b$, where a and b represent one-half of the ellipse´s major and minor axes, respectively.

All 53 rats were coded and randomised into two groups — AM and control group. In the AM group, wounds were covered with AM and a sodium chloride-moistened wound dressing (Aquacel; ConvaTec

References

1 Bourne, G.L. The microscopic anatomy of human amnion and chorion. Am J Obstet Gynecol. 1960; 79: 1070–1073.

2 Mohamad, H. Anatomy and embryology of human placenta, amnion and chorion. Sci Basis Tissue Trans. 2001; 5: 139–148.

3 Akle, C.A., Adinolfi, M., Welsh, K.I. et al. Immunogenicity of human amniotic epithelial cells after transplantation into volunteers. Lancet. 1981; 2: 8254, 1003–1005.

Inc.), whereas in the control group they were covered only with the moistened wound dressing, as shown in Fig 1d and 1e. Mepilex and Mepilex Lite were found to be unsuitable, due to poor attachment to the wound surface.

Within groups, follow-up periods were 0, 3, 7, 14 or 21 days. On day 0, five rats were studied without treatment, immediately after creation of the wound, to establish the baseline conditions of the wound. All other time points consisted of 12 rats, six rats in the AM group and six rats in the control group.

Follow-up

Throughout the experiment, the animals were individually caged and on *ad libitum* diet. Weight loss and need for postoperative pain medication were monitored to ascertain the general wellbeing of the animals. If needed, postoperative pain was relieved using subcutaneous injection of 0.002mg/100g body weight buprenorfine (Temgesic; Schering-Plough Europe Inc.), once a day.

After 3, 7, 14 and 21 days, rats were anaesthetised again. Wound measurements were conducted by an investigator blinded as to the group allocation and the wound area calculated, as above. Five millilitres of blood was collected via heart puncture. Blood samples were centrifuged to separate serum. Serum samples were stored at –80°C for IL-4 analysis (Rat IL-4 ELISA kit, Diaclone; Gen-Probe Life Sciences Inc.). The rats were then euthanised with CO_2. Thereafter, the entire scalp with the skull underneath was excised to collect the whole wound area for histological analysis. Immediately after the wound sites were excised, they were put into 10% formalin to 'freeze' the tissue in its state at the moment of excision. The wound area retained its natural conformation for histological analysis when the skull underneath was also excised.

Histology

Transverse sections of the whole wound area, including the underlying tissue, were embedded in paraffin and stained with haematoxylin-eosin, which is widely used in evaluation of skin constructs.[28] Histological analysis was blinded to group allocation and follow-up. Epithelialisation was described by the percentage covering the wound, at that time point, using a microscopical ten-grid.

Microscopical 10-grid is an assisting 'device', which creates a square grid consisting of smaller 10×10 squares in the microscopical view. Using the grid, it is possible to evaluate distances from the microscopical view, but it also outlines the area under examination. Oedema and fibrin were analysed from three different views, using four-time magnification. Oedema showed as puffy swelling within skin structure; fibrin identified as a clot around the wound surface, with varying thickness.

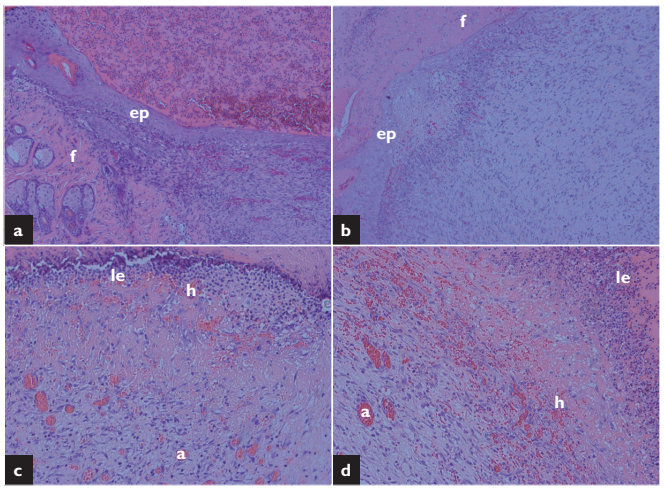

Fig 2. Histological images from 7-day follow-up. Pictures a and c were taken from an AM wound. Pictures b and d from a control wound. (a=angiogenesis, ep=epithelialisation, f=fibrin, h=haemorrhage, le=leukocytes)

Haemorrhage, angiogenesis and necrosis were analysed from six views, using 25-time magnification. Red blood cells are clearly visible in the HE-dying and the more red blood cells there are outside the vessels, the greater the haemorrhage is. Angiogenesis showed as occurrence of small veins that differed from original skin structure. For the possibility of necrosis, cell structures were inspected.

Oedema, fibrin, haemorrhage, angiogenesis and necrosis were scored 0–3, in comparison to categorise them as none, minimal, medial and maximal. A score of 0 meant that the parameter was not visible in relation to normal skin structure and a score of 3 meant the greatest possible state. Scores were defined visually (Fig 2).

Leukocytes were also counted using 25-time magnification; leukocytes were identified due to their property of turning dark blue with HE-dying and cell morphology.

IL-4 analysis

Serum samples were stored at –80°C and thawed prior to IL-4 analysis. IL-4 expression was measured using the Rat IL-4 ELISA kit, which was performed following the manufacturers instructions precisely. Three samples from each rat were analysed in parallel, on a multilabel counter with 450nm wavelength (Victor 1420 Multilabel Counter).

Statistical analysis

Results were analysed using SPSS for Windows (v16.0; SPSS Inc.). Continuous variables were analysed using unpaired Student´s t-test and scored parameters with Mann-Whitney test. Results for

4 Maral, T., Borman, H., Arslan, H. et al. Effectiveness of human amnion preserved long-term in glycerol as a temporary biological dressing. Burns. 1999; 25: 7, 625–635.

5 Gajiwala, K., Gajiwala, A.L. Evaluation of lyophilised, gamma-irradiated amnion as a biological dressing. Cell Tissue Bank. 2004; 5: 2, 73–80.

6 Davis, J.W. Skin transplantation with a review of 550 cases at the Johns Hopkins hospital. Johns Hopkins Med J. 1910; 15: 307–396.

7 Trelfor, J.D., Trelford-Sauder, M. The amnion surgery, past and present. Am J Obstet Gynecol. 1979; 134: 7, 833–845.

8 Ashworth, M.F., Morton, K.E., Dewhurst, J. et al. Vaginoplasty using amnion. Obstet Gynecol. 1986; 67: 3, 443–446.

9 Szabo, A., Haj, M., Waxsman, I., Eitan, A. Evaluation of seprafilm and amniotic membrane as adhesions prophylaxis in mesh repair of abdominal wall hernia in rats. Eur Surg Res. 2000; 32: 125–128.

10 Kudriashov, A.F., Artarian, A.A., Putsillo, M.V. Use of amnion to repair dural defect [in Russian]. Zh Vopr Neirokhir Im N Burdenko. 1981; 5: 37–40.

continued on page 6 ▶

Table 1. The results of the seven parameter histological analysis

	Parameter	AM group	Control group	p-value
Day 0				
	Epitheliasation (%)	—	0.0%	—
	Oedema (score)	—	0.5 (0.0–0.8)	—
	Fibrin (score)	—	0.0 (0.0–0.7)	—
	Haemorrhage (score)	—	0.4 (0.3–0.8)	—
	Angiogenesis (score)	—	0.0 (0.0–0.5)	—
	Leukocytes (n)	—	24 ± 9	—
Day 3				
	Epitheliasation (%)	9.5 ± 3.0%	6.7 ± 2.3%	0.101
	Oedema (score)	0.5 (0.0–0.8)	1.8 (1.3–2.0)	0.310
	Fibrin (score)	1.2 (0.7–1.7)	1.2 (1.0–1.7)	0.937
	Haemorrhage (score)	1.0 (0.8–1.3)	1.2 (1.0–1.7)	0.937
	Angiogenesis (score)	0.2 (0.0–0.5)	0.3 (0.0–0.7)	0.589
	Leukocytes (n)	68 ± 23	72 ± 30	0.834
Day 7				
	Epitheliasation (%)	19 ± 10%	15 ± 6.5%	0.385
	Oedema (score)	1.8 (0.7–2.7)	1.8 (0.8–2.8)	0.937
	Fibrin (score)	2.0 (0.2–3.0)	1.8 (1.3–2.5)	1.000
	Haemorrhage (score)	0.7 (0.2–0.8)	0.9 (0.6–0.9)	0.093
	Angiogenesis (score)	0.3 (0.0–1.1)	0.7 (0.3–1.3)	0.310
	Leukocytes (n)	68 ± 40	60 ± 17	0.649
Day 14				
	Epitheliasation (%)	45 ± 31%	34 ± 15%	0.470
	Oedema (score)	1.2 (0.3–1.5)	1.0 (0.2–1.5)	0.589
	Fibrin (score)	1.5 (0.3–2.5)	0.8 (0.7–1.8)	0.589
	Haemorrhage (score)	0.5 (0.3–1.1)	0.6 (0.2–0.8)	0.937
	Angiogenesis (score)	1.3 (0.6–2.3)	1.5 (0.8–2.3)	0.589
	Leukocytes (n)	57 ± 23	68 ± 26	0.422
Day 21				
	Epitheliasation (%)	60 ± 14%	72 ± 26%	0.359
	Oedema (score)	0.3 (0.0–0.5)	0.3 (0.0–0.7)	0.818
	Fibrin (score)	0.9 (0.0–1.3)	1.0 (0.3–3.0)	0.699
	Haemorrhage (score)	0.5 (0.3–0.6)	0.5 (0.2–0.8)	0.937
	Angiogenesis (score)	1.6 (0.3–2.1)	1.2 (0.7–1.5)	0.240
	Leukocytes (n)	62 ± 15	55 ± 26	0.595

Necrosis was not present in any of the wounds and is thus excluded from the table; Scores are given as median (range), all other results are given as mean ± SD

continuous variables are presented as mean and standard deviations, while scored parameters are presented as median and range. Statistical significance was set as $p<0.05$. Outliers were identified by the statistical programme used (SPSS), defined as those results that diverged considerably from the main group; these were considered to be outliers due to the extremely compact range on 21-day control.

Results

Pilot tests showed that rat skin is more stable on the scalp due to fixation to the ear lobes and facial region. Based on these preliminary studies, we decided to place the wound on the scalp. Suture fixation of the dressing was found to increase scratching and animals habituated better with lighter wound dressing on top of the wound. Moisturised Aquacel was found to be most suitable.

In the beginning of the follow-up the animals weighed 430 ± 50g. During the first 3 days animals' weight loss was 9–10%, after which all the animals regained their original weight by day 14, at the latest. There were no statistically significant differences in weight between the two groups, at any time point. There was no need for analgesia after the second postoperative day.

On day 3, the was a statistically significant difference in wound size in the control group (81 ± 13% of the original wound size) compared with the AM group was observed (60 ± 12%; Fig 3; p=0.009). By day 7, the corresponding percentages were 66 ± 4% in the control group and in the AM group 64 ± 9%, but showed no statistical significant difference (p=0.559). There was also no statistically significant difference observed between the groups on day 14 (p=0.547) or day 21 (p=0.652).

The day 3 time-point showed epithelial coverage in both groups. On day 21, the control group epithelialisation was 72 ± 26% of the original wound size, whereas in the AM group it was 60 ± 14% (p=0.359; Table 1). Although the epithelialisation was somewhat larger in the AM group on day 3, 7 and 14 days the difference was not statistically significant.

Immediately after wound preparation (day 0) only mild oedema and fibrin were discovered (Table 1). Highest oedema score in the control group was on days 3 and 7, where AM group oedema score was at its highest on day 7. Fibrin scores were highest on day 7 in both groups (AM 2.0 [0.2–3.0] vs control 1.8 [1.3–2.5], respectively; Fig 2). There was no statistically significant difference between the groups either in oedema or fibrin scores at any time point (Table 1).

Day 0 samples showed minimal haemorrhage scores of 0.4 (0.3–0.8) and 0.0 (0.0–0.5) for angiogenesis (Table 1). Haemorrhage reached its maximum on day 3. In the control group, the highest score in angiogenesis was seen on day 14. Maximal angiogenesis in the AM group was seen on day 21. There were no statistically significant differences between groups at any time-point. Necrosis was not discovered from any wound.

The leukocyte count on day zero was 24 ± 9. There was strong leukocytosis in the wounds starting from day 3 (counts 68 ± 23 and 72 ± 30 for AM and control group, respectively). This reaction did not subside during the 21-day follow-up. No statistically significant differences were observed between the two study groups.

In both groups, IL-4 absorbance levels descended from early stage to day 21 (Fig 3b). The decrease in

both groups between day 0 and day 21 was statistically significant ($p<0.05$). No statistically significant differences were observed between the groups.

Discussion

Despite limitations, rats are commonly used in wound research.[29] Good availability, low costs and small size support the selection of rat as a test animal, although histo-anatomical differences between rodent and human skin are obvious.

The wound site was selected after pilot tests. The skin of the scalp is better attached to the subcutaneous tissue than in the body regions. This is because of skin attachment to ear lobes and the facial region. Better subcutaneous attachment should minimise contraction and thus match human skin better. In the pilot tests we also observed that light dressing is suitable to prevent scratching. We tested standard commercially available dressing products and used suture fixation, which irritated the rats. Based on low need for extra pain medication, the final procedure was considered atraumatic for the animals.

Not all wounds need exceptional medical attention and, in chronic wounds, the treatment should focus on the underlying pathophysiology; however, local treatment is a major part of the healing process. AM provides an interesting choice to enhance local healing conditions, whether the wound is chronic or acute. This study showed that AM had a positive effect on wound size in 3-day follow-up. Mean wound size reduced to 60% of the original size compared with a mean reduction to 81% in the control group; this difference was statistically significant.

After the 3-day time point, wound size reduction plateaued. It has been shown that dermal fibroblast proliferation occurs rapidly after injury, which leads to collagen-rich matrix formation within 3–4 days of wound formation.[30] This initiates the contraction process, which then suppresses as healing proceeds. Contraction might have a greater role in the healing process where AM is involved and that is why significant difference was only discovered at early stage of the healing process. It also could be that AM gradually degrades from the wound surface at early stage and thus the effect deteriorates. In fact, it has not been reliably ascertained how long AM remains even on ocular wound surface.[31]

Another possible reason is that AMs effects manifest during inflammation and early proliferation stage. However, we did not find statistically significant differences in epithelialisation, oedema or leukocytosis in histological analysis. It has been shown that AM promotes corneal epithelialisation.[16] Corneal and dermal epithelialisation cannot be stated as equal because corneal wound healing is thought to be a simpler process than when the healing process occurs in the skin. For instance cornea lacks blood vessels in the cornea.[32] A recent study suggests that AM promotes skin epithelialisation in massive post-traumatic wounds but the study is an uncontrolled case report of two human patients with post-traumatic wounds.[20]

In this study, we used glycerol cryo-preserved AM. However, processing and storage conditions for AM

Fig 3. Histogram of wound size as percentages of the original size after the follow-up time, (a), and of IL-4 absorbance during the follow-up time, (b)

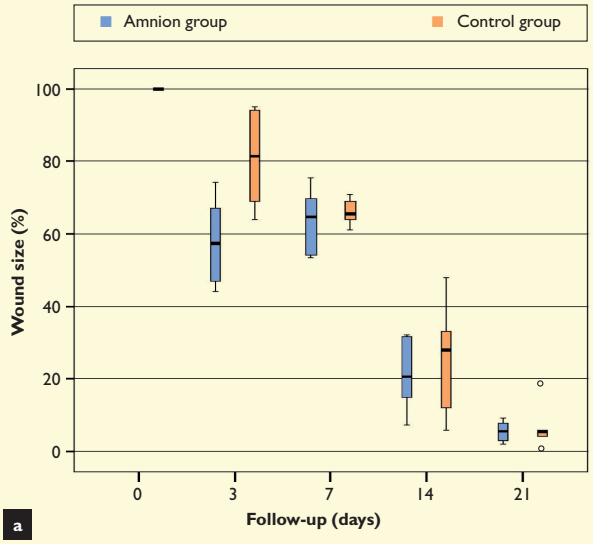

a

On day 3, statistically significant difference between the groups was observed ($p<0.01$);

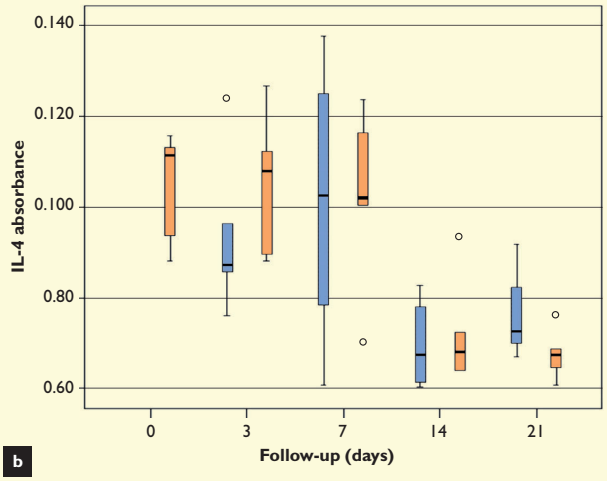

b

IL-4 levels decreased from early to late stage of the healing process; significant difference was observed between the AM and control group in the 21 day follow-up ($p=0.08$);
Circles indication outliers

The authors would like to thank to all collaborators at the Institute of Biomedical Technology and the Department of Plastic Surgery, as well as the personnel in Tampere University Animal Laboratory, who gave irreplaceable assistance. They would also like to thank Heini Huhtala for professional statistical advice.

may vary between studies.[4,5] The method to remove the epithelial cell layer might affect the usage of AM.[33–35] Our differences to the AM Maral et al. used can be considered minor, even though prolonged incubation of AM with dispase II has been suggested to enhance the degradation of AM.[33] In our study dispase incubation could be partly responsible for the fact that AM seemed to promote healing only during the early phase. We used overnight dispase incubation to remove the cell layer, which is long according to the references but our incubation temperature was only 4°C and not 37°C, where enzymatic activity increases. Also our dispase concentration was low and we did not use dispase II, which is a more potent enzyme.[29,33]

According to earlier studies, on tissue level, AM also has properties affecting the anti-inflammatory response,[18,19] and angiogenesis.[22,23] Our method revealed no clear anti-inflammatory qualities because there were no significant findings in oedema or leukocytosis. There was no statistically significant difference between the groups in angiogenesis, but earlier results considering angiogenesis are contradictory. It has been reported, *in vitro*, that AM expresses various antiangiogenic proteins, but also factors promoting angiogenesis, such as endothelin-2 and -3, vascular endothelial growth factor and vascular growth factor-B, has been identified from AM.[22,23]

Evidence show that IL-4 could promote wound closure when healing is impaired such as in infected wounds.[36] Although a crucial mediator in wound healing IL-4 has not previously been investigated in AM studies. The major cytokine related interest considering AM so far has been so called amnion-derived cellular cytokine solution which is a product secreted by amnion-derived multipotent progenitor cells.[37] In our study, serum IL-4 decreased over time both in AM and control groups following the observed healing course of the wounds. However, we did not find statistically significant differences in systemic IL-4 expression levels between groups, even though on day three wound size was significantly smaller in the AM than in the control group. The occasionally wide range of the results, for instance on day 7 in the AM group, has of course an impact to the statistical result and the effect might be so local that it does not show on systemical level.

Conclusion

According to this study, the use of AM in wound healing is possible. AM reduces wound size in the early stage (3 days) of the healing process but the effect decreases in later stages which should be taken into consideration especially in clinical applications. Systematic IL-4 analysis showed no clear evidence that IL-4 contributes to the effect of AM on wound healing. ■

11 Samandari, M.H., Yaghmaei, M., Ejlali, M. et al. Use of amnion as a graft material in vestibuloplasty – a preliminary report. Oral Surg Oral Med Oral Pathol Oral Radiol Endod. 2004; 97: 5, 574–578.

12 Atiyeh, B.S., Hayek, S.N., Gunn, S.W. New technologies for burn wound closure and healing – review of the literature. Burns. 2005; 31: 8, 944–956.

13 Bennett, J.P., Matthews, R., Faulk, W.P. Treatment of chronic ulceration of the legs with human amnion. Lancet. 1980; 1: 8179, 1153–1156.

14 Sabella, N. Use of foetal membranes in skin grafting. Med Rec NY. 1913; 83: 478–481.

15 Dua, H.S., Azuara-Blanco, A. Amniotic membrane transplantation. Br J Ophthalmol. 1999; 83: 6, 748–752.

16 Nakamura, T., Koizumi, N., Tsuzuki, M. et al. Successful regrafting of cultivated corneal epithelium using amniotic membrane as a carrier in severe ocular surface disease. Cornea. 2003; 22: 1, 70–71.

17 Subrahmanyam, M. Honey-impregnated gauze versus amniotic membrane in the treatment of burns. Burns. 1994; 20: 331–333.

18 Robson, M.C., Krizek, T.J. The effect of human amniotic membranes on the bacteria population of infected rat burns. Ann Surg. 1973; 177: 2, 144–149.

19 Kjaergaard, N., Hein, M., Hyttel, L. et al. Antibacterial properties of human amnion and chorion *in vitro*. Eur J Obstet Gynecol Reprod Biol. 2001; 94: 2, 224–229.

20 Insausti, C.L., Alcaraz, A., García-Vizcaíno, E.M. et al. Amniotic membrane induces epithelialization in massive posttraumatic wounds. Wound Rep Reg. 2010; 18: 4, 368–377.

21 Burd, A., Chiu, T. Allogenic skin in the treatment of burns. Clin Dermatol. 2005; 23: 4, 376–387.

22 Hao, Y., Ma, D.H., Hwang, D.G. et al. Identification of anti-angiogenic and anti-inflammatory proteins in human amniotic membrane. Cornea. 2000; 19: 3, 348–352.

23 Marvin, K.W., Keelan, J.A., Eykholt, R.L. et al. Expression of angiogenic and neurotrophic factors in the human amnion and choriodecidua. Am J Obstet Gynecol. 2002; 187: 3, 728–734.

24 Brown, M.A., Hural, J. Functions of IL-4 and control of its expression. Crit Rev Immunol. 1997; 17: 1, 1–32.

25 Le Gros, G., Ben-Sasson, S.Z., Seder, R. et al. Generation of interleukin 4 producing cells *in vivo* and *in vitro*: IL-2 and IL4 are required for *in vitro* generation of IL-4-producing cells. J Immunol. 2008; 181: 5, 2943–2951.

26 Kucukcelebi, A., Harries, R.H.C., Hennessey, P.J. et al. *In vivo* characterization of interleukin-4 as a potential wound healing agent. Wound Rep Reg. 1995; 3: 1, 49–58.

27 Adds, P.J., Hunt, C., Hartley, S. Bacterial contamination of amniotic memrane. Br J Ophthalmol. 2001; 85: 2, 228–230.

28 Lammers, G., Verhaegen, P.D., Ulrich, M.M. et al. An overview of methods for the *in vivo* evaluation of tissue-engineered skin constructs. Tissue Eng Part B Rev. 2011; 17: 1, 33–55.

29 Dorsett-Martin, W.A. Rat models of skin wound healing: A review. Wound Rep Reg. 2004, 12: 6, 591–599.

30 Martin, P. Wound healing — aiming for perfect skin regeneration. Science. 1997; 276: 5309, 75–81.

31 Tosi, G.M., Traversi, C., Schuerfeld, K. et al. Amniotic membrane graft: Histopathological findings in five cases. J Cell Physiol. 2005; 202: 3, 852–857.

32 Wilson, S.E., Mohan, R.R., Mohan, R.R. et al. The corneal wound healing response: cytokine-mediated interaction of the epithelium, stroma, and inflammatory cells. Prog Retin Eye Res. 2001; 20: 5, 625–637.

33 Lim, L.S., Riau, A., Poh, R. et al. Effect of dispase denudation on amniotic membrane. Mol Vis. 2009. 15: 1962–1970.

34 Wilshaw, S.P., Kearney, J.N., Fisher, J., Ingham, E. Production of an acellular amniotic membrane matrix for use in tissue engineering. Tissue Eng. 2006; 12: 8, 2117–2129.

35 Yang, L., Shirakata, Y., Shudou, M. et al. New skin-equivalent model from de-epithelialized amnion membrane. Cell Tissue Res. 2006; 326: 1, 69–77.

36 Salmon-Ehr, V., Ramont, L., Godeau, G. et al. Implication of Interleukin-4 in wound healing. Lab Invest. 2000; 80: 8, 1337–1343.

37 Steed, D.L., Trumpower, C., Duffy, D. et al. Amnion-derived cellular cytokine solution: a physiological combination of cytokines for wound healing. Eplasty. 2008; 8: e18.

Chitosan membranes in a rat model of full-thickness cutaneous wounds: healing and IL-4 levels

• **Objective:** The aim of this study was to examine the effect of chitosan membrane on wound healing.
• **Method:** The effect of chitosan membranes was evaluated in an experimental rat model. On day 0, circular full-thickness skin sections were excised from the scalps of rats. The wounds were then measured and the surrounding area tattooed. Rats were sacrificed either immediately after excision, or randomised into control and chitosan groups and followed up on day 3, 7, 14 or 21. Control group wounds were covered with Aquacel (wound dressing). Chitosan group wounds were covered with chitosan membranes and the wound dressing. Wounds and the distances between the tattooed marks were measured on follow-up, the wound sites were harvested and histologically examined, and serum interleukin (IL-4) levels were analysed.
• **Results:** A total of 54 rats were examined and all time points included 6 control and 6 chitosan treated animals, except for day 0 which consisted of control animals only. On day 3, wounds in the chitosan group were significantly ($p<0.05$) smaller (60 ± 6% versus 78 ± 19% of the original wound area) than in the control group. Chitosan membranes were found to degrade at the wound sites between days 7 and 14. Leukocyte counts were lower in the chitosan group than in the control group on day seven ($p<0.05$). IL-4 levels were significantly higher on day 7 ($p<0.001$) and 14 ($p<0.0001$) in the chitosan group.
• **Conclusion:** According to our results chitosan membrane may promote early wound healing, reduce inflammation and affect the IL-4 pathway, however, the membrane degrades at the wound site after day 7.

• **Declaration of interest:** . The authors state no conflict of interest. This study was financially supported by the Competitive Research Funding of the Tampere University Hospital (Grant 9H041 and 9J047) and the Finnish Cultural Foundation.

chitosan; chitosan membrane; full-thickness; wound healing; IL-4

Chitin after cellulose is the second most common polysaccharide in the world. It occurs in marine arthropod shells like crabs and shrimp, and also in the cell walls of fungi and yeast from which chitin and chitosan can be extracted.[1] Chitosan is soluble in acidic, neutral and alkaline solutions, which makes it versatile.[2–3] It is produced from chitin by deacetylation to obtain properties different from chitin. Degradation of chitosan, which increases when the degree of deacetylation decreases, is thought to be affected by enzymes, tissue constituents, the conditions of application and the preparation methods.[4–5] Earlier studies show that chitin and chitosan are biocompatible and biodegradable,[6] both degrade from the wound surface due to the enzymatic activity of N-acetyl-D-glucosaminidase, lysozyme and lipases.[5,7,8]

Chitosan has been studied in a range of dermal applications including ulcers and skin substitution.[5] Other epithelial surfaces where chitosan has been investigated include uroepithelium in urogenital repair and corneal wound healing.[9,10] In addition, chitosan has been studied in renal functionality and in nerve, meniscus and bone defects.[5]

In the wound healing process, the ability of chitosan to enhance inflammatory cell migration is thought to be crucial.[11] Macrophage activation has been suggested as the main mechanism behind chitosan's positive effect.[5] It has also been proposed that chitosan and chitin have antimicrobial and non-toxic qualities.[12,13] Chitosan has also been shown to stimulate deposition, assembly and orientation of collagen fibrils in extracellular matrix components.[5,14] In addition, re epithelialisation has occurred faster in wounds treated with chitosan.[15–17]

Interleukin 4 (IL-4) is a cytokine involved in anti-inflammatory processes, cell growth, immune regulation and lymphocyte and macrophage differentiation.[18] In wound healing, IL-4 accelerates the synthesis of proteins important in the healing process such as fibronectin, and collagens I and II.[19] Interestingly, chitin has been found to enhance the synthesis of collagen I, II and IV.[20] However, IL-4 has not been investigated in studies in the presence of chitosan.

The aim of this study was to investigate the effect

P. H. Nordback,[1,2,3] MD;
S. Miettinen,[1,2,3] PhD;
M. Kääriäinen,[4] MD, PhD;
A-M. Haaparanta,[2,6] Dr Tech;
M. Kellomäki,[2,6] Professor, Dr Tech;
H. Kuokkanen,[4] Professor;
R. Seppänen,[1,2,5,6] MD, DDS, PhD, FeBoMS, Dr Tech (h.c.), Professor;
1 Institute of Biomedical Technology, University of Tampere, Tampere, Finland
2 BioMediTech, University of Tampere and Tampere University of Technology, Tampere, Finland
3 Science Center, Tampere University Hospital, Tampere, Finland
4 Department of Plastic Surgery, Tampere University Hospital, Tampere, Finland

Continued page 246 ▶

5 Department of Eye, Ear and Oral Diseases, Tampere University Hospital, Finland
6 Department of Electronics and Communications Engineering, Tampere University of Technology, Finland

of 73% deacetylated chitosan membrane (CM) on wound healing in a experimental full-thickness rat model. Assessing wound area, contraction, systemic IL-4 levels, and the histology of epithelialisation, oedema, fibrin, necrosis, haemorrhage, angiogenesis and leucocytosis to describe any tissue effects.

Materials and methods

Chitosan membrane preparation

Microcrystalline chitosan (Novasso Inc., Tampere, Finland) with a deacetylation degree of 73% and molecular weight 240kDa was used to make chitosan membranes (CMs). The CMs were made by dissolving chitosan in deionised water/acetic acid (Sigma-Aldrich Inc., St. Louis, Missouri, USA) solution. The solution contained chitosan and solvent at a ratio of 1:1 w/v. The chitosan solution was 1.5 weight-percentage. The solution was then poured into structured polytetrafluoroethylene-moulds dried in a laminar flow cabinet for 48 hours, and then for a week in a vacuum at room temperature.

Due to the use of acetic acid, CMs had to be neutralised by incubation for 30 minutes in 5M sodium hydroxide (Baxter Healthcare Ltd., Norfolk, England) at +22ºC. After which the CMs were rinsed ten times with sodium chloride and five times with Dulbecco's phosphate buffered saline (Lonza Inc., Verviers, Belgium). The neutralisation was confirmed with pH-paper (Merck & Co. Inc., New Jersey, USA). The initial thickness of the manufactured CMs was 120µm.

Animal model

Adult male Sprague Dawley rats were housed in the Animal Laboratory of Tampere University. The experiment was conducted under license from the Board of Animal Experiments (ESLH-2008-04691/Ym-23) according to The National Research Council's Guide for the Care and Use of Laboratory Animals. The rats were anaesthetised using intraperitoneal medetomidine-ketamine injection with a dose, according to weight, of 0.05mg/100g medetomidine (Domitor, Orion Inc., Espoo, Finland) and 7.5mg/100g ketamine (Ketalar, Parke Davis Inc., Caringbah, NSW, Australia). The site of the wounds was determined on the basis of pilot tests and our previous study.[21]

Under general anaesthesia, a circular 15mm diameter skin section was marked and excised to the bottom of the dermis on the scalp with surgical scissors (Fig 1). After wound formation, the wound site was tattooed with dot-like marks to detect contraction. The created wound was measured from two directions perpendicular to each other. Using these measurements, the wound area was defined using the mathematical formula for ellipse area:

$$\text{wound} = \pi \times A \times B$$

where A and B represent one-half of the ellipse´s major and minor axes.

The distance between the tattooed dots was measured and the area outlined was defined using the above equation as for the wound area. The rats were randomised into two groups: a chitosan membrane group (CM group) and a control group. The wounds in the CM group were covered with chitosan membranes and an wound dressing Aquacel (ConvaTec Inc., Espoo, Finland). The CM was tailored to fit the wound just before it was placed on top of the wound (Fig 1a and 1c). Control group wounds were covered only with the absorbent dressing. Before covering the wound, the absorbent dressing was moistened with 0.9 % sodium chloride (Baxter Healthcare Ltd.). Under primary anaesthesia, the animals were given subcutaneous 0.002mg/100g buprenorphine (Temgesic, Schering-Plough Europe Inc., Brussels, Belgium) injections for pain relief, which were repeated as required.

Follow-up

Animal were individually caged and on an ad libitum diet. Follow-up occurred on days 0, 3, 7, 14 or 21. Examination of the control group on 0 day took place under primary anaesthesia immediately after wound excision. On days 3,7,14 and 21 six animals from each group were anaesthetised again with intraperitoneal medetomidine-ketamine injections (0.05/7.5mg/100g weight) and assessed.

Assessment included measurements of the wound site to ascertain wound area and contraction as well as blood sampling and tissue collection. Wound areas are presented as percentages from the baseline

Fig 1. Chitosan and wound preparations

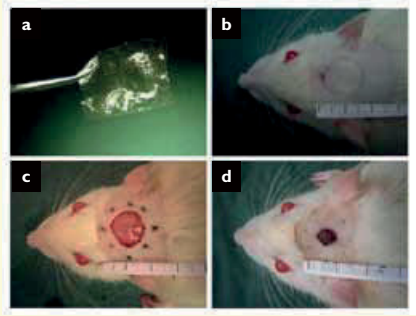

Chitosan was neutralised and cut into pieces immediately before use (a). After shaving and cleansing the scalps, the wound site was outlined (b), executed and tattooed (c). In the chitosan group, wounds were covered with chitosan and sodium chloride-moistened dressing whereas in the control group, wounds were covered only with the same dressing. At the final time point, the tattooed marks are still clearly visible (d)

Table 1. Weight, wound area, contraction and epithelialisation.

0 day	CM	Control	p-value
Weight (%)	-	100 ± 0	-
Wound area (%)	-	100 ± 0	-
Contraction (%)	-	100 ± 0	-
Epithelialisation (%)	-	0 ± 0	-
3 day			
Weight (%)	89 ± 4	89 ± 5	0.784
Wound area (%)	60 ± 6	78 ±19	0.048*
Contraction (%)	81 ± 6	80 ± 8	0.778
Epithelialisation (%)	15 ± 4	14 ± 8	0.641
7 day			
Weight (%)	96 ± 7	100 ± 9	0.397
Wound area (%)	60 ± 15	53 ± 6	0.299
Contraction (%)	74 ± 8	73 ± 11	0.903
Epithelialisation (%)	34 ± 7	32 ± 9	0.669
14 day			
Weight (%)	100 ± 1	101 ± 4	0.623
Wound area (%)	17 ± 10	20 ± 5	0.560
Contraction (%)	62 ± 11	59 ± 5	0.538
Epithelialisation (%)	41 ± 21	40 ± 15	0.897
21 day			
Weight (%)	113 ±13	115 ± 17	0.838
Wound area (%)	4 ± 2	5 ± 3	0.282
Contraction (%)	63 ± 5	65 ± 8	0.709
Epithelialisation (%)	88 ± 15	96 ± 11	0.361

The percentage values were derived by comparing the onset measurements to the end point measurements.

CM – chitosan membrane; * $p<0.05$.

throughout the study. The distances between the tattooed dots were also measured to discover contraction and presented as percentages from the original distances (contraction percentage). All measurements were carried out by a blinded researcher.

Following wound assessment animals were anaesthetised and a blood sample of approximately 5ml was drawn by cardiac puncture for IL-4 analysis. The puncture was followed by CO_2 euthanasia, which took place when the animals were still under anaesthesia. For histological analysis, the whole wound area was excised including the skull underneath and preserved in 10% formaldehyde.

Histology

The samples were formaldehyde fixed, embedded in paraffin and stained with hematoxylin-eosin. Hematoxylin-eosin staining has been used earlier in chitosan-related *in vivo* studies.[16,21,25] Paraffin-embedded samples were cross-sectioned throughout their entire length and one half of the block was sectioned parallel to the first section, generating two separate tissue samples from each wound for histological examination. Epithelialisation, oedema, fibrin, necrosis, haemorrhage, angiogenesis and leucocytosis were analysed as described in our previous study.[21]

Briefly, epithelialisation was described as percentages covering the original wound and was calculated using a microscopical ten-grid. Oedema and fibrin were scored from zero to three with five different views using x4 magnification. Necrosis, haemorrhage and angiogenesis were also scored from zero to three but from nine different views and with x25 magnification. Leucocytes were defined as cell count with x25 magnification. Beside epithelialisation and leucocyte count, all other parameters in the histological examination were defined as scores from zero to three where zero represented normal rat skin structure.

The histological examination was performed blind. Furthermore, histological sections were used to detect presence of chitosan membrane.

Interleukin 4

Blood samples were centrifuged (5 minutes, 1000 rpm) to separate the serum, which was stored at -80°C. The samples were thawed before IL-4 analysis, which was performed using a Rat IL-4 ELISA kit (Diaclone / Gen-Probe Life Sciences Inc., Besancon Cedex, France) according to the manufacturer's instructions and our previous study.[21]

Statistical analysis

Statistical analysis was carried out using SPSS 16 for Windows program (SPSS Inc., Chicago, USA). The statistical test for measured numeric parameters was unpaired Student's t-test and the results were presented as mean ± standard deviation (SD). Scores were analysed with the Mann–Whitney U test and presented as median and minimal and maximal values. Statistically significant difference was set at $p<0.05$.

Results

The animals needed no extra pain medication after the second postoperative day. In the CM group, the weight was 89 ± 4% of their baseline at the three-day follow-up. The corresponding percentage in the control group was 89 ± 5%. The animals completely regained their original weight in 14 days (Table 1).

Wound healing

The wound area was significantly smaller in the CM group at the three-day follow-up, CM group being 60 ± 6% of the original area compared to 78 ± 19% in the control group ($p=0.048$, Table 1). At the same time point, the contraction was 81 ± 6% in the CM

group and 80 ± 8 % in the control group. At the 7, 14 or 21-day follow-up no statistically significant differences were observed. By 21 days, the remaining wound areas were 4 ± 2% (CM) and 5 ± 3% (control) of the original area.

Histology

Epithelialisation, oedema, fibrin, necrosis, haemorrhage, angiogenesis and leuccocytes were analysed from histological sections (Table 2, Fig 2). The leucocyte count was the only histological parameter where statistically significant difference was observed between the CM and control group. On day 7, the count was lower in the CM group than in the control group (55 ± 10 and 75 ± 16, respectively, p=0.0031).

Epithelialisation was up to 88 ± 15% of the original area in the CM group at the 21-day time point, and to 96 ± 11% in the control group. Due to a relatively wide standard deviation, the difference was not statistically significant (Table 1).

Oedema score was highest on day 3 in both groups. Oedema scores reverted to day 0 levels on day 21. Peak fibrin score was reached on day 7 in both groups. No necrosis was observed.

In the CM group, the haemorrhage level remained steady through days 3, 7 and 14. In the control group the highest haemorrhage score was observed on day 7. Angiogenesis peaked on day 21 in the CM group but on day 14 in the control group.

In the histological analysis, CM was visible on days 3 and 7 in the CM group but we could not detect CM on days 14 and 21 in any of the samples (Fig 3).

Fig 2. Histological views

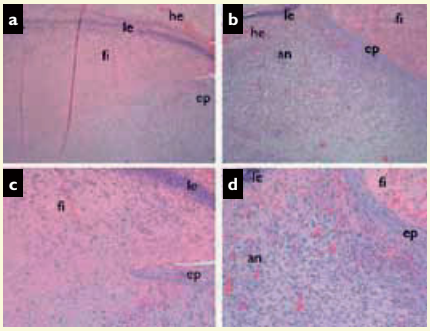

Image a is a x4 magnification of a wound site from the control group, whereas image b is a x4 magnification of a wound site from the CM. Images c and d are the respective x10 magnifications. All of these images were taken on day 7. Abbreviations: an – angiogenesis; fi – fibrin; ep – epithelialisation; h – haemorrhage; le – leucocytosis.

Table 2. Histological analysis

0 day	CM	Control	p-value
Oedema (score)	-	0.5 (0–1)	-
Fibrin (score)	-	0.0 (0–1)	-
Haemorrhage (score)	-	1.0 (1–1)	-
Angiogenesis (score)	-	0.0 (0–0)	-
Leucocytes (count)		17 ± 5	-
3 day			
Oedema (score)	2.0 (2–2)	2.0 (1–2)	0.138
Fibrin (score)	1.8 (1–2)	1.3 (1–2)	0.093
Haemorrhage (score)	1.0 (1–1)	1.0 (1–2)	0.138
Angiogenesis (score)	0.3 (0–2)	0.2 (0–1)	0.902
Leucocytes (count)	72 ± 12	75 ± 21	0.809
7 day			
Oedema (score)	1.8 (1–2)	2.0 (1–2)	1.000
Fibrin (score)	2.3 (2–3)	2.0 (2–3)	0.523
Haemorrhage (score)	1.0 (1–1)	1.0 (1–2)	0.317
Angiogenesis (score)	1.0 (1–2)	1.5 (0–2)	0.523
Leucocytes (count)	55 ± 10	75 ± 16	0.031*
14 day			
Oedema (score)	1.0 (0–1)	1.0 (1–1)	0.317
Fibrin (score)	1.0 (0–2)	1.5 (1–2)	0.116
Haemorrhage (score)	1.0 (1–1)	1.0 (0–1)	0.317
Angiogenesis (score)	1.0 (0–2)	2.0 (1–2)	0.162
Leucocytes (count)	58 ± 15	71 ± 29	0.334
21 day			
Oedema (score)	0.5 (0–1)	0.0 (0–1)	0.241
Fibrin (score)	0.5 (0–1)	0.0 (0–1)	0.575
Haemorrhage (score)	1.0 (0–2)	0.0 (0–1)	0.212
Angiogenesis (score)	1.0 (1–2)	1.0 (0–3)	0.445
Leucocytes (count)	42 ± 15	38 ± 12	0.673

Scored parameters (oedema, fibrin, haemorrhage and angiogenesis) were tested with the Mann-U Whitney test and presented as median (range) values. Leucocyte counts were tested with unpaired Student's t-test and presented as mean ± standard deviation. Necrosis was also examined but not seen.

CM – chitosan membrane; * p<0.05.

Interleukin 4 levels

At day 7 the difference between the groups was statistically significant (p=0.007, Fig 4) being higher in the CM group than in the control group. The same trend continued on day 14, where IL-4 expression was still significantly (p=0.003) higher in the CM group (Fig 4). There was no difference between the groups on day 21.

Discussion

Rats are commonly used in wound healing studies and in this study we examined the effects of ▶

Fig 3. Histological view at days 3 (a) and 21 (b) of the chitosan membrane group .The chitosan can be seen on top of the wound on day 3 and is no longer present by day 21.This image is a x25 magnification

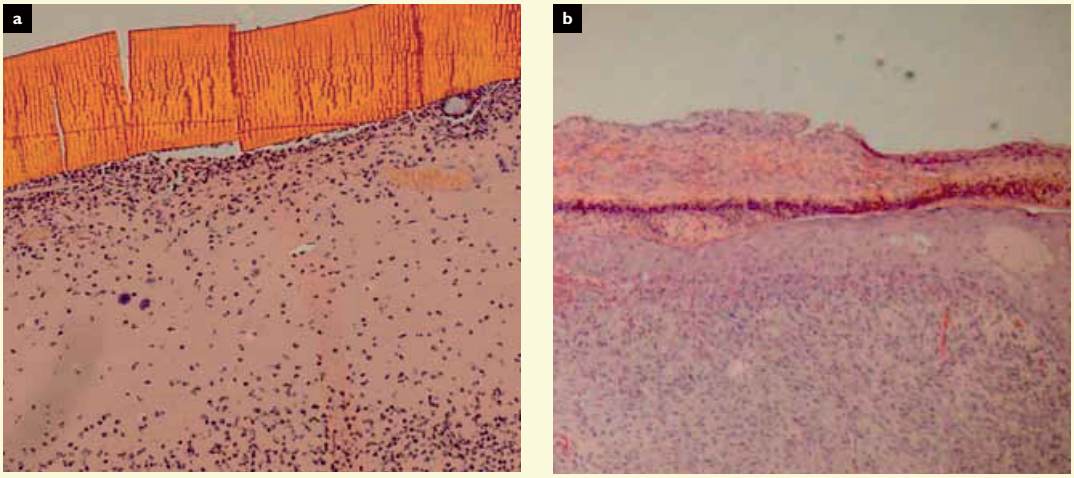

chitosan on wound healing, observing wound area, contraction, histology and systemic IL-4 levels using an experimental rat model described in our previous study.[21–23] The need for minimal extra pain medication and minor weight loss showed our method was tolerable for the animals.

Chitosan is biodegradable and is decomposed by chitinases, lysozyme and lipases.[5–7] Using chitosan beads, it has been shown that lower deacetylation of chitosan enhances the degradation and thus degradation is slower when the deacetylation degree is over 73%.[24,25] Our chitosan was 73% deacetylated, which can be considered average. The histological examination showed that chitosan degrades from the wound sites between 7–14 days. This gradual biodegradation may explain why the positive effect on wound area was only seen on day 3 and in the CM group. When chitosan starts to degrade due to enzymatic activity, chito-oligomers promotes the organisation of collagen fibrils during wound healing.[5]

Previous studies have shown that chitosan enhances wound healing being antimicrobial and effecting collagen organisation, macrophage activation and vascularisation.[5,11–13,15] The difference in wound area on day 3 is not explained with faster re epithelialisation because our histological analysis showed minor epithelialisation with no difference between the groups. It is known that fibrin clot formation and inflammation dominate early stage wound healing and re epithelialisation has a bigger role later in the healing cascade.[26]

Contraction occurs in the early stage of wound healing and chitosan may support wound contraction, something Burkatovskaya et al. described as the 'clamping effect' of their chitosan acetate bandage—the bandage had a positive effect on the first days of wound healing.[12,26] Nevertheless, our

Fig 4. Histogram of IL-4 levels. The systemic IL-4 level was significantly higher in the CM group on days 7 (p=0.007) and 14 (p=0.003)

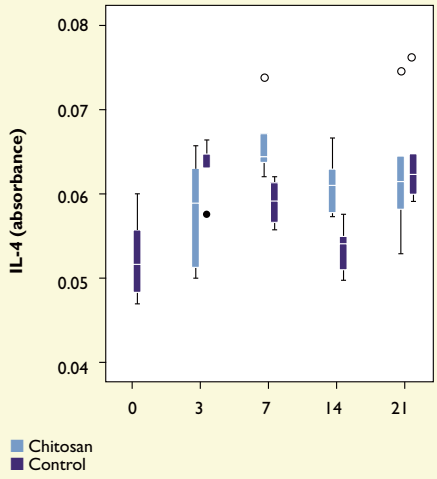

© 2015 MA Healthcare Ltd

measurements did not show a positive effect of chitosan in contraction in any time point.

In the histological analysis, no necrosis or significant oedema was found, which supported the idea of non-toxicity.[13] In earlier investigations, chitosan has been found to be haemostatic.[17,27] In our study however, there were no statistically significant differences in fibrin, haemorrhage or angiogenesis between the groups.

The inflammatory stage of wound healing commonly takes place from the first minutes to several days.[26] Our histological results showed a significantly lower leukocyte count in the CM group on day 7. This result indicates that CM may accelerate and shorten the duration of an inflammatory stage, which can be seen as faster descending leucocyte levels when chitosan covers the wound. Acceleration of the inflammatory stage could partly explain the significant difference in wound area on day 3.

Macrophage activation is thought to be one of the principal mechanisms of action of chitosan in wound healing.[5] It is known that IL-4 production activates local macrophages, which in turn promotes extracellular matrix formation and especially collagen synthesis.[28] IL-4 is also one of the first innate signal pathways to activate in tissue damage.[29] Our results showed that systemically measured IL-4 levels were significantly higher in the CM group on day 7 and 14 following the course of chitosan degradation.

Limitations

The differences between the two groups were mild, however, the positive early effect of chitosan in reducing wound size should be considered when planning other studies or clinical application. Changing methodolgy could help extend the early beneficial effects seen.

Conclusions

Our results indicate that CM promotes early-stage wound healing and degrades from the wound site after day 7. The degradation time should be taken under consideration when planning wound treatments with chitosan. The mechanism behind the enhanced healing may be related to inflammatory stage progression and IL-4 pathway, and requires further investigation. ■

Acknowledgements
We are very grateful to our collaborators at the Institute of Biomedical Technology, BioMediTech and the Department of Plastic Surgery in Tampere University Hospital. The personnel in Tampere University Animal Laboratory gave irreplaceable help during our experiments and deserve our special gratitude. We also thank Heini Huhtala for professional statistical advice.

References

1 Jayakumar, R., Prabaharan, M., Nair, S.V., Tamura, H. Novel chitin and chitosan nanofibers in biomedical applications. Biotechnol Adv 2010; 28: 1, 142–150.

2 Pillai, C.K.S., Paul, W., Sharma, C.P. Chitin and chitosan polymers: chemistry, solubility and fiber formation. Prog Polym Sci 2009; 34: 641–678.

3 Dong, Y., Xu, C., Wang, J et al. Influence of degree of acetylation on critical concentration of chitosan/dichloroacetic acid liquid-crystalline solution. J Appl Polym Sci 2002; 83: 1204–1208.

4 Howling, G.I., Dettmar, P.W., Goddard, P.A. et al. The effect of chitin and chitosan on the proliferation of human skin fibroblasts and keratinocytes in vitro. Biomaterials 2001; 22: 22, 2959–2966.

5 Muzzarelli, R.A., Mattiol-Belmonte, M. et al. Biochemistry, histology and clinical uses of chitins and chitosans in wound healing. EXS 1999; 87: 251–264.

6 Nagahama, H., New, N., Jayakumar, R. et al. Novel biodegradable chitin membranes for tissue engineering applications. Carbohydr Polym 2008; 73: 295–302.

7 Saimoto, H., Takamori ,Y., Morimoto, M. et al. Biodegradation of chitin with enzymes and vital components. Macromol. Symp 1997 120, 11–18.

8 Eijsink, V., Hoell, I., Jaaje-Kolstada, G. Structure and function of enzymes acting on chitin and chitosan. Biotechnol Genet Eng Rev 2010; 27: 331–366.

9 Bartone FF, Adickes ED. Chitosan: effects on wound healing in urogenital tissue: preliminary report. J Urol 1988; 140: (5 Pt 2), 1134–1137.

10 Sall, K.N., Krete, J.K., Keates, R.H. The effect of chitosan on corneal wound healing. Ann Opthalmol 1987; 19: 1, 31–33.

11 Willi, P., Sharma, C.P. Chitosan and alginate wound dressings: a short review. Trends Biomater Artif Organs 2004; 18: 1, 18–23.

12 Burkatovskaya, M., Castano, A.P., Demidova-Rice, T.N et al. Effect of chitosan acetate bandage on wound healing in infected and noninfected wounds in mice. Wound Repair Regen 2008; 16: 3, 425–431.

13 Kean, T., Thanou, M. Biodegradation, biodistribution and toxicity of chitosan. Adv Drug Deliv Rev 2010; 62: 1, 3–11.

14 Kojima, K., Okamoto, Y., Kojima, K. et al. Effects of chitin and chitosan on collagen synthesis in wound healing. J Vet Med Sci 2004; 66: 12, 1595–1598.

15 Stone, C.A., Wright, H., Clarke, T. et al. Healing at skin graft donor sites dressed with chitosan. Br J Plast Surg. 2000; 53: 7, 601–606.

16 Alsarra, I.A. Chitosan topical gel formulation in the management of burn wounds. Int J Biol Macromol 2009; 45: 1, 16–21.

17 Azad, A.K., Sermsintham, N., Chandrkrachang, S., Stevens, W.F. Chitosan membrane as a wound-healing dressing: characterization and clinical application. J Biomed Mater Res B Appl Biomater 2004; 69:2, 216–222.

18 Chamberlain, C.S., Leiferman, E.M., Frisch, K.E. et al. The influence of interleukin-4 on ligament healing. Wound Repair Regen 2011; 19: 3, 426–435.

19 Kucukcelebi, A., Harries, R.H.C., Hennessey, P.J. et al. In vivo characterization of interleukin-4 as a potential wound healing agent. Wound Repair Regen 1995; 3: 1, 49–58.

20 Kojima, K., Okamoto, Y., Miyatake, K. et al. Collagen typing of granulation tissue induced by chitin and chitosan. Carbohydr. Polym 1998; 37: 109–113.

21 Nordback, P.H., Miettinen, S., Kääriäinen, M. et al. Amniotic membrane reduces wound size in early stages of the healing process. J Wound Care 2012; 21: 4, 190–197.

22 Hirose, K., Onishi, H., Sasatsu, M. et al. In vivo evaluation of Kumazasa extract and chitosan films containing the extract against deep skin ulcer model in rats. Biol Pharm Bull 2007; 30: 12, 2406–2411.

23 Dorsett-Martin, W.A. Rat models of skin wound healing: A review. Wound Repair Regen 2004; 12: 591–599.

24 Kofuji, K., Ito, T., Murata, Y., Kawashima, S. Biodegradation and drug release of chitosan gel beads in subcutaneous air pouches of mice. Biol Pharm Bull 2001; 24: 2, 205–208.

25 Kofuji, K., Ito, T., Murata, Y., Kawashima, S. The controlled release of a drug from biodegradable chitosan gel beads. Chem Pharm Bull (Tokyo) 2000; 48: 4, 579–581.

26 Martin P. Wound healing – Aiming for perfect skin regeneration. Science 1997; 276: 5309, 75–81.

27 Taravel, M.N., Domard, A. Collagen and its interaction with chitosan. II. Influence of the physicochemical characteristics of collagen. Biomaterials 1995; 16: 11, 865–871.

28 Mosser, D.M., Edwards, J.P. Exploring the full spectrum of macrophage activation. Nat Rev Immunol 2008; 8: 12, 958–969.

29 Loke, P., Gallagher. I., Nair, M.G. et al. Alternative activation is an innate response to injury that requires CD4+T cells to be sustained during chronic infection. J Immunol 2007; 79: 6, 3926–3936.

TISSUE ENGINEERING: Part A
Volume 24, Numbers 1 and 2, 2018

DOI: 10.1089/ten.tea.2016.0245

termis
Tissue Engineering
& Regenerative Medicine
International Society

ORIGINAL ARTICLE

Comparison of Poly(L-lactide-co-ε-caprolactone) and Poly(trimethylene carbonate) Membranes for Urethral Regeneration: An *In Vitro* and *In Vivo* Study

Reetta Sartoneva, PhD, MD, MSc,[1,2,*] Panu H. Nordback, MD,[1,2,*] Suvi Haimi, PhD,[3] Dirk W. Grijpma, PhD,[4,5] Kalle Lehto, MSc,[1] Niall Rooney, PhD,[6] Riitta Seppänen-Kaijansinkko, MD, DDS, PhD,[3] Susanna Miettinen, PhD,[1,2] and Tuija Lahdes-Vasama, PhD, MD[2,7]

Urethral defects are normally reconstructed using a patient's own genital tissue; however, in severe cases, additional grafts are needed. We studied the suitability of poly(L-lactide-co-ε-caprolactone) (PLCL) and poly(trimethylene carbonate) (PTMC) membranes for urethral reconstruction *in vivo*. Further, the compatibility of the materials was evaluated *in vitro* with human urothelial cells (hUCs). The attachment and viability of hUCs and the expression of different urothelial cell markers (cytokeratin 7, 8, 19, and uroplakin Ia, Ib, and III) were studied after *in vitro* cell culture on PLCL and PTMC. For the *in vivo* study, 32 rabbits were divided into the PLCL ($n=15$), PTMC ($n=15$), and control or sham surgery ($n=2$) groups. An oval urethral defect 1×2 cm in size was surgically excised and replaced with a PLCL or a PTMC membrane or urethral mucosa in sham surgery group. The rabbits were followed for 2, 4, and 16 weeks. After the follow-up, urethrography was performed to check the patency of the urethra. The defect area was excised for histological examination, where the epithelial integrity and structure, inflammation, and fibrosis were observed. There was no notable difference on hUCs attachment on PLCL and PTMC membranes after 1 day of cell seeding, further, the majority of hUCs were viable and maintained their urothelial phenotype on both biomaterials. Postoperatively, animals recovered well, and no severe strictures were discovered by urethrography. In histological examination, the urothelial integrity and structure developed toward a normal urothelium with only mild signs of fibrosis or inflammation. According to these results, PLCL and PTMC are both suitable for reconstructing urethral defects. There were no explicit differences between the PLCL and PTMC membranes. However, PTMC membranes were more flexible, easier to suture and shape, and developed significant epithelial integrity.

Keywords: poly(L-lactide-co-ε-caprolactone), poly(trimethylene carbonate), urethral defects, urethral tissue engineering, urothelial cell

Introduction

Urethral defects due to congenital causes, trauma, or infection are fairly common. For instance the prevalence of hypospadia, which is a common congenital anomaly, has increased during the last decades now being ~1/250 to 1/300 live births.[1] Small urethral defects are traditionally reconstructed using the patient's own genital tissue. However, reconstruction of large urethral defects requires additional grafts, such as buccal mucosa. Nevertheless,

[1]Adult Stem Cell Research Group, BioMediTech, Faculty of Medicine and Life Sciences, University of Tampere, Tampere, Finland.
[2]Science Centre, Tampere University Hospital, Tampere, Finland.
[3]Department of Oral and Maxillofacial Diseases, University of Helsinki and Helsinki University Hospital, Helsinki, Finland.
[4]Department of Biomaterials Science and Technology, MIRA Institute for Biomedical Technology and Technical Medicine, University of Twente, Enschede, The Netherlands.
[5]Department of Biomedical Engineering, W.J. Kolff Institute, University Medical Centre Groningen, University of Groningen, Groningen, The Netherlands.
[6]Proxy Biomedical Ltd., Galway, Ireland.
[7]Pediatric and Adolescent Surgery Unit, Pediatric Research Centre and Tampere University Hospital, Tampere, Finland.
*These authors contributed equally to this work.

complications, such as urethral strictures, diverticulas, and fistula formation, are relatively common in these operations. Further, using the patient's own tissue as a graft material leads to donor site morbidity.[2,3] Thus, there is a clear clinical need for new reconstruction techniques of urethral defects.

Tissue engineering could provide a novel method to overcome problems associated with traditional reconstructive surgery. Several natural tissue grafts, such as bladder acellular matrix graft (BAMG) and collagen and small intestine mucosa with and without cells, have previously been studied for urethral reconstruction. For instance, Orabi *et al.* studied the BAMG seeded with urothelial and smooth muscle cells for urethral reconstruction in an *in vivo* beagle model with promising results. They compared the cell-seeded BAMG with the noncellular BAMG and observed that, in the noncellular group, the number of urethral strictures and fistulas was remarkably higher.[4] The disadvantage of natural biomaterials is the high batch-to-batch variation, and large-scale manufacturing and modification of mechanical properties are difficult. Thus, the development of novel graft materials for urethral reconstruction is essential to develop new treatment options for remedying severe urethral defects.[2,3,5,6]

The selection of an appropriate biomaterial for the application is crucial, and the biomaterial for urethral reconstruction should meet the requirements of being biocompatible, nontoxic, biodegradable without disadvantageous tissue reactions, and able to promote urothelial tissue regeneration. Furthermore, for urethral reconstruction, the biomaterial should be elastic and flexible and should mimic the basement membrane of the urothelium, generating a suitable matrix for urothelial cells to attach and proliferate. Additionally, the biomaterial should be suturable and easily molded into a tubular structure.[2,6]

Aliphatic poly(α-esters), such as polyglycolide (PGA), polylactide (PLA), polycaprolactone (PCL), and their copolymers, are the most commonly studied synthetic biomaterials for tissue engineering, and they have also been studied in urological applications with promising results.[7–9] Tubular PGA:poly(lactide-co-glycolide acid) (PLGA) scaffolds seeded with urothelial and smooth muscle cells were used to reconstruct urethras for five boys suffering from severe urethral defects with favorable results. After the operation, a narrowing of the urethra developed for one patient, but it was repaired with a surgical incision. After a 6-year follow-up, no strictures or diverticula were detected, and the urethral histology was normal after 3 months.[8]

Furthermore, PLGA scaffolds were also used to reconstruct *de novo* bladders for children suffering from neurogenic bladders; however, the results of this study were not positive. In this study, PLGA scaffolds seeded with urothelial cells and smooth muscle cells were used to reconstruct *de novo* bladders for 10 children. Severe adverse effects, either bowel obstruction or bladder rupture, were detected in four patients.[9] Furthermore, Pariente *et al.* have demonstrated excellent biocompatibility of PGA, poly-L-lactic acid (PLLA), and PLGA when cultured with urothelial cells *in vitro*.[7] Although the aliphatic poly(α-esters) are considered as potential biomaterials for urological applications, intensive research is required before tissue-engineered urethral grafts can be used as an everyday treatment method for urethral defects. In particular, the development of optimal scaffold material and design is essential.

In our previous studies, we have shown that human urothelial cells (hUCs) attach, remain viable, and proliferate on poly(L-lactide-ε-caprolactone) (PLCL) membranes *in vitro*.[10,11] PLCL is a biocompatible copolymer of L-lactide and ε-caprolactone with variable mechanical properties depending on the monomer ratio. Increasing the ε-caprolactone content results in a more flexible and elastic polymer. PLCL degrades mainly via hydrolysis, although enzymes may also affect the degradation at later stages.[12,13] Furthermore, PLCL has been previously studied in other soft tissue engineering applications, such as vascular and esophageal tissue engineering, with encouraging results, and due to its excellent biocompatibility and elasticity, it is an interesting biomaterial for urethral reconstruction.[12,14]

Poly(trimethylene carbonate) (PTMC) is a benign, degradable, biocompatible polymer prepared from trimethylene carbonate that possesses good mechanical properties.[15,16] PTMC is glass-like at temperatures below approximately −15°C but is flexible at room temperature.[15] PTMC degrades via surface, not bulk, erosion, and enzymatically without acidic end products *in vivo*.[17–20] PTMC has been studied in various tissue engineering applications, for instance, for cardiomyocyte and Schwann cell cultivation, guided bone regeneration and abdominal surgery. Further, PTMC has been studied for vascular tissue engineering applications with good results.[15,19] Due to its flexibility, biocompatibility, and potential for soft tissue engineering applications, we considered it an interesting biomaterial for urothelial applications. Further, at least to our knowledge, PTMC has not been previously studied for urothelial tissue engineering.

Due to the unmet medical need of nonurological grafts, we tested PLCL and PTMC membranes for urothelial tissue engineering. The aim of this study was to compare the suitability and *in vivo* biocompatibility of PLCL and PTMC for urethral reconstruction in an *in vivo* rabbit model.

Materials and Methods

Biomaterial membranes

The 70/30 poly(L-lactide-co-ε-caprolactone) surface-textured membranes were provided by Proxy Biomedical (Proxy Biomedical Ltd, Galway, Ireland). The PLCL membranes were manufactured by film molding, resulting in 200-μm thick membranes. Surface texturing of the films was accomplished with a 100 W CO_2 laser micromachining device (Preco-Europe, Inc., Canterbury, United Kingdom) giving a pitted surface texture. The samples were sterilized using gamma irradiation at 25 kGy.

PTMC was synthesized by ring polymerization of trimethylene carbonate (Boehringer Ingelheim, Ingelheim am Rhein, Germany) under a blanket of nitrogen at 150°C, using stannous octoate (Sigma Aldrich, St. Louis) as a catalyst and water as an initiator. The polymer was melted using a compression molder (Fontijne laboratory press THB400, Vlaardingen, The Netherlands) at 160°C and up to 100 kN for 1 min, followed by a two-step compression molding cycle. Membranes with a thickness of 250 μm were obtained; their molecular weight was ~275 kg/mol. The membranes were cut to appropriate size and packed in PET/ALU/PE peel pouches (Riverside medical packaging Ltd., Derby, United Kingdom), vacuum sealed, and gamma irradiated at 25 kGy using a ^{60}Co source (Synergy Health, Ede,

The Netherlands) for sterilization and cross-linking. The PTMC membranes were prepared in a similar manner as described in previous studies.[16,17]

The X-ray microtomography (μCT) images of PLCL and PTMC membranes were acquired by using commercial Zeiss Xradia MicroXCT-400 (Zeiss, Pleasanton) system (Fig. 1). PLCL and PTMC membranes were imaged, respectively, with the following parameters: 60 kV source voltage, 10 W tube power; 40 mm source-to-object distance; 8 mm object to image-receptor distance; 20×, 10× objective; 2 binning; 1600 projections; full 360° projection circle; and 5.0, 2.5 s exposure time. The three-dimensional image stacks were reconstructed using Zeiss Xradia XRMreconstructor software (8.1; Zeiss) resulting in 1.1 and 2.3 μm isotropic voxel sizes and the data were visualized in Zeiss Xradia TXM3DViewer (1.1.6; Zeiss).

In vitro *cell culture*

For this study, human urothelial tissue samples were isolated during a routine surgery from one pediatric patient in the Tampere University Hospital with the approval of the Ethics Committee of Pirkanmaa Hospital District, Tampere, Finland (R071609). Further, the urothelial cells were isolated and expanded as previously described.[10,21] PLCL and PTMC membranes were attached to the cell culture devices (CellCrown48, Scaffdex, Tampere, Finland) and preincubated for 24 h in urothelium medium containing EpiLife (Invitrogen, MA) supplemented with 1% of EpiLife Defined Growth Supplement (EDGS; Invitrogen), 0.1% of $CaCl_2$ (Invitrogen), and 0.35% of antibiotics (100 U/mL penicillin and 0.1 mg/mL streptomycin; Lonza, BioWhittaker, Verviers, Belgium).

In vitro *attachment and viability*

The cell attachment was verified by determining the DNA amount using CyQUANT Cell Proliferation Assay kit (Invitrogen). Briefly, 20,000 urothelial cells from one patient were seeded on to three parallel PLCL and PTMC membranes and cultured for 24 h. The cells were lysed with 0.1% Triton-X-100 buffer (Sigma-Aldrich) and stored at −70°C until analysis. The samples were thawed and 20 μL of each sample was mixed with 180 μL of working solution containing CyQUANT GR dye and lysis buffer. The fluorescence at 480/520 nm was measured with a multiplate reader (Victor 1420 Multilabel Counter; Wallac, Turku, Finland).

To verify the viability of hUCs on PLCL and PTMC membranes, we used qualitative live/dead fluorescent staining. The urothelial cells from one patient, 30,000 cells/cm^2, were seeded on to two parallel membranes and the viability of urothelial cells was verified after 1 and 2 weeks of cell culture as described before.[10,11] Briefly, the cells were incubated at room temperature with a mixture of 0.25 μM calcein AM (green fluorescence; Molecular Probes, Waltham) and 0.3 μM ethidium homodimer-1 (red fluorescence, EthD-1; Molecular Propes) for 30 min. A fluorescence microscope (IX51S8F-2, camera DP71; Olympus, Tokyo, Japan) was used to image viable cells (green fluorescence) and dead cells (red fluorescence).

Quantitative real-time PCR

The relative expression of urothelium marker genes was studied after 14 days of cell culturing on PLCL or PTMC with quantitative real-time reverse transcription–polymerase chain reaction (qRT-PCR). The cell culture polystyrene (PS) served as a control material. For the experiment 50,000 cells/cm^2 from one patient was seeded on to three parallel PLCL, PTMC, or PS wells and cultured until analyses. First, the total RNA was isolated with Nucleospin kit reagent (Macherey-Nagel GmbH & Co. KG, Düren, Germany). Thereafter, the RNA was reverse transcribed to cDNA using the High-Capacity cDNA Reverse Transcriptase Kit (Applied Biosystems, Life Technologies). The expression of cytokeratin (CK) 7, CK8, CK19, uroplakin (UP) Ia, UPIb, and UPIII was analyzed. The expression data were normalized to the expression of housekeeping gene RPLP0 (large ribosomal protein P0). The sequences of primers (Oligomer Oy, Helsinki, Finland) and the accession numbers are presented in the Table 1. The qRT-PCR mixture contained cDNA, forward and reverse primers, and SYBR Green PCR Master Mix (Applied Biosystems). The reactions were conducted with AbiPrism 7000 Sequence Detection System (Applied Biosystems) with initial enzyme activation at 95°C for 10 min, followed by 45 cycles at 95°C for 15 s and 60°C for 60 s. The previously described mathematical model was used to calculate the relative expression.[22]

In vivo *experiment*

The animal experiment was conducted under the license of the Board of Animal Experiments (ESLH-2009-06718/Ym-23), and the National Research Council's Guide for the Care and Use of Laboratory Animals was followed. Adult

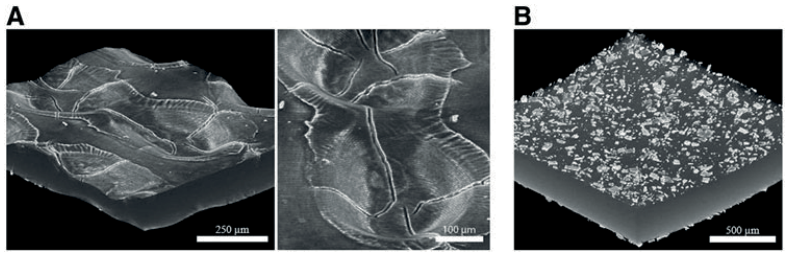

FIG. 1. The PLCL **(A)** and PTMC **(B)** membranes were imaged with micro-CT showing the surface characteristic of the membranes. The maximum diameter of the pit in PLCL membrane is 400 μm. The granules on the PTMC membranes are glucose, which makes the membranes easier to handle. CT, computed tomography; PLCL, poly(L-lactide-co-ε-caprolactone); PTMC, poly(trimethylene carbonate).

TABLE 1. THE SEQUENCES FOR QUANTITATIVE REAL-TIME REVERSE TRANSCRIPTION-POLYMERASE CHAIN REACTION PRIMERS USED IN THIS STUDY

Name		*5′- sequence -3′*	*Product size (bp)*	*Accession number*
CK7	Forward	CATCGAGATCGCCACCTACC	80	NM_005556.3
	Reverse	TATTCACGGCTCCCACTCCA		
CK8	Forward	CCATGCCTCCAGCTACAAAAC	68	M34225.1
	Reverse	AGCTGAGGTTTTATTTTGGGACC		
CK19	Forward	ACTACACGACCATCCAGGAC	80	NM_002276.4
	Reverse	GTCGATCTGCAGGACAATCC		
UPIa	Forward	GGGATCTCCAGTTGTGGTGG	80	NM_007000.3
	Reverse	TCTCAGCAAACAGGGACAGG		
UPIb	Forward	AGTCACCAAAACCTGGGACAG	64	NM_006952.3
	Reverse	TGATGGACCATTTACGCCACA		
UPIII	Forward	TCAGTGCAAGACAGCACCAA	65	AB010637.1
	Reverse	GTCCTCCCACCCTCTGTTTG		
RPLP0	Forward	AATCTCCAGGGGCACCATT	70	NM_001002
	Reverse	CGCTGGCTCCCACTTTGT		

male New Zealand White rabbits ($n = 34$, Harlan Laboratories, The Netherlands) were housed in the Animal Laboratory of the University of Tampere throughout the study. The rabbits were divided into the following three reconstruction groups: 15 rabbits with a PLCL membrane, 15 rabbits with a PTMC membrane, and 2 rabbits serving as a control group with urethral mucosa for reconstruction.

First, the rabbits were weighed and then anesthetized using a combination of 0.3 mg/kg medetomidine (Domitor, Orion, Inc., Espoo, Finland) and 0.3 mg/kg ketamine (Ketalar, Parke Davis, Inc., Caringbah, NSW, Australia), which were given intramuscularly. Additionally, the prophylactic antibiotic 2.5 mg/kg enrofloxacin (Baytril vet 50 mg/mL; Bayer Animal Health GmbH, Leverkusen, Germany) was given intramuscularly prior to the surgery. The rabbits were catheterized using 8F catheters (Mediplast AB, Malmo, Sweden). An incision ~2 cm long was created in the rabbit skin from the inguinal to the penile region, and the urethral mucosa was exposed (Fig. 2A). First, a 2×1-cm oval-shaped defect was created to the urothelial mucosa of the rabbit's anterior urethra. Holding sutures made of 6/0 nonabsorbable polypropylene (Premilene®; B. Braun Medical AS, Melsungen, Germany) were placed in every defect quarter and left in place after the operation as marking sutures. The defect site was replaced with the same sized on-lay PLCL or PTMC membrane (Fig. 2B), which was tailored just before transplantation using surgical scissors. The biomaterial membranes were sutured to the free edges of the urothelial mucosa with bioabsorbable 6/0 poly(p-dioxanone) sutures (PDS II®, Ethicon, Inc., NJ) and aligned with the catheter (Fig. 2C). For control rabbits, we did a sham surgery, removed a similar patch of urethral mucosa and sutured it back as a graft to the defect area to investigate the inflammation caused by the operation and the absorbable suture. After the suturing, the skin wound was closed with an intracutaneous suture using absorbable 4/0 polyglactin 910 sutures (Vicryl®, Ethicon, Inc., NJ), and the catheter was removed. The adequate analgesia was administered, and all the rabbits received 4 mg/kg carprofen (Norocarp vet, Norbrook Laboratories Ltd., Newry, Northern Ireland) and 0.05 mg/kg buprenorphine (Temgesic, Schering-Plough Europe, Inc., Brussels, Belgium) subcutaneously during the operation. The 0.05 mg/kg buprenorphine (Schering-Plough Europe, Inc.) was continued until 24 h after the operation, and the carprofen (Norbrook Laboratories Ltd.) was given daily 2 days after the operation. Pain medication was continued longer, if required. The rabbits in both the PLCL and PTMC groups were followed up for 2, 4, or 16 weeks, individually caged on an *ad libitum* diet. The sham surgery rabbits were followed up for 2 or 4 weeks.

In vivo *follow-up*

After the follow-up, the animals were weighed, anesthetized as described in the *In vitro* Attachment and Viabilitysection, and subjected to urethrographic examination. The animals were catheterized, and the 8F catheter (Mediplast AB) was

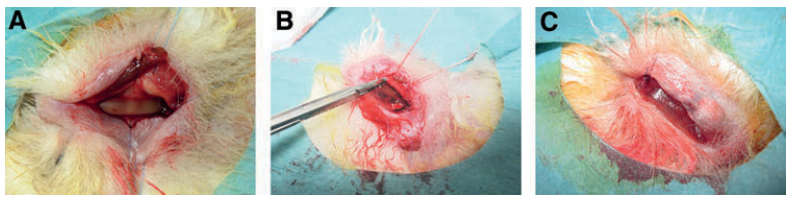

FIG. 2. At the beginning of the surgery, the rabbits were catheterized. An incision ~2 cm long was made in the inguinal region. The urethra was exposed, and a 2×1-cm oval defect was created in the rabbits' anterior urethra **(A)**. Subsequently, biomaterial membrane of equal size was sutured to the defect area **(B)**, and the biomaterial was aligned with the catheter **(C)**. Color images available online at www.liebertpub.com/tea

fixed with sutures distal from the defect area, which was palpated during catheterization. The urethrographic examination was performed by administering 180 mg/mL iohexol (Omnipaque, GE Healthcare AS, Oslo, Norway) by syringe as a radiocontrast agent via the catheter toward the bladder and by taking simultaneous X-ray pictures (Philips Oralix, Amsterdam, Holland) to detect severe strictures. Severe strictures block urine flow and thus prevent normal urination. After the examination, the animals were euthanized using 1 mg/kg intravenous pentobarbital (Mebunat, Orion, Inc., Espoo, Finland). The defect area was then excised, cut perpendicular from the middle of the reconstructed urethra to get the defect center to the histological analyses, and stored in 4% paraformaldehyde (Sigma-Aldrich) until histolgical analyses.

Histology

Paraformaldehyde-fixed tissue samples from rabbit urethras were embedded in paraffin and stained with hematoxylin and eosin (H&E) (Reagena Oy, Finland) or Masson's trichrome (Sigma-Aldrich) for microscopic examination. Epithelial integrity and structure were determined from the H&E-stained samples 2, 4, and 16 weeks after the operation. Epithelial integrity was categorized as discontinuous or continuous, whereas epithelial structure was categorized as no structure, monolayered or layered, that is, stratified structure.[23] Edema and the presence of inflammatory cells in the H&E-stained samples were evaluated to discover inflammation. Edema was scored from 0 to 3: 0 = none, 1 = mild, 2 = moderate, and 3 = severe.[23] Similarly, the presence of inflammatory cells was scored from 0 to 3. Normal inflammatory cell appearance was scored as 0; less than 25% of all cells was scored as 1; 25–50% was scored as 2, and over 50% was scored as 3.[24] The epithelial integrity and structure and inflammation-related parameters were examined at 40× magnification. Fibrosis was determined from Masson's trichrome-stained samples and scored. A score of 0 indicated no fibrosis, 1 indicated mild fibrosis (less than 25%), 2 indicated moderate fibrosis (25–50%), and 3 indicated severe fibrosis (more than 50%).[25] The histological examination was performed without knowing the group to which the sample belonged.

Immunohistochemistry

Immunohistochemistry with the pancytokeratin marker was used to study the urothelial epithelium after 2, 4, and 16 weeks of follow-up. Briefly, the samples were fixed with 5% paraformaldehyde and embedded in paraffin. The antigen retrieval was performed by microwaving the samples in 10 mM EDTA buffer (pH 9; Sigma-Aldrich), after which the samples were blocked in 3% hydrogen peroxide (Sigma-Aldrich). The samples were incubated overnight in diluted primary antibody (1:100, AE1/AE3; Thermo Fisher Scientific, MA). On the following day, the secondary antibody (1:200, goat anti-mouse IgG; Thermo Fisher Scientific) was used to detect the primary antibody.

Statistical analysis

Statistics were analyzed using IBM SPSS Statistics version 22 (IBM Corp., Armonk, NY). Edema, inflammation cell appearance, epithelial structure, fibrosis, and cell attachment on membranes were analyzed using the Mann–Whitney *U* test. Kruskal–Wallis test with Dunn's multiple comparison test was used with qRT-PCR results. Significant differences in epithelial integrity were analyzed using Fisher's test. Statistical significance was set to a p-value of <0.05.

Results

Cell attachment and viability on PLCL and PTMC membranes in vitro

The QyQUANT assay illustrated that there was small, yet statistically significant difference on the hUCs attachment on PLCL or PTMC membranes after 1 day of cell implantation (Fig. 3A, $p < 0.05$). Live/dead staining confirmed that the majority of cells were viable on both the PLCL and PTMC membranes and that the number of dead cells was negligible after the 1- and 2-week assessment periods (Fig. 3B). According to the qualitative analysis, the number of urothelial cells was notably lower on PLCL compared to the PTMC, especially after 1 week of cell culture.

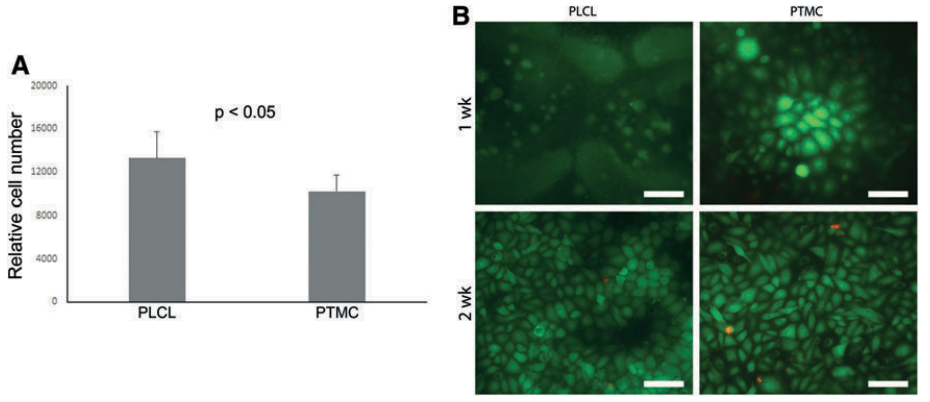

FIG. 3. The adhesion of urothelial cells on PLCL and PTMC was assessed after 1 day of cell implantation **(A)**. There was a statistically significant difference on cell attachment between PLCL and PTMC ($p < 0.05$). **(B)** Illustrates representative images of viable (green fluorescence) and dead (red fluorescence) urothelial cells on PLCL and PTMC after 1 week and 2 weeks. Scale bar: 100 μm. Color images available online at www.liebertpub.com/tea

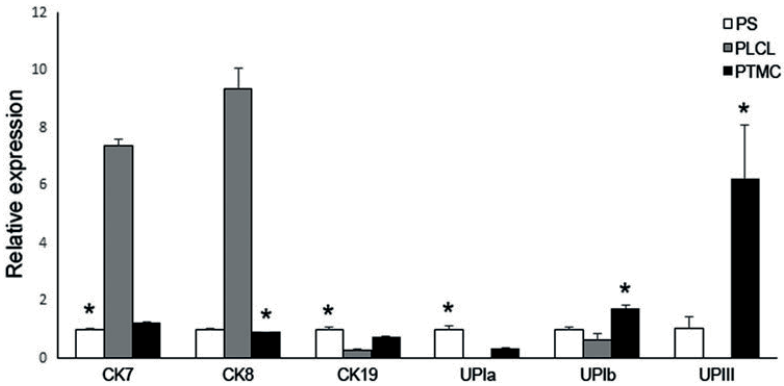

FIG. 4. The urothelial cells cultured on PLCL, PTMC, and PS expressed different urothelial markers, CK7, CK8, CK19, UPIa, UPIb, and UPIII, after a 2-week *in vitro* assessment period. $*p < 0.05$ with respect to PLCL. CK, cytokeratin; PS, polystyrene; UP, uroplakin.

Expression of urothelium markers

The expression of different urothelial markers was studied after 14 days of cell culture on PLCL and PTMC membranes with qRT-PCR (Fig. 4). On both PLCL and PTMC membranes, the hUCs expressed CK7, CK8, and CK19, which are known to be present in all layers of multilayered urothelium. On the PLCL, the expression of CK7 and CK8 was statistically higher compared to the PS and PTMC, respectively ($p < 0.05$). However, the CK19 expression of hUCs was significantly lower on PLCL compared to PS ($p < 0.05$). Additionally, on the PTMC the hUCs expressed all the studied UPs, UPIa, UPIb, and UPIII, which are more specific markers for urothelial cells. The hUCs on the PLCL expressed only the UPIb marker, whereas, no UPIa and UPIII expression was detected. The expression of UPIa was statistically higher with PS and the expression of UPIb and UPIII was statistically higher with PTMC compared to the PLCL ($p < 0.05$).

In vivo *experiment*

During the operation, the PTMC membranes appeared more flexible and were easier to suture and mold into tubular structures around the catheter compared with the PLCL membrane.

The rabbits recovered well after the operation. Most of the rabbits started to eat and drink normally and urinated spontaneously 1–3 days after the surgery. One rabbit from the PLCL group did not urinate and eat normally until 4 days after the operation. Further, two rabbits from PTMC group died 2 days after the operation, and those rabbits were excluded from the study. Both rabbits underwent autopsy, which revealed no biomaterial related causes of death.

The urethrographic examination performed at 2, 4, and 16 weeks detected no severe strictures, and the radiocontrast agent passed through the defect area in all rabbits (Fig. 5). The postoperative spontaneous urination supported our

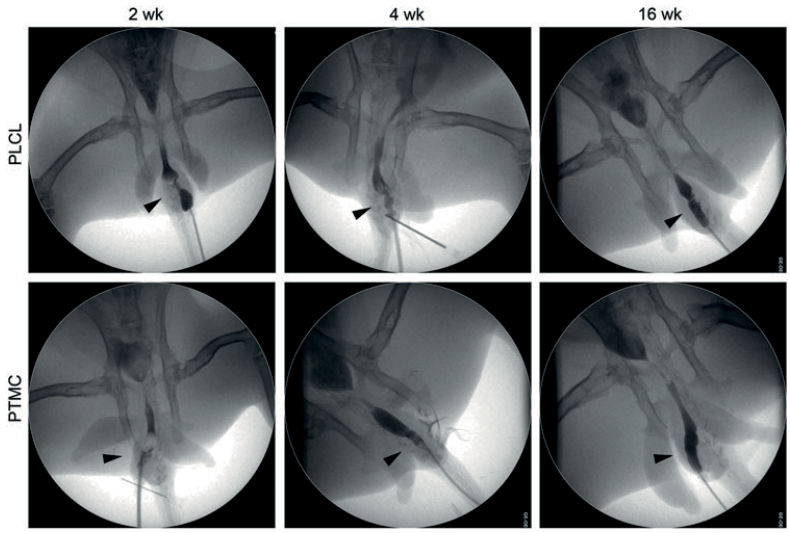

FIG. 5. Urethrographic examination illustrated the free passage of the radiocontrast agent through the defect area. After the follow-up, no severe strictures were detected in the PLCL or PTMC biomaterial groups. The *arrowhead* is indicating the graft area.

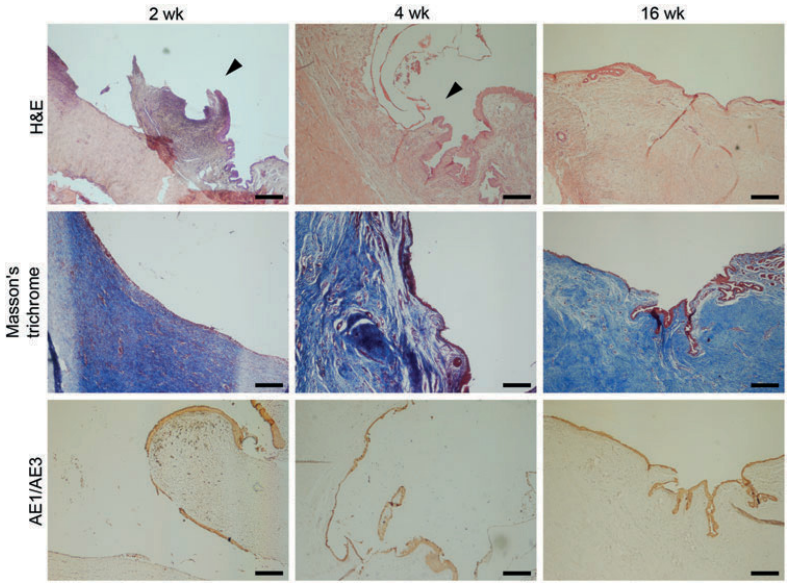

FIG. 6. Images show example histological views of the PLCL group at the 2-, 4-, and 16-week ($n=5$) time points stained with H&E and Masson's trichrome. The *third row* of histological images shows pancytokeratin (AE1/AE3)-staining. The implantation area in each panel is located in the centrum of the specimen view. The scale bar is 250 μm and the *arrowhead* is indicating the margin of natural tissue and biomaterial graft. H&E, hematoxylin and eosin. Color images available online at www.liebertpub.com/tea

urethrographic findings. The biomaterials in both the PLCL and PTMC groups could not be seen anymore at the 16-week time point.

Histology

The histological examination showed that the epithelial integrity approached that of the normal urothelial state in both groups (Figs. 6 and 7). By week 16, the epithelium was continuous, and, in the majority of samples, the epithelium was stratified (Table 2). Within the PTMC group, the difference in epithelial integrity between the 2- and 16-week follow-up was statistically significant ($p=0.048$). In the sham surgery rabbit group, inflammation was negligible after the 2- and 4-week follow-up (Fig. 8). The biomaterials used in this study caused only mild inflammation throughout the follow-up

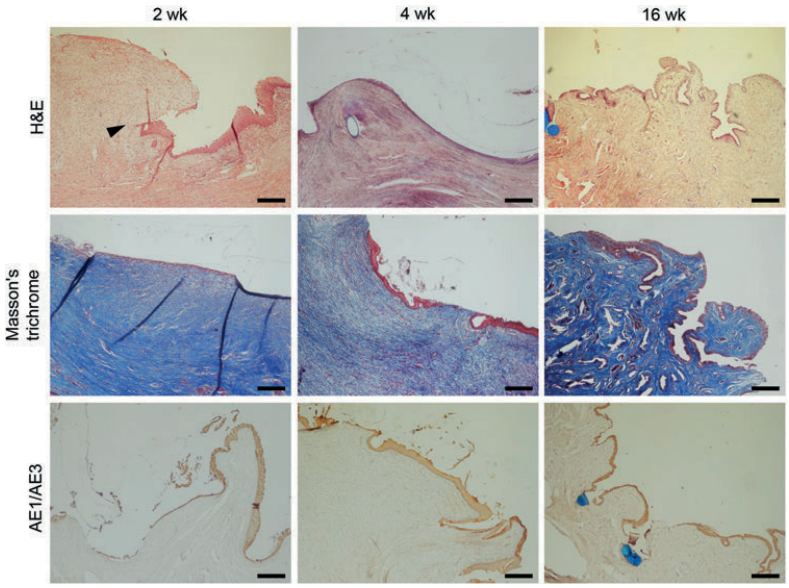

FIG. 7. Images show example views of the PTMC group at 2-, 4-, and 16-week time points stained with H&E, Masson's trichrome, or pancytokeratin (AE1/AE3). The implantation area in each panel is located approximately in the center of the specimen view. The *arrowhead* is indicating the margin of urothelium tissue and biomaterial graft and the *blue spheres* are nonbiodegradable marking sutures. Scale bar 250 μm. Color images available online at www.liebertpub.com/tea

Table 2. Epithelial Structure and Appearance of Inflammation or Fibrosis After 2, 4, or 16 Weeks of Follow-Up

Parameter	*Control*	*PLCL*	*PTMC*	p
2 Weeks				
Inflammation				
Cells	1	1 [0–2]	1 [1–2]	0.310
Edema	1	1 [0–2]	0 [0–1]	0.222
Epithelial integrity				
Discontinuous	100% (1)	60% (3)	80% (4)	1.000
Continuous	0% (0)	40% (2)	20% (1)	
Epithelial structure				
None	0% (0)	20% (1)	20% (1)	1.000
Monolayer	100% (1)	60% (3)	60% (3)	
Layered	0% (0)	20% (1)	20% (1)	
Fibrosis	1	1 [1–2]	1 [1–2]	1.000
4 Weeks				
Inflammation				
Cells	0	1 [0–2]	2 [0–3]	0.310
Edema	0	1 [0–1]	0 [0–1]	0.690
Epithelial integrity				
Discontinuous	0% (0)	60% (3)	100% (5)	0.444
Continuous	100% (1)	40% (2)	0% (0)	
Epithelial structure				
None	0% (0)	20% (1)	40% (2)	0.348
Monolayer	0% (0)	60% (3)	60% (3)	
Layered	100% (1)	20% (1)	0% (0)	
Fibrosis (total)	0	1 [1–2]	2 [1–2]	0.067
16 Weeks				
Inflammation				
Cells	—	0 [0–1]	0 [0–2]	0.841
Edema	—	0 [0–1]	1 [0–2]	0.548
Epithelial integrity				
Discontinuous	—	0% (0)	0% (0)	1.000
Continuous	—	100% (5)	100% (5)	
Epithelial structure				
None	—	0% (0)	0% (0)	0.545
Monolayer	—	40% (2)	20% (1)	
Layered	—	60% (3)	80% (4)	
Fibrosis	—	2 [1–2]	2 [1–2]	0.545

Inflammation and fibrosis scores are represented as median and range scores. Parameters related to the epithelium are represented as percentages and sample count. Significance was set to a p-value of <0.05. Epithelial integrity within the PTMC group between weeks 2 and 16 was statistically significant ($p=0.048$).

PLCL, poly(L-lactide-co-ε-caprolactone); PTMC, poly(trimethylene carbonate).

period. The highest scores of inflammatory cells (score 2 [0–3]) were discovered at the 4-week time point in the center defect area in the PTMC group, but the difference between the groups was not statistically significant ($p=0.310$). However, especially in the PLCL group, edema (score 0) and inflammatory cells (score 0) appeared to decrease by the last 16-week time point without a significant difference from the PTMC group (score 1 [0–2] and score 0 [0–2], respectively). No differences in edema or presence of inflammatory cells could be detected in any samples between the groups. Signs of fibrosis varied from mild to moderate during the follow-up. There were no statistically significant differences between the groups. At the 4-week time point, fibrosis was mild in the PLCL group and moderate in the PTMC group (Table 2). In the histological examination, there were no membrane remnants at the 16-week time point in either group.

Immunohistochemistry

Immunohistochemical staining with the CK marker (AE1/AE3) demonstrated the formation of *de novo* urothelium (Figs. 6 and 7). Hence, in the stainings, no differences between the PLCL and PTMC biomaterial groups were detected at any time point. Further, the *de novo* urothelium developed toward normal stratified urothelium during the assessment period.

Discussion

In this study, we investigated the suitability of the PLCL and PTMC membranes for urethral reconstruction in a rabbit model. Reconstruction of severe urethral defects is problematic because additional nonurological tissue grafts are needed, and those operations are highly susceptible to complications. Furthermore, nonurological grafts should fulfill the versatile challenging requirement, from biocompatibility to formable structure.

PLCL was selected because our previous *in vitro* studies have shown its suitability as a growth surface for hUCs.[10,11] It is a biocompatible biomaterial that has been studied in various soft tissue engineering applications with encouraging results.[12,14] Furthermore, Kloskowski *et al.* have previously demonstrated that PLCL was more suitable for ureter segment reconstruction compared with the acellular aortic arch in a rat model.[26] Additionally, PTMC has been shown to be a biocompatible biomaterial, and it has been studied in particular in soft tissue engineering applications with promising results.[15,19] At least to our knowledge, this is the

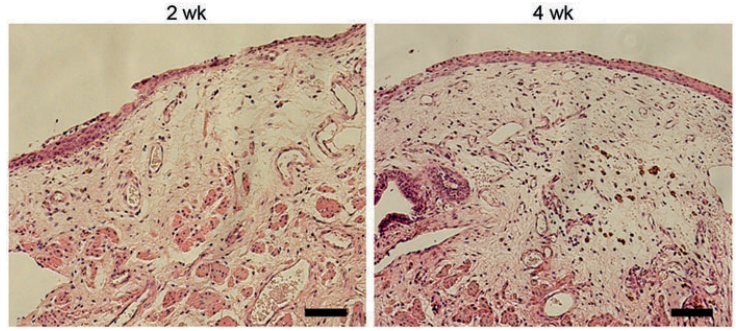

FIG. 8. Images show the effect of sham surgery at 2- and 4 week time points. The H&E staining illustrates that the inflammation and fibrosis after 2 and 4 weeks is extremely low indicating the small effect of sham surgery and sutures. Scale bar 250 μm. Color images available online at www.liebertpub.com/tea

first study comparing the synthetic biomaterials PLCL and PTMC for urethral reconstruction.

We demonstrated that the attachment of hUCs was significantly higher on PTMC compared to PLCL. However, the hUCs retained their viability on both materials, which was expected since both PLCL and PTMC are known to be biocompatible. During this study we also evaluated the phenotype of hUCs after 2-weeks *in vitro* culturing period on both biomaterials. We analyzed the markers CK7, CK8, and CK19 since those are generally expressed in multilayered epithelium and throughout all layer in urothelium. Further, the UPs were analyzed due to their specificity for superficial urothelial cells.[21,27] Both biomaterials appeared to support the maintenance of the hUCs phenotype further indicating their potential for urothelial applications. Interestingly, the PTMC appeared to support the expression of UP markers superiorly compared to the PLCL, however, evaluating the significance of these results requires further *in vitro* and *in vivo* studies.

The majority of the rabbits recovered well after membrane implantation and started to eat and urinate within a few days after the operation. One rabbit from the PLCL group had a slight delay in recovering. Two rabbits from the PTMC group died the second postoperative day. These rabbits did not eat after the operation and drank only remotely before they died; however, both rabbits urinated after the operation. The other rabbit had a hematoma at the defect area, but no specific reason could be identified for the death. Nevertheless, we concluded that the deaths were unlikely to be biomaterial-related.

In this study, we also evaluated the applicability of the biomaterial membranes for urological applications. During the operation, PTMC was easier to suture and mold into a tubular structure than PLCL, even though both biomaterials were flexible and easy to handle.

An appropriate biomaterial for urethral reconstruction should not cause disadvantageous tissue effects, such as excessive scar formation, leading to urethral strictures, causing decreased urinary flow and predisposing the patient to urinary tract infections. In our study, the animals were sacrificed 2, 4, or 16 weeks after the operation, and urethrographic examinations were performed to ensure the openness of the urethra. At the 2-week time point, a narrowing of the urethra was detected in both biomaterial groups, but this may be due to the inflexibility of the biomaterial membranes compared to the native urothelial tissue. No severe strictures were detected at the 16-week time point. However, in the PLCL group, a mild narrowing of the urethra was detected at the proximal defect area, whereas the distribution of the radiocontrast agent was uniform when the urethra was reconstructed with the PTMC membrane.

According to a visual inspection after sacrifice, both the PLCL and PTMC membranes were still present after the 4-week follow-up but had fully degraded by 16 weeks, which is consistent with previous degradation studies.[11,17,18] However, at the 2- and 4-week time points, the PLCL membrane appeared to be more unevenly degraded or more peeled off than the PTMC membranes. PLCL was more rigid than PTMC at 2 and 4 weeks when the defect area was revealed. However, visual inspection showed no substantial differences in the *de novo* urethral membrane after the 16-week assessment period, and there were no macroscopically observable strictures or fibrosis.

The histological results based on the H&E and AE1/AE3 staining showed that the urothelium in both groups developed toward a normal urothelium with regards to integrity and epithelial structure. The positive staining of AE1/AE3 further illustrates the epithelial phenotype of these cells. We hypothesized that the urothelial cells could migrate on the biomaterial membranes from the margin of the graft from the intact urothelium. The development of epithelial integrity was significant in the PTMC group between the 2- and 16-week follow-ups. After 2 weeks, the margin between the defect area and the normal urothelium was evident in both biomaterial groups. However, the defect margin was no longer distinguishable after 16 weeks, and the *de novo* epithelium showed stratification characteristic of the urothelium.

Invasive treatment always causes fibrosis of some degree. The fibrotic changes on a histological level in our study varied from mild to moderate. The level of observed fibrosis did not cause clinically demonstrable problems, such as urinary retention. Our urethrographic examination proved that the postoperative urethral lumen was open and that the animals started to urinate rapidly after the operation, in other words no severe strictures were detected. In urothelial tissue engineering, the studied biomaterials should not cause severe inflammatory responses.[3] Regarding PTMC, van Leeuwen *et al.* concluded that the tissue reaction on a histological level to PTMC membranes implanted in the mandible was mild and transient.[16] There are no previous data on the tissue response of the urethra to PTMC, but our low inflammatory cell and edema counts suggest that the reaction is mild. Likewise, our results showed mild inflammatory tissue responses in the PLCL group as well. Some results show that PLCL causes an even milder cellular inflammatory response than collagen, which might be related to the slow biodegradation process of PLCL.[28] Based on our histological evaluation, both PLCL and PTMC caused only mild inflammation throughout the follow-up, which establishes their potential.

Conclusion

Our aim was to investigate and compare the use of PLCL and PTMC for urethral reconstruction in a rabbit model. In addition, we confirmed the attachment, viability, and phenotype of hUCs on both biomaterials *in vitro*, which further indicated the excellent biocompatibility of the PLCL and PTMC membranes. Our urethrographic examination results and reversion of spontaneous urination after the operation did not reveal clinically remarkable problems, such as strictures. Further, there were no significant differences between the PLCL and PTMC groups in the integrity or structure of the *de novo* urothelium, and therefore, both biomaterials could be considered potential for urothelial applications. However, PTMC showed significant development of urothelial integrity. Based on our histological evaluation, both PLCL and PTMC caused only mild inflammation throughout the follow-up. Invasive treatment naturally always causes fibrosis to some degree, but the fibrotic changes on the histological level in our study varied only from mild to moderate, and the fibrosis did not cause clinically demonstrable problems. Both biomaterials showed suitability for this purpose without significant differences

from each other. In particular, PTMC, which has not been previously investigated for urethral reconstruction and was easier to handle than PLCL, should be considered as a potential biomaterial for urological tissue engineering. The limitation of this research was that we used unseeded biomaterial grafts, and therefore, our next step is to study cell-seeded PLCL and PTMC grafts for urethral reconstruction. Additionally, in the future it would be beneficial to compare these biomaterials to, for instance, PGA or BAMG, which are one of the most frequently studied biomaterials for urethral tissue engineering with promising results.[4,8] Further, it would be interesting to study different composite biomaterials, as PLCL or PTMC meshes combined, for instance, with polyethylene glycol (PEG) hydrogel[29] for urethral reconstruction to facilitate the regeneration of urethra.

Acknowledgments

We most deeply thank our colleagues in BioMediTech, Pirkanmaa Hospital District and University of Twente. We sincerely appreciate the expertise of pathologist Marita Laurila, statistician Heini Huhtala, and laboratory technologist Sari Kalliokoski. Without the knowledge and experience of the personnel in the animal laboratory of the University of Tampere, this study would not have been completed. This study was financially supported by the Finnish Research Foundation of Children's Diseases, Competitive State Research Financing of the Expert Responsibility area of Tampere University Hospital and The Finnish Cultural Foundation.

Disclosure Statement

No competing financial interests exist.

References

1. Baskin, L.S. Hypospadias and urethral development. J Urol **163,** 951, 2000.
2. Atala, A. Regenerative medicine and tissue engineering in urology. Urol Clin North Am **36,** 199, 2009.
3. Orabi, H., Bouhout, S., Morissette, A., Rousseau, A., Chabaud, S., and Bolduc, S. Tissue engineering of urinary bladder and urethra: advances from bench to patients scientific. ScientificWorldJournal **24,** 154, 2013.
4. Orabi, H., AbouShwareb, T., Zhang, Y., Yoo, J.J., and Atala, A. Cell-seeded tubularized scaffolds for reconstruction of long urethral defects: a preclinical study. Eur Urol **63,** 531, 2013.
5. Yamzon, J., Perin, L., and Koh, C.J. Current status of tissue engineering in pediatric urology. Curr Opin Urol **18,** 404, 2008.
6. Atala, A. Tissue engineering of human bladder. Br Med Bull **97,** 81, 2011.
7. Pariente, J.L., Kim, B.S., and Atala, A. In vitro biocompatibility assessment of naturally derived and synthetic biomaterials using normal human urothelial cells. J Biomed Mater Res **55,** 33, 2001.
8. Raya-Rivera, A., Esquiliano, D.R., Yoo, J.J., Lopez-Bayghen, E., Soker, S., and Atala, A. Tissue-engineered autologous urethras for patients who need reconstruction: an observational study. Lancet **377,** 1175, 2011.
9. Joseph, D.B., Borer, J.G., De Filippo, R.E., Hodges, S.J., and McLorie, G.A. Autologous cell seeded biodegradable scaffold for augmentation cystoplasty: phase II study in children and adolescents with spina bifida. J Urol **191,** 1389, 2014.
10. Sartoneva, R., Haimi, S., Miettinen, S., Mannerström, B., Haaparanta, A.-M., Sándor, G., Kellomäki, M., Suuronen, R., and Lahdes-Vasama, T. Comparison of poly(lactide-ε-caprolactone) membrane and amniotic membrane for urothelium tissue engineering applications. J R Soc Interface **8,** 671, 2011.
11. Sartoneva, R., Haaparanta, A.-M., Lahdes-Vasama, T., Mannerström, B., Kellomäki, M., Salomäki, M., Sándor, G., Seppänen, R., Miettinen, S., and Haimi, S. Characterizing and optimizing poly-l-lactide-co-e-caprolactone membranes for urothelial tissue engineering. J R Soc Interface **9,** 3444, 2012.
12. Burks, C.A., Bundy, K., Fotuhi, P., and Alt, E. Characterization of 75:25 poly(1-lactide-co-ε-caprolactone) thin films for the endoluminal delivery of adipose-derived stem cells to abdominal aortic aneurysms. Tissue Eng **12,** 2591, 2006.
13. Kellomäki, M., Puumanen, K., Ashammakhi, N., Waris, T., Paasimaa, S., and Törmälä, P. Bioabsorbable laminated membranes for guided bone regeneration. Technol Health Care **10,** 165, 2002.
14. Zhu, Y., Leong, M.F., Ong, W.F., Chan-Park, M.B., and Chian, K.S. Esophageal epithelium regeneration on fibronectin grafted poly(L-lactide-co-caprolactone) (PLLC) nanofiber scaffold. Biomaterials **28,** 861, 2007.
15. Song, Y., Wennink, J.W., Kamphuis, M.M., Sterk, L.M., Vermes, I., Poot, A.A., Feijen, J., and Grijpma, D.W. Dynamic culturing of smooth muscle cells in tubular poly(-trimethylene carbonate) scaffolds for vascular tissue engineering. Tissue Eng Part A **17,** 381, 2011.
16. Van Leeuwen, A.C., Van Kooten, T.G., Grijpma, D.W., and Bos, R.R. In vivo behaviour of a biodegradable poly(-trimethylene carbonate) barrier membrane: a histological study in rats. J Mater Sci Mater Med **23,** 1951, 2012.
17. Pêgo, A.P., Van Luyn, M.J., Brouwer, L.A., van Wachem, P.B., Poot, A.A., Grijpma, D.W., and Feijen, J. In vivo behavior of poly(1,3-trimethylene carbonate) and copolymers of 1,3-trimethylene carbonate with D,L-lactide or epsilon-caprolactone: degradation and tissue response. J Biomed Mater Res A **67,** 1044, 2003.
18. Zhang, Z., Kuijer, R., Bulstra, S.K., Grijpma, D.W., and Feijen, J. The in vivo and in vitro degradation behavior of poly(trimethylene carbonate). Biomaterials **27,** 1741, 2006.
19. Pêgo, A.P., Siebum, B., Van Luyn, M.J., Gallego, Y., Van Seijen, X.J., Poot, A.A., Grijpma, D.W., and Feijen, J. Preparation of degradable porous structures based on 1,3-trimethylene carbonate and D,L-lactide (co)polymers for heart tissue engineering. Tissue Eng **9,** 981, 2003.
20. Vogels, R.R., Bosmans, J.W., van Barneveld, K.W., Verdoold, V., van Rijn, S., Gijbels, M.J., Penders, J., Breukink, S.O., Grijpma, D.W., and Bouvy, N.D. A new poly(1,3-trimethylene carbonate) film provides effective adhesion reduction after major abdominal surgery in a rat model. Surgery **157,** 1113, 2015.
21. Southgate, J., Masters, J.R.W., and Trejdosiewicz, L.K. Culture of human urothelium. In: Freshney, R.I., and Freshney, M.G., eds. Culture of Epithelial Cells. NY: John Wiley & Sons, Inc., 2002, pp. 381–399.
22. Pfaffl, M.W. A new mathematical model for relative quantification in real-time RT-PCR. Nucleic Acids Res **29,** 2002, 2001.
23. Villoldo, G.M., Loresi, M., Giudice, C., Damia, O., Moldes, J.M., DeBadiola, F., Barbich, M., and Argibay, P.

Histologic changes after urethroplasty using small intestinal submucosa unseeded with cells in rabbits with injured uretra. Urology **81,** 1380, 2013.
24. Sayeg, K., Freitas-Filho, L.G., Waitzberg, Å.F., Arias, V.E., Laks, M., Egydio, F.M., and Oliveira, A.S. Integration of collagen matrices into the urethra when implanted as onlay graft. Int Braz J Urol **39,** 414, 2013.
25. Uyeturk, U., Gucuk, A., Firat, T., Kemahli, E., Kukner, A., and Ozyalvacli, M.E. Effect of mitomycin, bevacizumab, and 5-Fluorouracil to inhibit urethral fibrosis in a rabbit model. J Endourol **28,** 1363, 2014.
26. Kloskowski, T., Jundzill, A., Kowalczyk, T., Nowacki, M., Bodnar, M., Marszalek, A., Pokrywczyńska, M., Frontczak-Baniewicz, M., Kowalewski, T.A., Chlosta, P., and Drewa, T. Ureter regeneration—the proper scaffold has to be defined. PLoS One **9,** e106023, 2014.
27. de Graaf, P., van der Linde, E.M., Peter, F.W.M., Rosier, P.F., Izeta, A., Sievert, K.-D., Bosch, J.L.H., and de Kort, L.M. Systematic review to compare urothelium differentiation with urethral epithelium differentiation in fetal development, as a basis of tissue engineering of the male urethra. Tissue Eng Part B Rev **23,** 257, 2016.
28. Taira, M., Araki, Y., Nakao, H., Takahashi, J., Hyon, S.H., and Tsutsumi, S. Cellular reactions to polylactide-based sponge and collagen gel in subcutaneous tissue. J Oral Rehabil **30,** 106, 2003.
29. Adelöw, C.A., and Frey, P. Synthetic hydrogel matrices for guided bladder tissue regeneration. Methods Mol Med **140,** 125, 2007.

Address correspondence to:
Reetta Sartoneva, MD, PhD, MSc
BioMediTech
University of Tampere
Lääkärinkatu 1, 4th floor
33520 Tampere
Finland

E-mail: reetta.sartoneva@fimnet.fi

Received: June 28, 2016
Accepted: April 17, 2017
Online Publication Date: July 21, 2017